DIGITAL COMPUTER MODEL STUDY OF A DESTROYER STEAM GENERATOR SYSTEM CONTROL

by

Humberto Medina Arellano

United States
Naval Postgraduate School

THESIS

DIGITAL COMPUTER MODEL STUDY OF A DESTROYER STEAM GENERATOR SYSTEM CONTROL

by

Humberto Medina Arellano

June 1970

This document has been approved for public release and sale; its distribution is unlimited.

T135266

Digital Computer Model Study of a Destroyer Steam Generator System Control

by

Humberto Medina Arellano
Lieutenant Commander, Venezuelan Navy

Submitted in partial fulfillment of the
requirements for the degree of

MASTER OF SCIENCE IN ELECTRICAL ENGINEERING

from the

NAVAL POSTGRADUATE SCHOOL
June 1970

ABSTRACT

The steam generator of a DLG-9 Class Destroyer is studied and simulated by means of the Digital Simulation Language DSL/360. Parameter plane studies are made for each one of the principal subloops of the control system and determination of optimal controller settings is attempted.

The entire steam generator and control system are simulated and the responses to small disturbances are analyzed.

Finally a linear interpolation is attempted for the nonlinear transfer functions, and the responses compared with data from an actual DLG-9 Test Boiler.

TABLE OF CONTENTS

LIST OF DRAWINGS

LIST OF SYMBOLS AND ABBREVIATIONS

ζ	Relative Damping Coefficient (zeta)
ω	Undamped Natural Frequency (omega)
σ	Real-axis Values of the s-plane (sigma)
NBTL	Naval Boiler and Turbine Laboratory
DSL	Digital Simulation Language
FDB	Forced Draft Blower
FP	Full Power Condition
Crsng	Cruising Condition
lb/hr	Pounds per hour of flow
psi	Pounds per square inch of pressure

ACKNOWLEDGEMENTS

The author wishes to express his appreciation to the following persons:

Doctor George J. Thaler, Professor at the U. S. Naval Postgraduate School, for providing the topic and guidance necessary to make this manuscript possible.

Lieutenant Charles A. Vinroot, USN, for the many helpful discussions that he and the author had during the preparation of this manuscript.

Professor Milton L. Wilcox, of the U. S. Naval Postgraduate School, and Mr. James W. Banham, Jr., of the Naval Boiler and Turbine Laboratory, for providing beneficial reference material.

I. INTRODUCTION

A. DISCUSSION

The Naval Boiler and Turbine Laboratory has conducted extensive dynamic and frequency response tests on a Babcock and Wilcox Company test boiler of the DLG-9 class, and through the use of the "pulse test" technique described in Ref. 1 a mathematical model was obtained of the steam generator system with its controls and auxiliary equipment.

This mathematical model is reported in NBTL PROJECT B-502-III and Figure 1, taken from that report is the block diagram of the model with its associated transfer functions. It is the objective of this thesis to simulate the steam generator using the Digital Simulation Language DSL/360 [2], with the transfer functions as reported in Ref. 1 and to establish the validity of the model; also using parameter plane techniques [3] to perform the analysis of each of the three principal sub-loops (air flow, oil flow and water level control systems) in the decoupled state. An attempt to improve the response of these loops will be made by changing the controllers gains; however, since the specifications for the performance of the loops in the decoupled state are not known, those specifications will be defined with the criterion of making the step response as fast as possible with little or no overshoot. A simulation of the complete steam generator will be

made with the parameter settings as chosen from above specifications and the response compared with those for the parameter settings as given in Ref. 1.

Finally a linear interpolation will be attempted for the nonlinear devices and responses of the simulation using the linear interpolation will be compared with actual responses of the boiler as reported in Ref. 4.

B. DESCRIPTION

The DLG-9 boiler utilizes the Bailey Combustion Control System, of which a general description will be given in this section, and a more detailed description will be given in later sections.

The primary functions of the automatic boiler control system are: to control the firing rate of the boilers to maintain a constant superheater outlet pressure under all conditions of boiler steam load; to proportion the combustion air (quantity of air needed to burn the fuel oil furnished to the boiler) and fuel in the proper ratio to maintain the optimum combustion efficiency; to reduce the firing rate to a stable minimum in the event of instrument failure; finally, through the feedwater control, to regulate the flow of feedwater to the boiler drum to maintain a normal boiler drum level.

The amount of fuel burned, the quantity of air required to burn that fuel and the amount of feedwater needed to maintain the boiler drum level, are determined by the amount of steam being used and the desired pressure to be maintained.

The amount of steam output demanded of the boiler, Gs, is measured, through its entire range (0 to 210000 lbs/hr), by the steam flow transmitter which develops a pneumatic signal, Pgs, (3 to 27 psi) proportional to the steam flow, which is sent, as demand signal, to the steam pressure controller and the water level control loop.

The desired superheater outlet pressure to be maintained is 1200 psi. This pressure is measured by the superheater steam pressure transmitter which develops a pneumatic signal, Pp, from 3 to 27 psi, in direct proportion to a range of superheater pressure variation from 900 psi to 1500 psi; therefore to 1200 psi of superheater pressure corresponds a signal of 15 psi which is compared to a reference or set point, Prp, of 15 psi also, so as to have a signal, Pep, that is a measure of the deviation of superheater pressure from 1200 psi. This signal is also sent to the steam pressure controller whose output depends on the two signals mentioned, Pep and Pgs. The output of the controller is sent to the fuel oil control loop to modify the firing rate according to the demand, and also is sent to air control loop to modify the amount of air flow in accordance to the change in the firing rate which is going to take place.

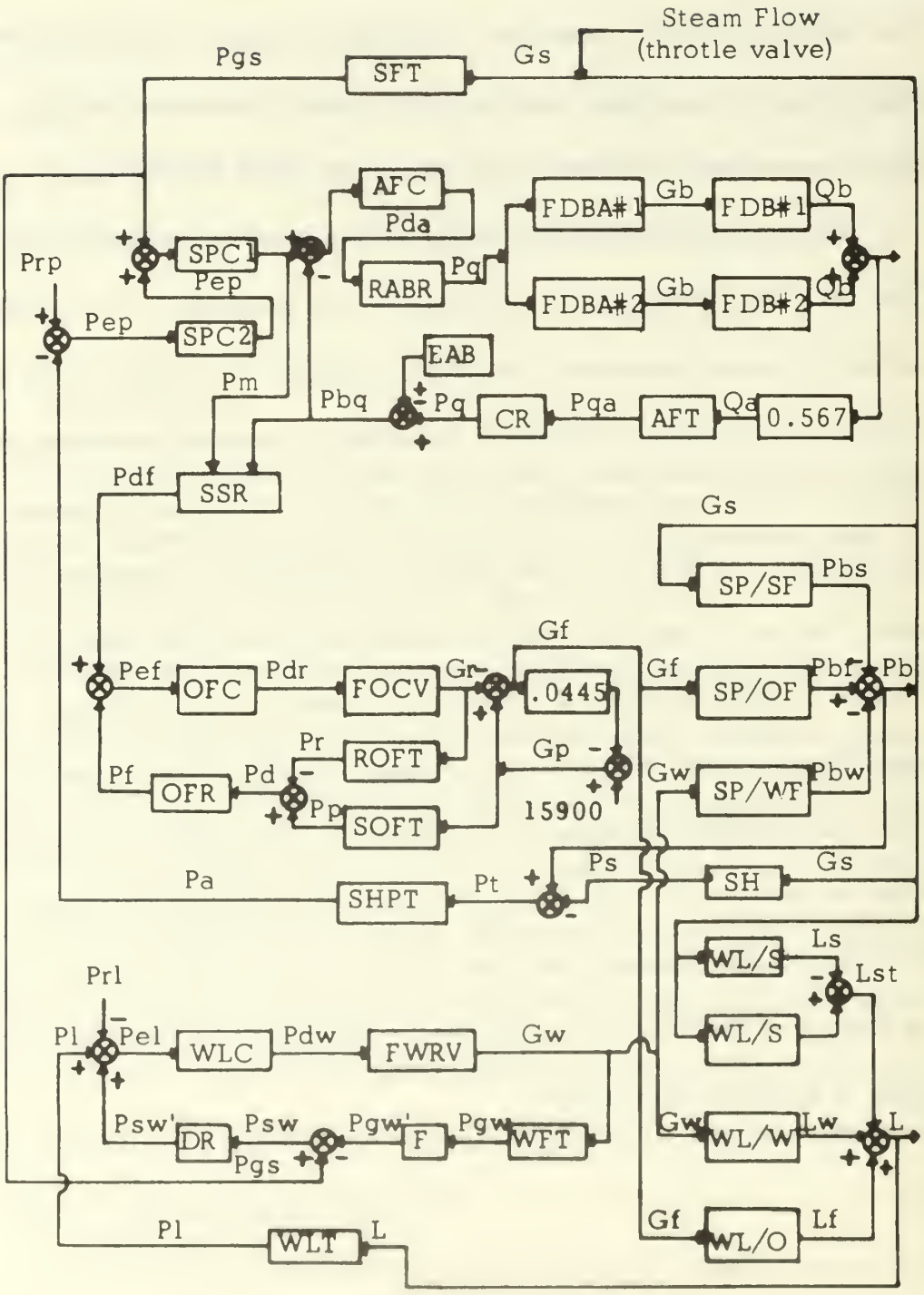

FIGURE 1
SCHEMATIC DIAGRAM OF BOILER CONTROLS

TABLE I

TRANSFER FUNCTIONS CORRESPONDING TO FIGURE 1

SFT	Steam Flow Transmitter:
	$(1.14 \times 10^{-4})/(1 + 1.36S + 0.052S^2)$
SPC1	Steam Pressure Controller:
	$(2.5)/(1 + 0.034S)$
SPC2	Steam Pressure Controller:
	$(1.0)/(1 + 0.038S + 0.004S^2)$
AFC	Air Flow Controller:
	$(0.944 + 0.106/S)/(1 + 0.04S + 0.003S^2)$
RABR	Rate Action Booster Relay:
	$(1 + 0.895)/(1 + 0.079S + 0.01S^2)$
FDBA	Forced Draft Blower Actuators #1 and #2:
	Crsng: $(512/(1+S))/(1 + 0.28S + 0.5S^2)$
	90% FP: $(950/(1+S))/(1 + 0.28S + 0.5S^2)$
FDB	Forced Draft Blowers #1 and #2:
	Crsng: $(6.83 \times 10^{-3})/(1 + 10.0S)$
	90% FP: $(5.50 \times 10^{-3})/(1 + 6.35S)$
AFT	Air Flow Transmitter:
	$(0.254\exp(-0.45S))/(1 + 0.4S)$
CR	Calibrating Relay:
	$(1.05)/(1 + 0.034S)$

EAB Excess Air Bias:

Amount of excess air to be added or subtracted to produce smoke or to blow tubes.

SSR Signal Selector Relay:

Transmits the smaller value of Pbq and Pm

OFC Oil Flow Controller:

$(2.82 + 0.392/S)/(1 + 0.32S)$

FOCV Fuel Oil Flow Control Valve:

795.0

ROFT Return Oil Flow Transmitter:

$(1.2 \times 10^{-3})/(1 + 0.12S + 0.33S^2)$

SOFT Supply Oil Flow Transmitter:

Same as ROFT

OFR Oil Flow Relay:

$(1.05)/(1 + 0.034S)$

SHPT Superheater Steam Pressure Transmitter:

$(4.0 \times 10^{-2})/(1 + 0.012S + 0.02S^2)$

SH Superheater:

Crsng: 3.0×10^{-4}

90% FP: 8.2×10^{-4}

WLC Water Level Controller:

$(1.26 + 0.1/S)/(1 + 0.54S + 0.8S^2)$

FWRV Feedwater Regulating Valve:

$(3.12\exp(-0.25S))/(1 + 0.68S + 1.26S^2)$

WFT Water Flow Transmitter:

$$(1.14\times10^{-4})/(1 + 1.36S + 0.052S^2)$$

F Filter:

$$(1.0)/(1 + 4.5S)$$

DR Steam Flow-Water Flow Differential Relay:

$$(0.50)/(0.034S)$$

WLT Water Level Transmitter:

$$(1.0)/(1 + 0.6S + 0.25S^2)$$

SP/SF Steam Pressure / Steam Flow:

Crsng: $(1.65\times10^{-4})(1+35.70S)/(S(1+22.5S)(1+0.71S))$

90% FP: $(2.5\times10^{-1})(1+0.504S)/(S(1+2.23S++ 2.53S^2))$

SP/OF Steam Pressure / Oil Flow:

Crsng: $(2.83\times10^{-3})(1+35.6S)/(S(1+22.5S)(1+0.57S))$

90% FP: $(3.18\times10^{-3})(1+4.50S)/(S(1+2.50S)(1+0.71S))$

WL/S Water Level / Steam Flow:

Crsng: $(1.12\times10^{-6})/S$

90% FP: $(1.26\times10^{-6})/S$

WL/S Water Level / Steam Flow:

Crsng: $(5.62\times10^{-5})/((1+3.18S)(1+0.48S+0.63S^2))$

90% FP: $(4.04\times10^{-5})/((1+1.80S)(1+0.21S+0.13S^2))$

SP/WF Steam Pressure / Water Flow:

Crsng: $(0.389\times10^{-4})/(S(1 + 22.5S))$

90% FP: $(0.100\times10^{-4})/(S(1 + 6.0S + 100.0S^2))$

WL/W Water Level / Water Flow:

Crsng: $(1.12 \times 10^{-6})/(S(1 + 0.852S + 2.02S^2))$

90% FP: $(1.26 \times 10^{-6})/(S(1 + 0.320S + 0.63S^2))$

WL/O Water Level / Oil Flow:

Crsng: $(2.09 \times 10^{-4} \exp(-0.8S)/((1+0.45S)(1+1.9S+2.5S^2))$

90% FP: $(1.9 \times 10^{-4} \exp(-0.36S)/((1+2.0S)(1+2.0S+4.0S^2))$

II. AIR FLOW CONTROL SYSTEM

A. DESCRIPTION

The Air Flow Control System is shown in block diagram in Figure 2; it is a typical feedback system with two principal non-linearities, the steam control valves and the forced draft blowers. The system consists of the following elements:

1. The Controller

The Controller is a Bailey Meter Company "Mini-line" Standatrol, proportional plus reset controller; it has as input the loading pressure, Pe, that represents the difference between the master demand signal, Pm, from the steam pressure controller, and the signal from the air flow measurement. The controller is calibrated to maintain a constant output pressure as long as Pe is zero or when the air flow measurement is equal to the demand signal.

2. Rate Action Booster Relay

A Bailey Meter Company Rate Booster Relay, which is a proportional plus rate action controller, is introduced to provide increased phase margin in the blower control loop, thus allowing maximum loop gain. It is driven by the air flow controller, and if its input changes, the rate action booster relay will commence to increase or decrease its output at the rate set by the proportional band and reset settings until the air flow again balances the demand signal.

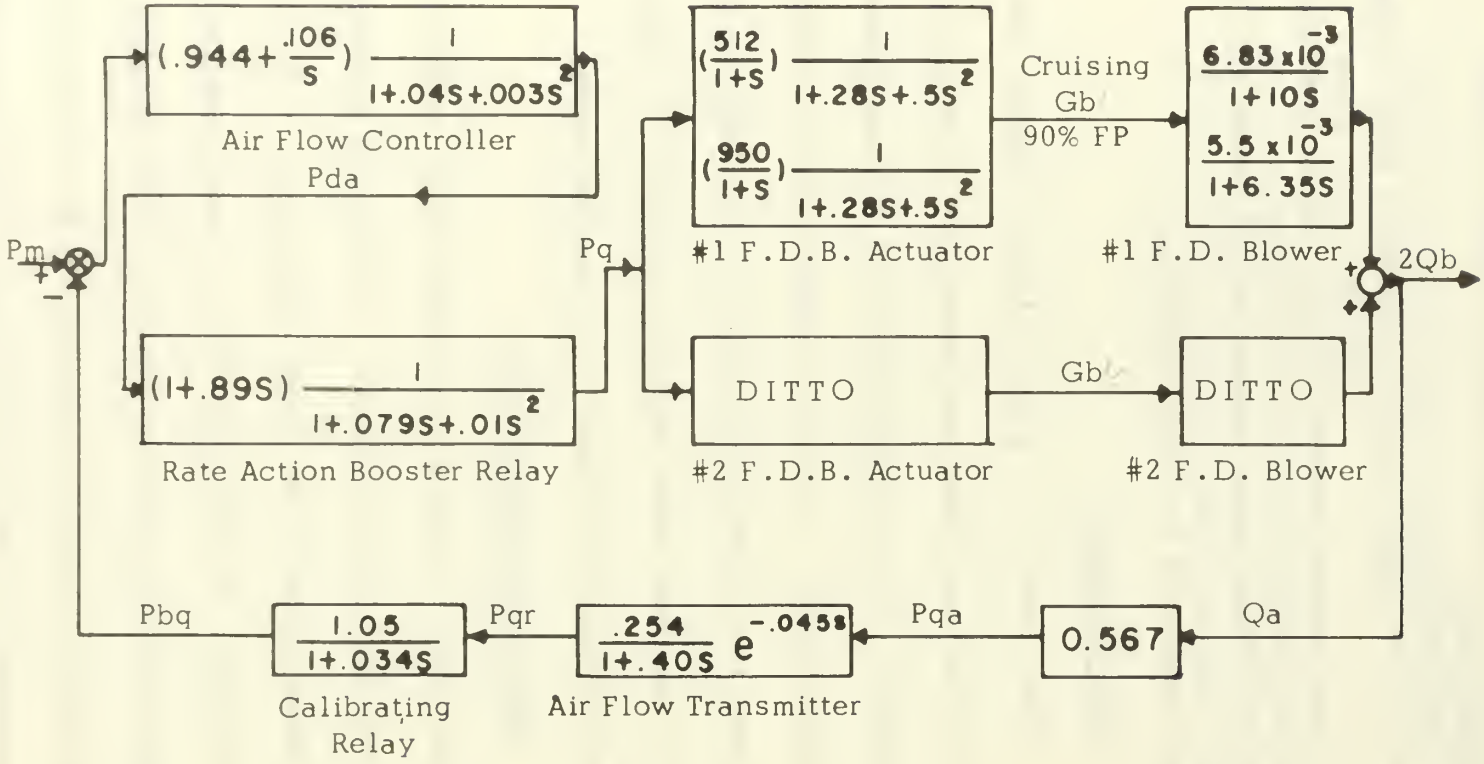

FIGURE 2
BLOCK DIAGRAM. AIR FLOW CONTROL SYSTEM

The output of this controller serves to position the forced draft blower throttles and the air flow control dampers.

3. Forced Draft Blower Actuator

Linkage and throttle valve, Bailey Meter Company Model AC-44 Control Drive and Mason-Neslan Control Valve, constitutes the steam regulating system for the main forced draft blowers. The throttle valve which admits the steam, Gb, to the forced draft blower's turbine is positioned according to the pneumatic signal, Pq, from the booster relay. The dynamics of the actuator are assumed to be linear for all blower speeds but the gain varies as the blower's speed is varied. This nonlinearity is due to the characteristics of the V-ported blower steam control valve.

4. Main Forced Draft Blower

Results obtained (NBTL Report) by generating a triangular pulse in the pneumatic signal to the actuators, indicates that the blowers can be represented by a first-order lag characterized by a natural frequency increasing with load, and a gain decreasing with load. This nonlinearity is due to the driving torque and retarding torque being nonlinear functions of turbine steam flow and blower speed.

5. Air Flow Transmitter

This is a Bailey Meter Company Type CJ-20 Differential Transmitter with Type KC-16 square root converter - transmitter.

This instrument in the feedback circuit of the air flow control loop, measures the pressure differential of the air flow across an orifice, extracts the square root of the differential pressure, and develops a pneumatic loading pressure that is proportional to the flow of air.

6. Air Flow Calibrating Relay

This relay, operating on the air flow transmitter output signal, is provided to permit scaling of the air flow open-loop gain in order to obtain optimum air/fuel ratio.

B. ANALYSIS AND SIMULATION

The Air Flow system was simulated using DSL, and using the transfer functions as given in Figure 2. The transient response to a unit step input is shown in Figure 3 for 90% Full Power condition and in Figure 4 for Cruising condition. As noted from Figure 3, there is some oscillation in the transient, and the settling time is about 30 seconds; the Cruising condition response is slower, about 40 seconds settling time.

It is desired to "optimize" the response of the loop, by adjusting the coefficients of the Air Flow Controller; therefore the Controller is defined as:

$$\text{Alpha} + \text{Beta} / s$$

where Alpha and Beta are the variable coefficients, which in the NBTL report are given as:

$$\text{Alpha} = 0.944$$

$$\text{Beta} = 0.106$$

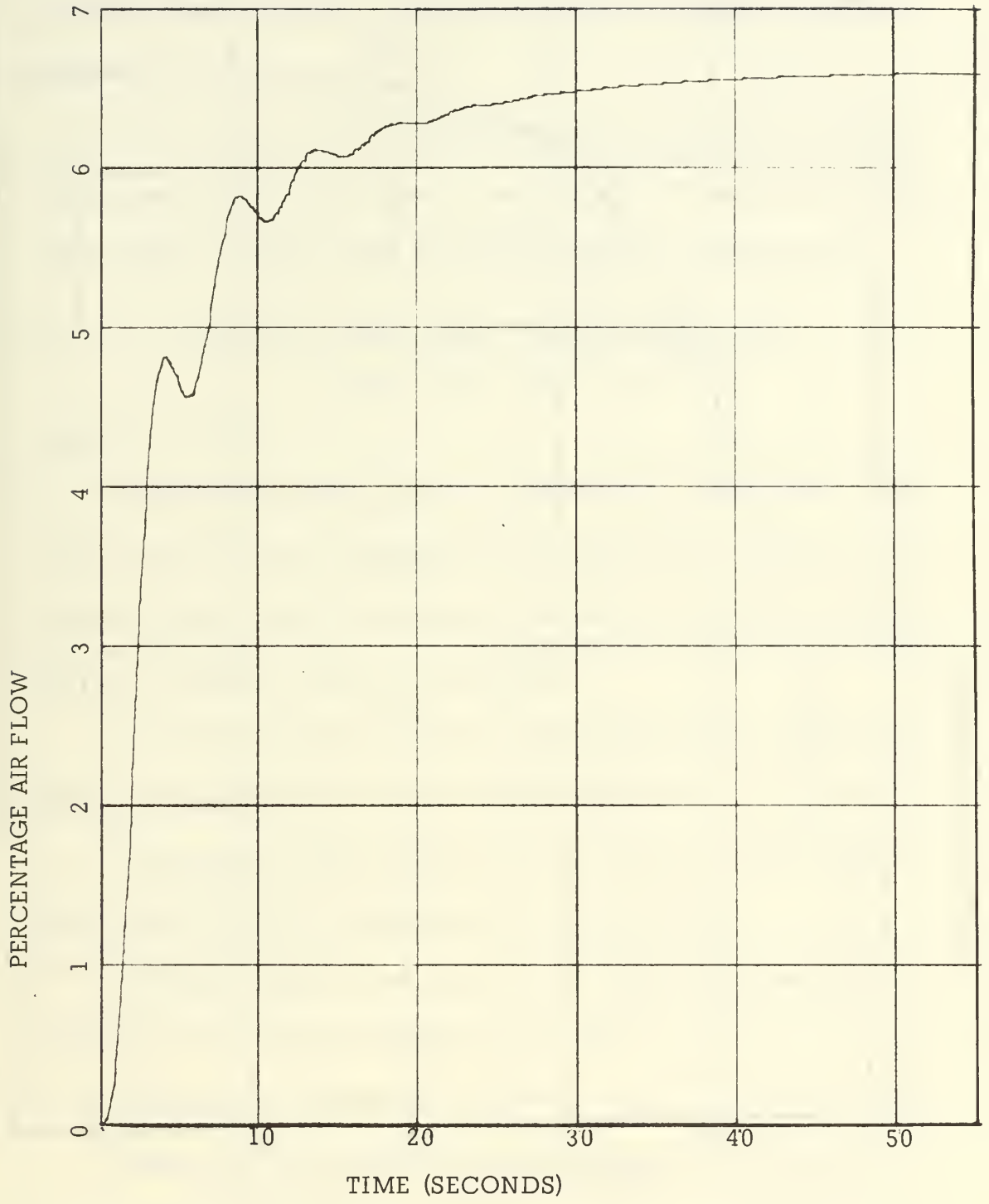

FIGURE 3. UNIT STEP RESPONSE
AIR LOOP (90%FP). ALPHA = 0.944, BETA = 0.106

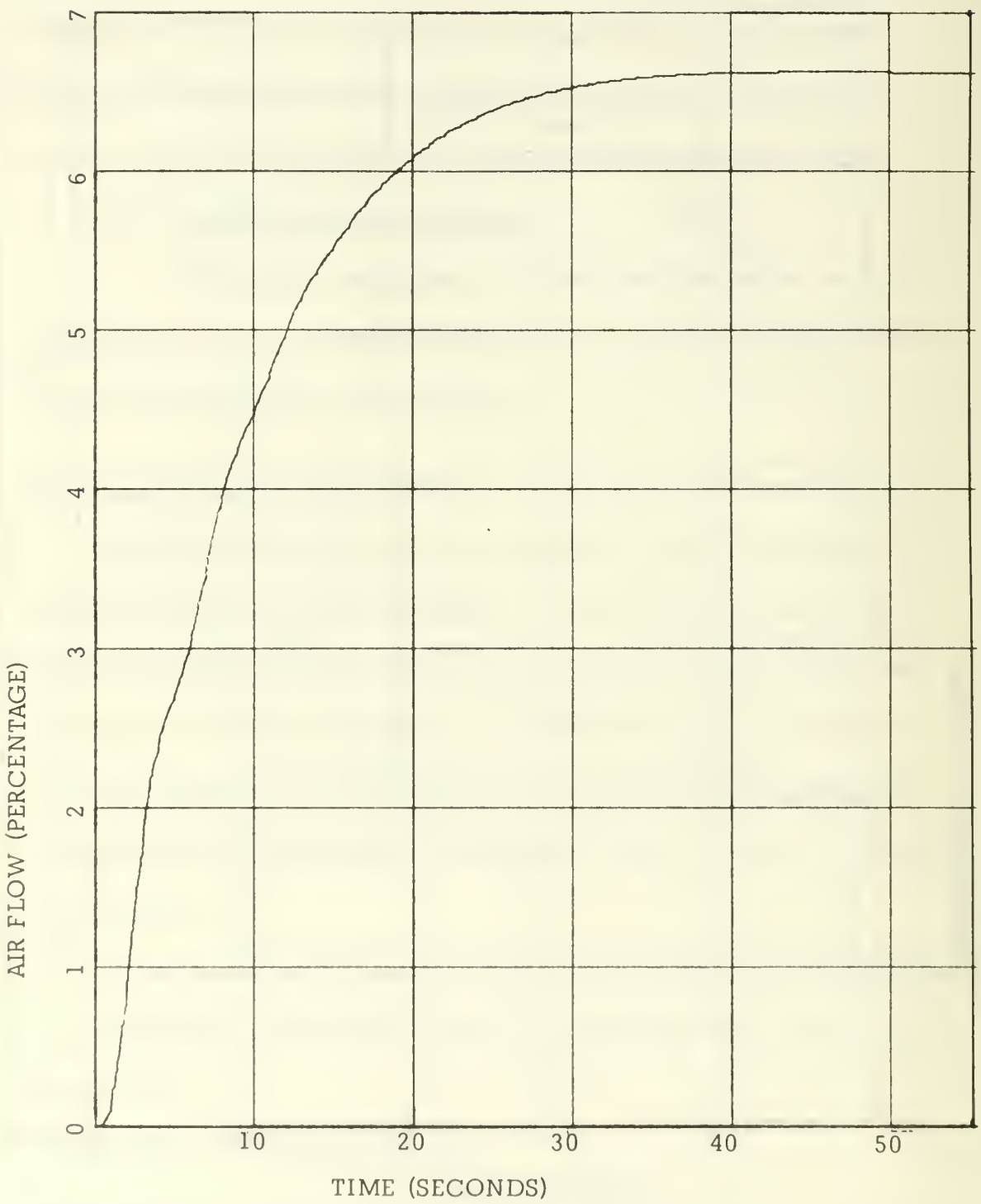

FIGURE 4. UNIT STEP RESPONSE
AIR LOOP (CRUISING). ALPHA = 0.944, BETA = 0.106

By optimizing the loop response it is assumed that the desired response is a faster one, and in the case of the 90% FP a smoother response is desired.

In order to calculate the characteristic equation for the loop a Pade approximation of the fourth order was made to represent the time delay shown in Figure 2; the Pade approximation in question is:

$$\exp(-x) = \frac{1680 - 840x + 180x^2 - 20x^3 + 4x^4}{1680 + 840x + 180x^2 + 20x^3 + x^4}$$

where $x = 0.045s$.

The resulting characteristic equation was of 15th order. Since there are two variable coefficients the best method of analysis is the parameter plane which is a graphical method that gives the following curves as function of the two parameters:

Constant zeta curves (maps of radial lines in the s-plane) for the range of frequency Wn, specified by the user.

Constant Wn curves (maps of circles centered at the origin of the s-plane) for a pre-programmed set of zeta values.

Constant sigma curves, each one of which is the map of a specific point in the real axis of the s-plane.

Constant zeta-Wn product curves.

Figure 5 is the parameter plane plot for the 90% FP condition. In this graph, for clarity only, the constant zeta curves were drawn to show that some regions of the graph are covered by two sets of zeta lines; this is so because within the range of Wn of interest there

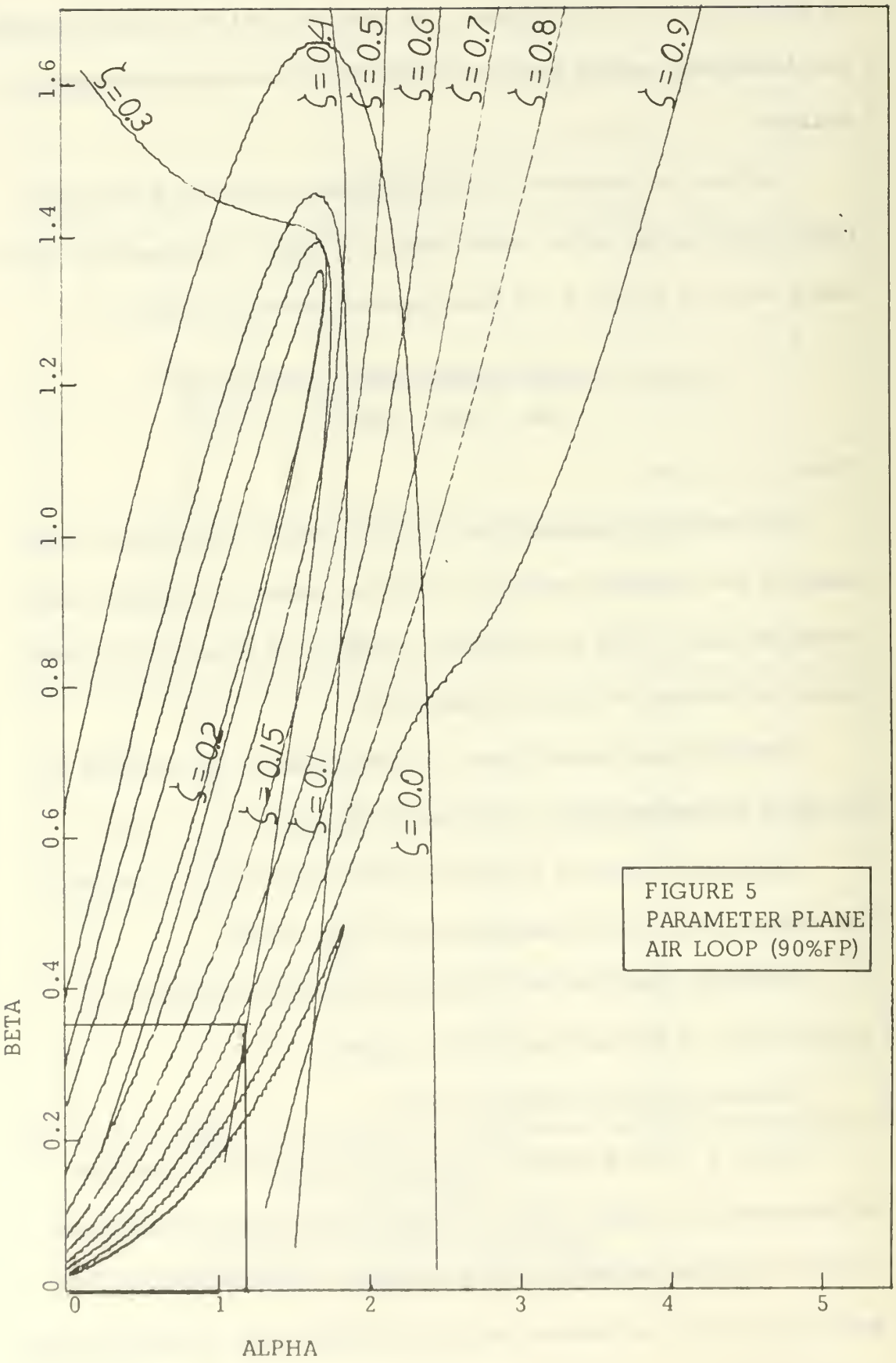

FIGURE 5
PARAMETER PLANE
AIR LOOP (90%FP)

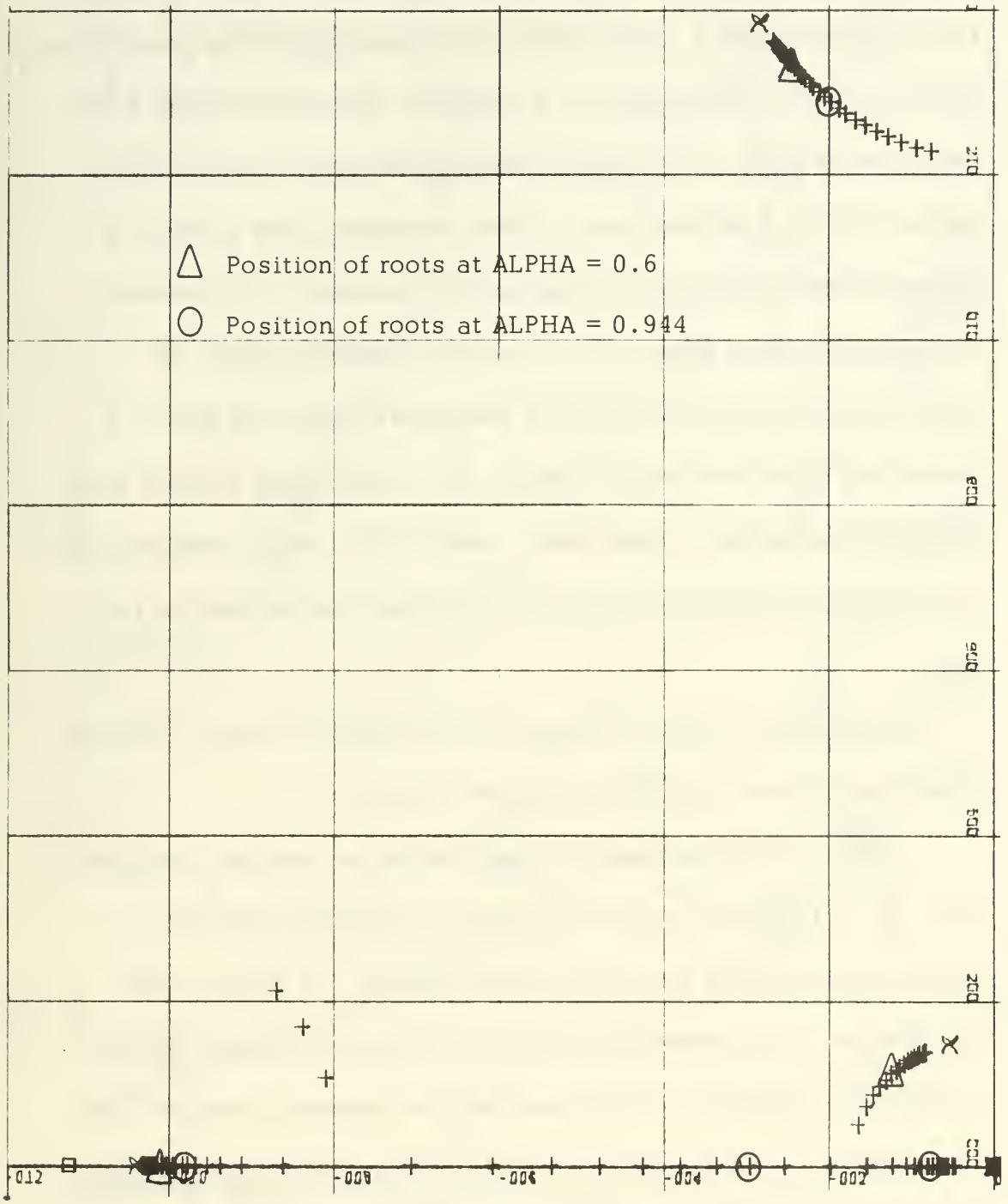

FIGURE 6. ROOT LOCUS PLOT
AIR LOOP (90%FP) ALPHA VARIABLE, BETA = 0.106
Scale = 0.2 units per inch

are two pairs of complex roots. This is more clearly seen in the Root Locus plot of Figure 6, made holding Beta constant at the given value of 0.106, and varying Alpha for 3 decades. The roots marked with a circle are at Alpha = 0.944 and those marked with a triangle are at Alpha = 0.60. It is seen that as Alpha decreases from 0.944 to 0.6 the real roots closer to the origin become complex. This is seen in the parameter plane Figure 5 by moving the operating point "B" (Alpha = 0.944, Beta = 0.106) in a horizontal line to the left, i.e., decreasing Alpha with Beta constant. At a point where Alpha $\doteq$ 0.66 begin the second set of zeta lines, zeta $\doteq$ 0.99, which indicates that at this point the real roots closer to the origin are leaving the real axis.

The outlined region in Figure 5 is expanded in Figure 7, which shows the constant zeta, sigma and Wn lines.

Figure 8 is the parameter plane plot for the cruising condition. Point "B" in Figures 7 and 8 indicates the operating point with parameter settings as given by the NBTL report. As stated in the Introduction, it is desired to reduce the rise time and have little or no overshoot; in Figure 7 it is seen that the dominant roots are real and at sigma $\doteq$ -0.1 and sigma $\doteq$ -0.35, which determine the general shape of the response. The high frequency oscillation noted in Figure 3 is due to the effect of the complex roots at zeta $\doteq$ 0.158 and Wn $\doteq$ 1.31; to speed up the rise time, zeta should be decreased, but for the 90% FP condition the rise time is determined by the real roots

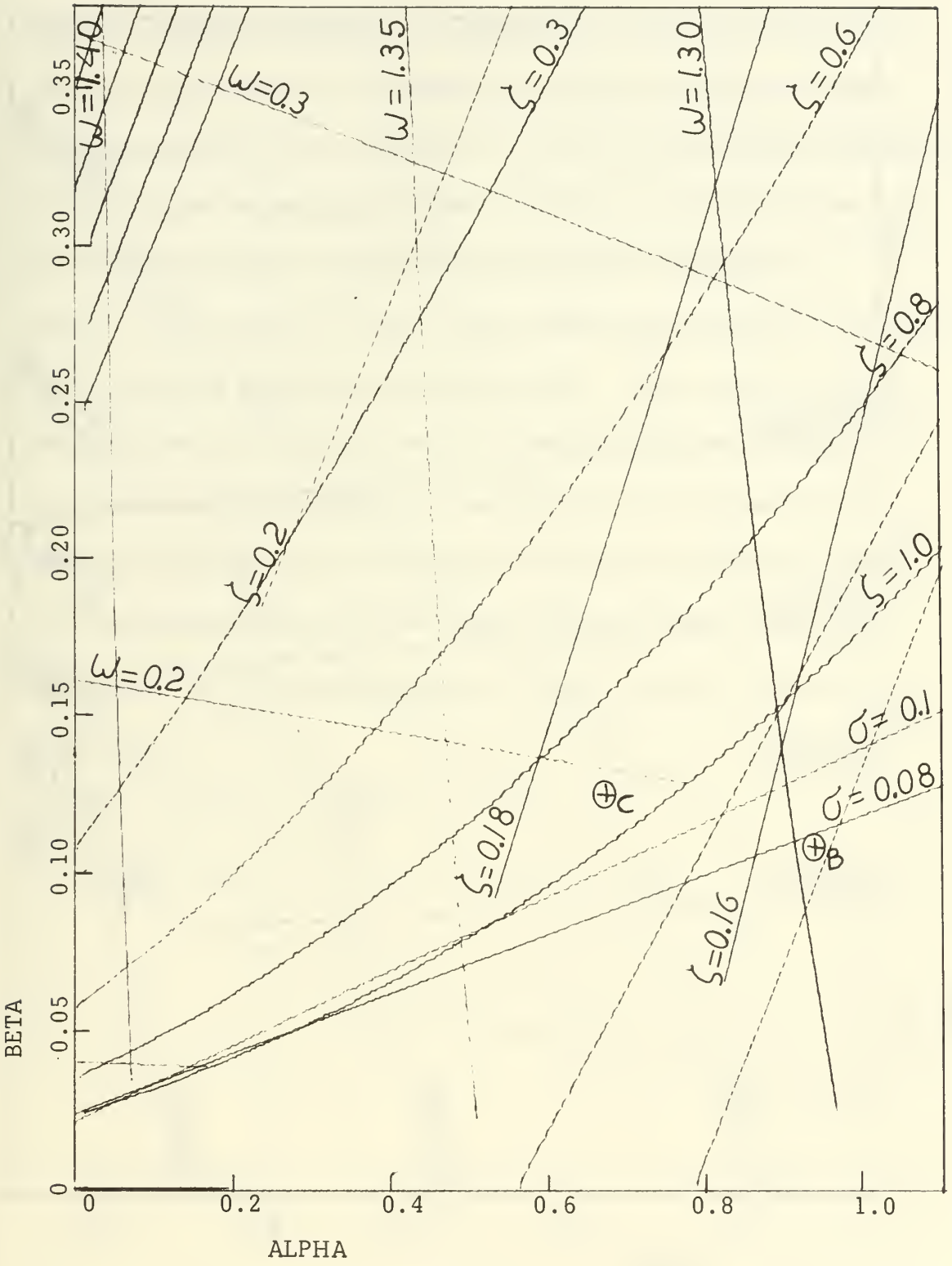

FIGURE 7. PARAMETER PLANE
AIR LOOP (90%FP)

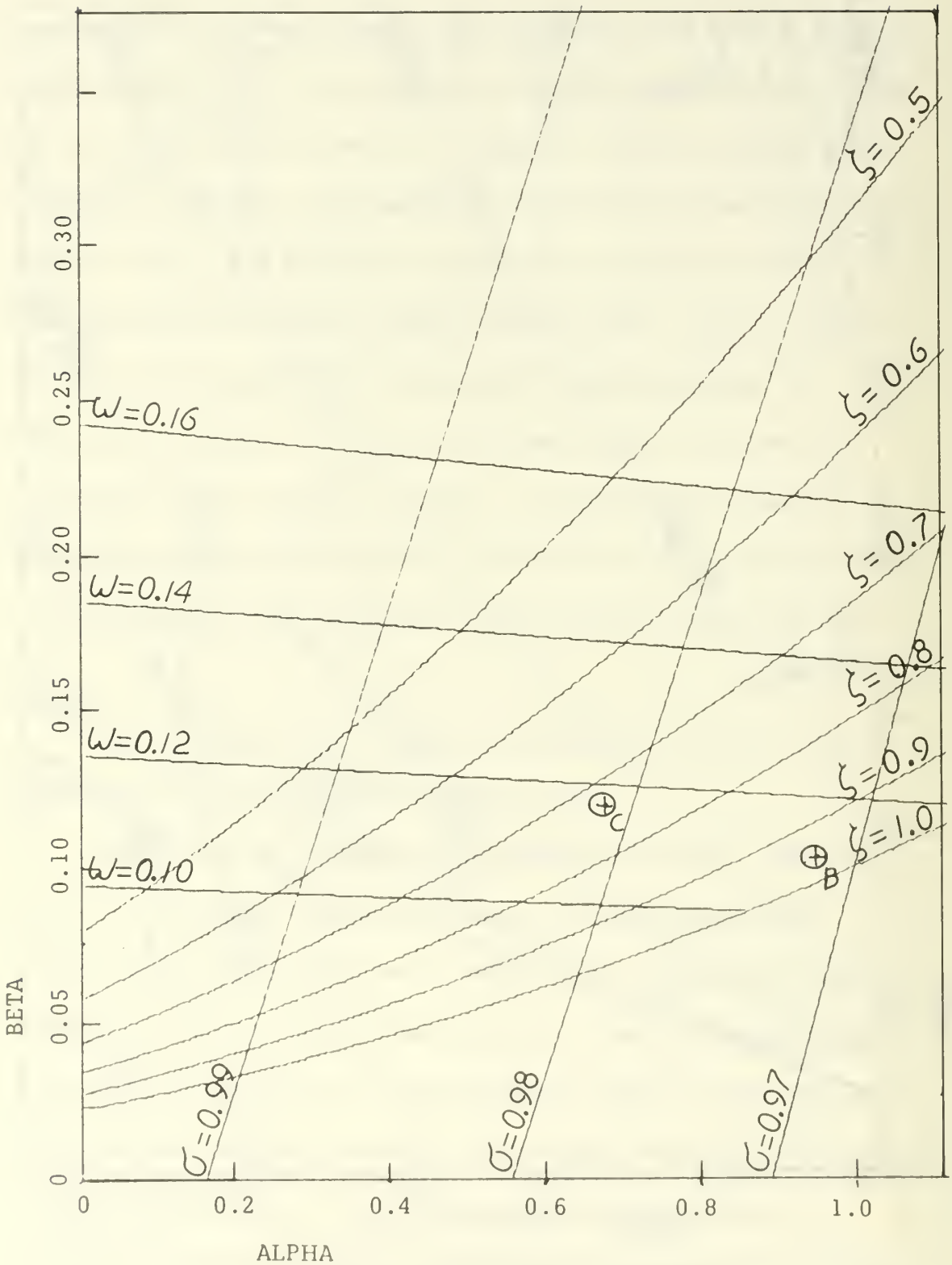

FIGURE 8. PARAMETER PLANE
AIR LOOP (CRUISING)

that are dominant, therefore, by choosing an operating point like "C" (Alpha = 0.68, Beta = 0.12) where the dominant roots have become complex with zeta $\doteq$ 0.9 and Wn $\doteq$ 0.18, the zeta have been effectively lowered hence decreasing the rise time, also it is noted that the zeta for the second pair of complex roots have been increased from zeta $\doteq$ 0.157 to zeta $\doteq$ 0.178, a very small increment which is believed to diminish the oscillation noted in Figure 3. The step response for operating point "C" and for 90% FP is shown in Figure 9 where it is compared with the response for operating "B" to show that the rise time has been decreased. Examination of Figure 8 shows that point "C" as chosen above will also lower the zeta for this, the cruising condition, but in this case a small overshoot appears as shown in Figure 10.

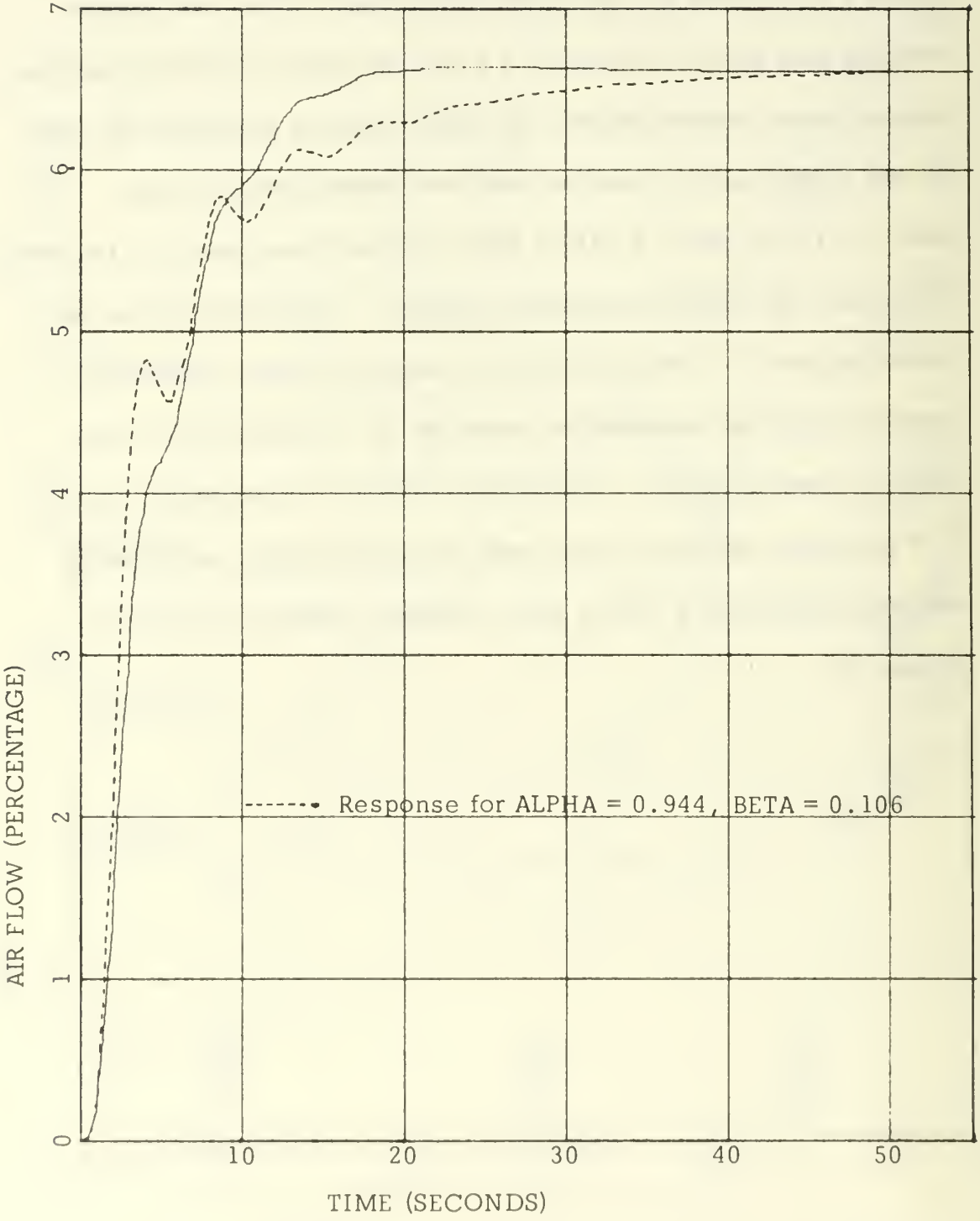

FIGURE 9. UNIT STEP RESPONSE
AIR LOOP (90%FP). ALPHA = 0.68, BETA = 0.12

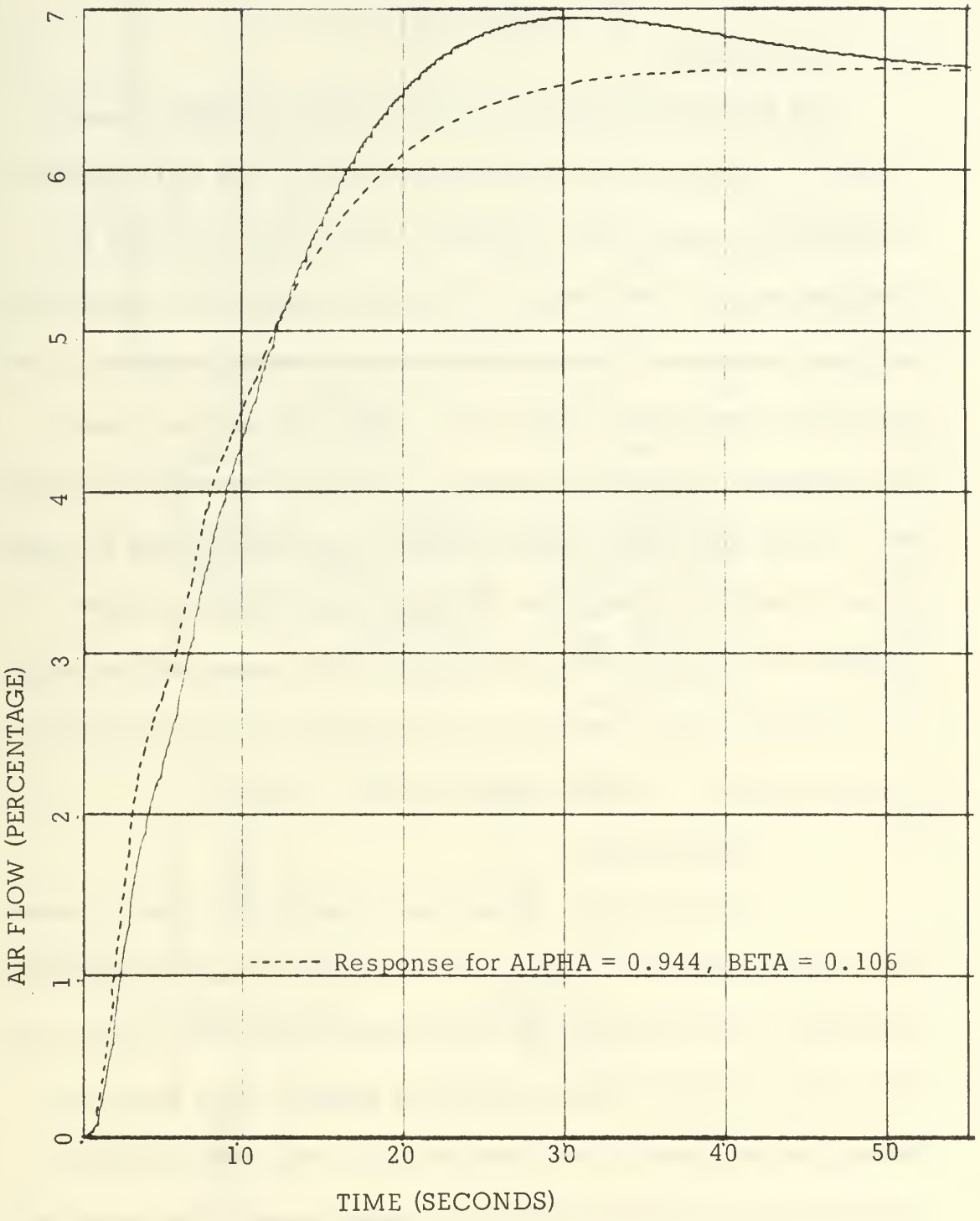

FIGURE 10. UNIT STEP RESPONSE
AIR LOOP (CRUISING). ALPHA = 0.68, BETA = 0.12

III. FUEL OIL CONTROL SYSTEM

A. DESCRIPTION

The fuel oil flow control system is shown in block diagram in Figure 11, it has as input the pneumatic signal, Pdf, as the demand index and the output is the fuel flow of the boiler, Gf. There is a constant input of 15900 lbs/hr. of fuel oil supplied to the system at a constant pressure of 1000 psi; effectively the amount supplied to the atomizers is not exactly 15900 lbs/hr. minus Gf, but less, due to back-pressure, since some pressure is needed to atomize the fuel oil; this is represented in the block diagram by making Gp equal to 15900 minus 0.0445 Gf; Gp being the effective supply of fuel oil. The system is of the return flow burner type, which means that the control is in the return line, done by the fuel oil control valve; the oil flow control system is composed of the following elements:

1. The Controller

This controller, as the one in the air flow control system, is a typical proportional plus reset "Mini-Line" Standatrol controller. The inputs to the controller are the pneumatic signals Pf, from the oil flow relay and Pdf from the fuel limiting selector relay; these two signals are balanced by the controller and if they differ an output signal, Pdr, is generated that is the control signal to the return fuel oil flow valve.

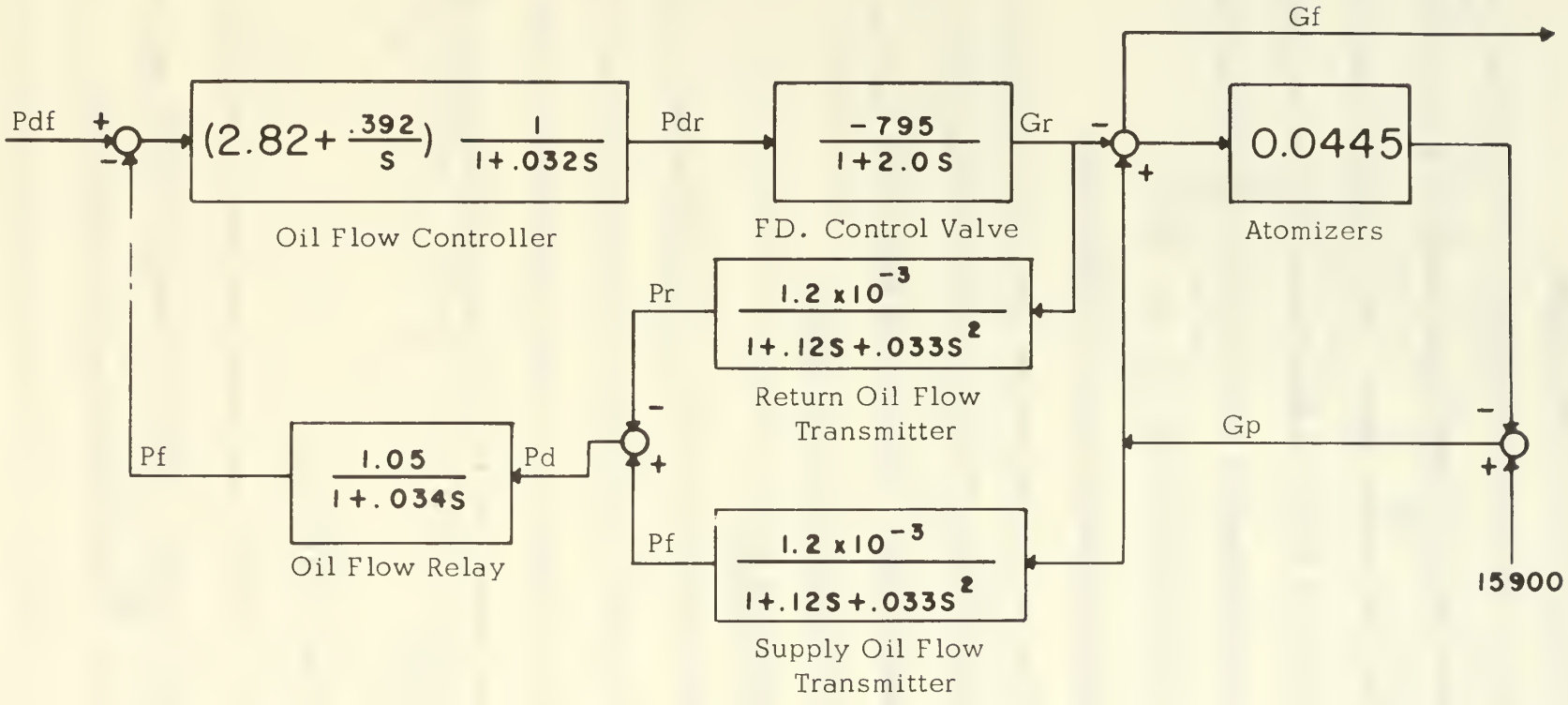

FIGURE 11
BLOCK DIAGRAM. FUEL OIL FLOW CONTROL SYSTEM

2. Return Fuel Flow Control Valve

This is a diaphragm-operated, V-ported valve, located in the fuel oil return line and controls the amount of fuel oil returned according to the input control signal. Note that the transfer function for this valve given in Figure 11 is different from the one shown in Figure 1; this discrepancy will be explained in the Analysis and Simulation part of this system.

3. Supply and Return Fuel Flow Transmitter

These two transmitters are area meters that measure the supply fuel flow Gp (lbs/hr), and the return fuel flow Gr (lbs/hr), by means of a metering valve, and each one transmits a pneumatic signal, representative of the amount of fuel flow.

4. Oil Flow Relay

This relay receives as input a signal which is obtained by subtracting the signal Pr, the output of the return fuel flow transmitter, from the signal Pp produced by the supply fuel flow transmitter. The relay develops an output, Pf, that is linearly proportional to the flow of fuel oil burned.

B. ANALYSIS AND SIMULATION

The oil flow control system when simulated on the digital computer using the transfer functions furnished by NBTL was unstable. The following block diagram reductions were made in order to find the characteristic equation of the loop and investigate the cause of the instability:

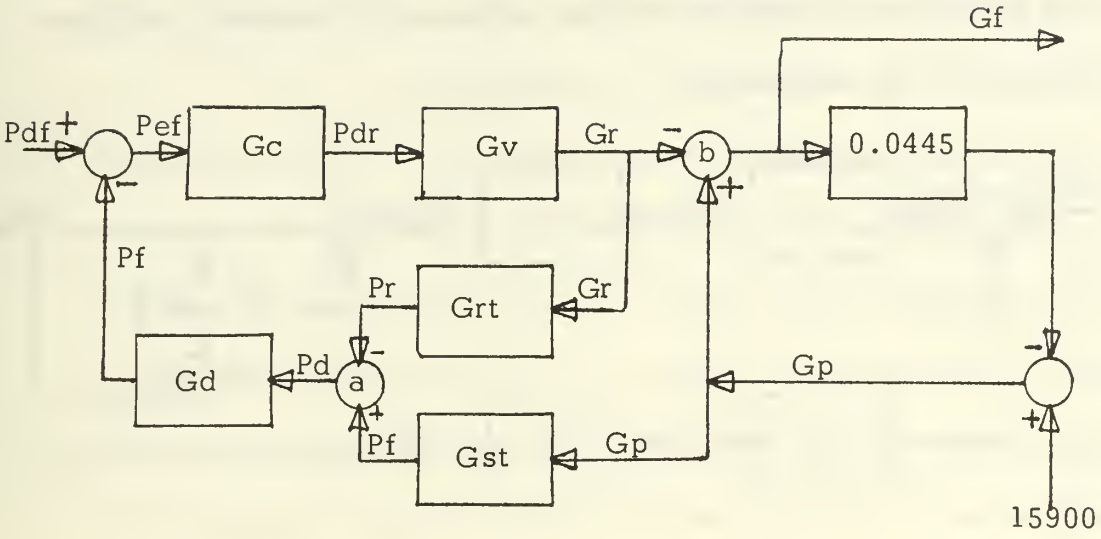

where transfer functions for the different components of Figure 11 are defined by the letters inside the corresponding blocks.

Moving the summing point 'a' to the input side of the transmitters, and reducing the two transmitters to one block since Grt is equal to Gst, the above block diagram is reduced to the following one:

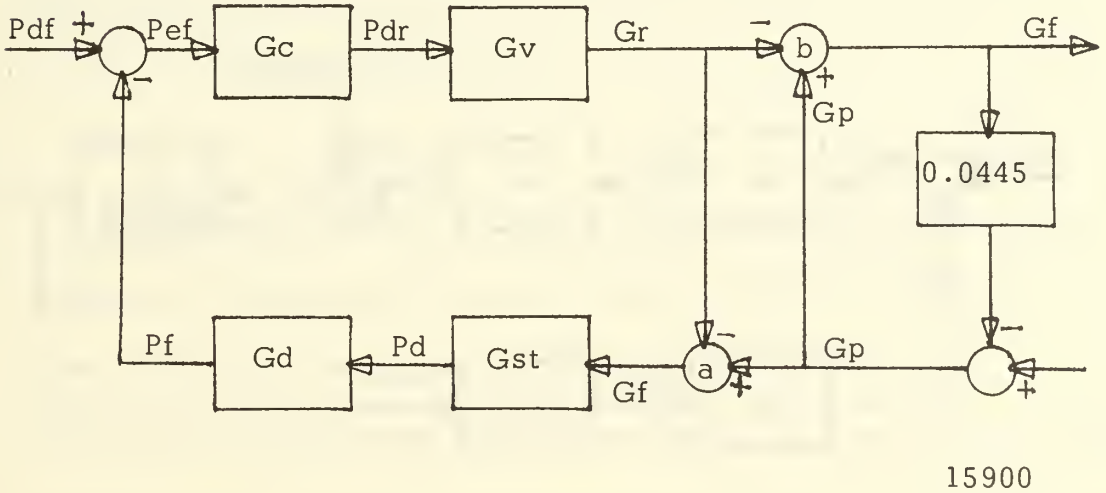

It is noted that the input to the Gst block is Gf; therefore, the block diagram can be reduced to:

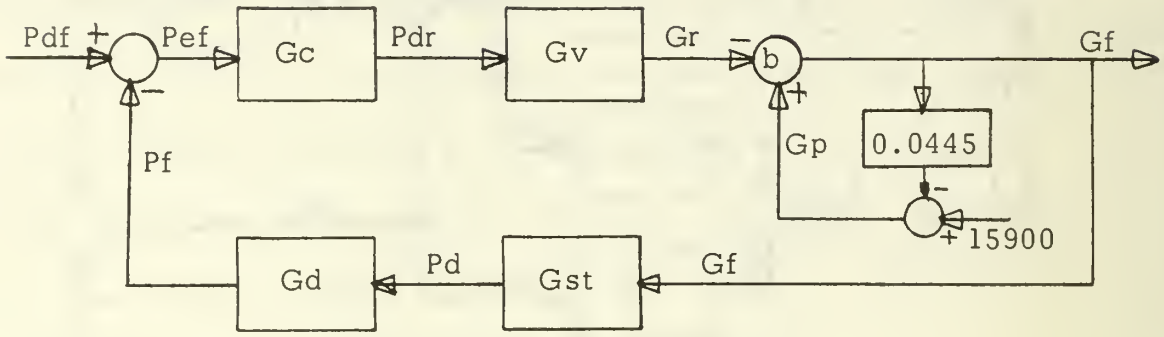

In order to eliminate the implicit loop around the constant 0.0445, the following substitutions were made:

$$Gf = Gp - Gr \quad (1)$$

$$Gp = 15900 - 0.0445Gf \quad (2)$$

Substituting (2) in (1)

$$Gf = 15900 - 0.0445Gf - Gr \quad (3)$$

$$Gf = (15900 - Gr)/1.0445 \quad (4)$$

And the block diagram was finally reduced to:

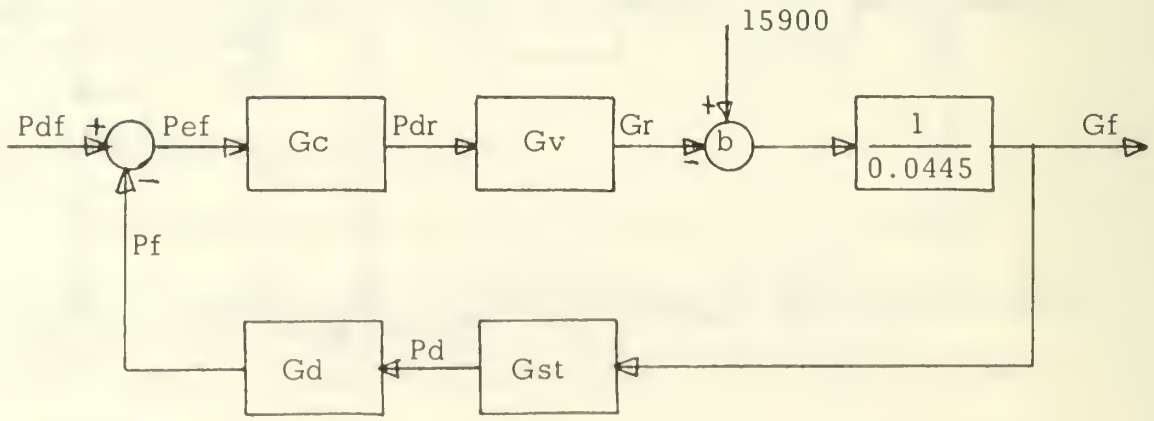

From this block diagram the characteristic equation was calculated as:

$$GcGvGdGst - 1.0445 = 0 \qquad (5)$$

When the numbers given by the report of NBTL for the indicated transfer functions were substituted in (5), the negative sign persisted giving a characteristic equation of mixed signs which indicates roots in the right half plane; therefore, a change in sign was indicated in the fuel oil flow loop in order to have a potentially stable system. This change of sign was made in the return valve, since an increase in the demand signal produces an increase in the control signal, Pdr, and the return valve should produce a decrease in the amount of fuel oil returned in order to meet the demand of more oil to be burned. For this action to take place the sign of the return valve has to be negative.

Making the indicated change in sign a parameter plane was plotted, Figure 12, for the resulting characteristic equation, and as before assuming the controller gains as variables, in this case:

$$Gamma + Delta / s$$

The values given for these parameters in the NBTL report are:

$$Gamma = 2.82$$

$$Delta = 0.392$$

It is clearly seen in Figure 12 that for the values given above, operating point marked "A" in the figure, the system is unstable because the operating point is outside of the region covered by the zeta curves, meaning that the complex roots are in the right half part of the s-plane. To make the system stable, the gain Gamma could be

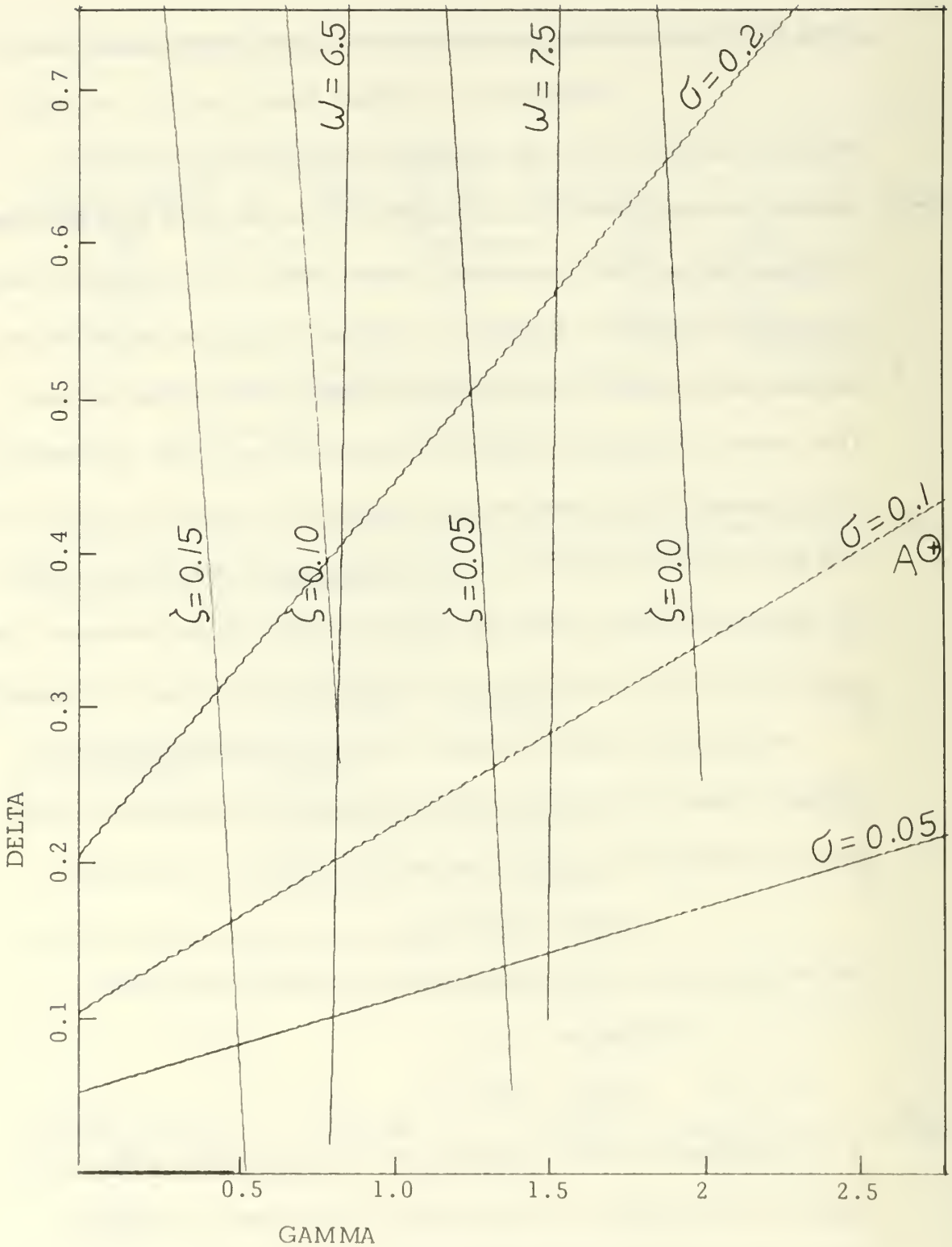

FIGURE 12. PARAMETER PLANE
FUEL OIL LOOP

reduced to a value less than 2.0, keeping Delta constant at the given value. A simulation was done with Gamma set to 1.8, which showed that the system was stable for this parameter setting, as expected. The author of this thesis, thinking that such a gross instability as the one exhibited by this loop could not have been unnoticed by the authors of the NBTL report, through personal letter brought his findings to their attention. As a result, the transfer function for the control valve was changed as explained in Appendix A.

Using, for the fuel oil return control valve, the transfer function indicated in Appendix A, a parameter plane was plotted, Figure 14. Again in this figure, the point marked "B" is for the parameters as given in NBTL report; the roots for this operating point are at zeta $\doteq$ 0.145, Wn $\doteq$ 4.93 and sigma $\doteq$ 0.075.

The fuel oil control system has a fast response, as seen on Figure 13, with some oscillation in the transient. If, as before, it is desired to eliminate this oscillation, the zeta of the complex roots should be increased, which is obtained by decreasing Gamma. But as Gamma is decreased, with Delta constant, Wn decreases and sigma does not change appreciably, and since the real root is so close to the origin, no significant change is obtained in the response. Therefore, it is necessary to move the real root farther from the origin, so as to make it less dominant, and let the variation in zeta have some noticeable effect. To increase sigma, Delta should be increased, so

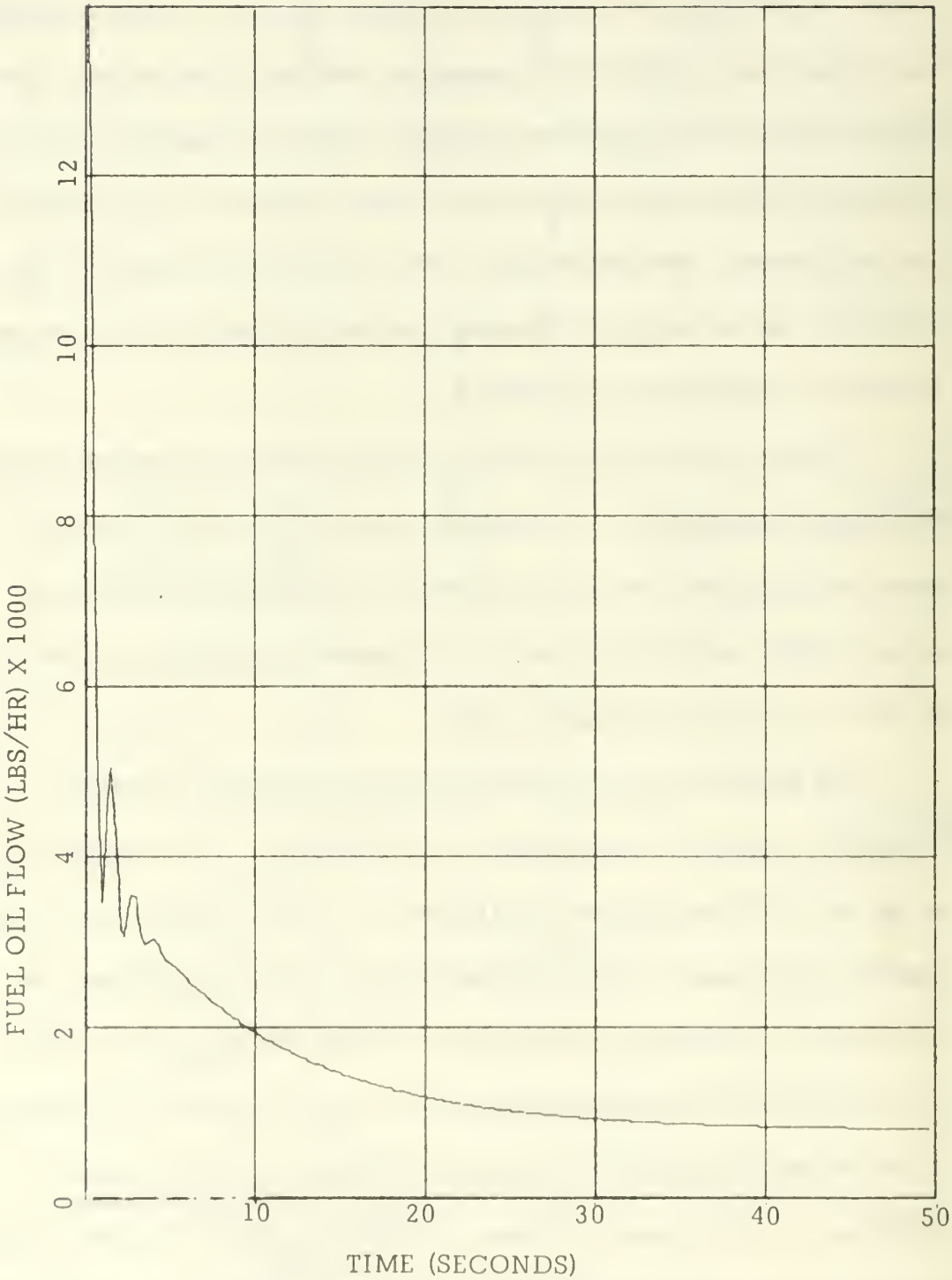

FIGURE 13. UNIT STEP RESPONSE
FUEL OIL LOOP. GAMMA = 2.82, DELTA = 0.392

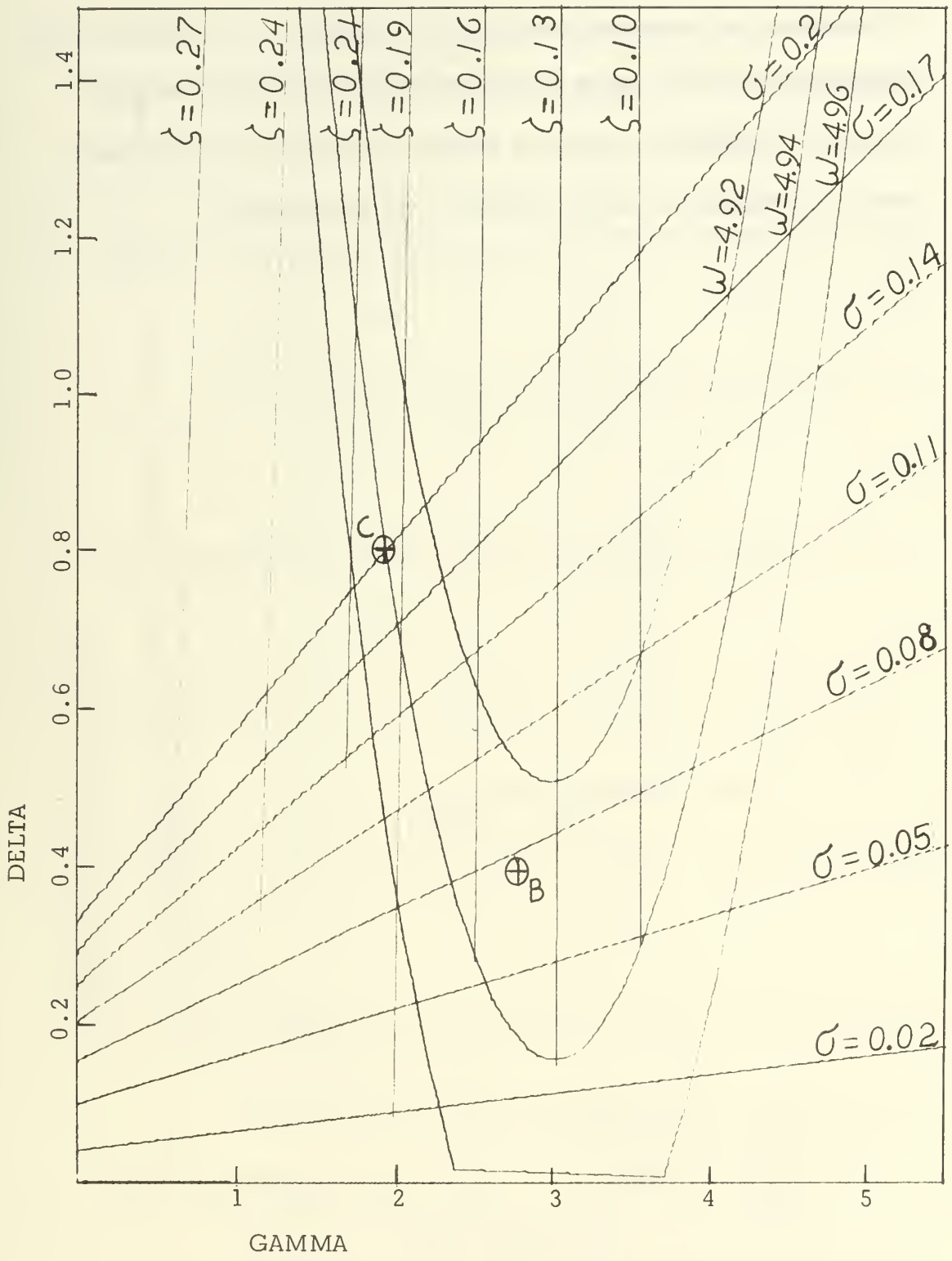

FIGURE 14. PARAMETER PLANE
FUEL OIL LOOP (CORRECTED DYNAMICS)

by choosing an operating point like "C" (Gamma - 2.0, Delta = 0.8) where zeta $\doteq$ 0.195, Wn $\doteq$ 4.94, and sigma $\doteq$ 0.185, a unit step response is obtained, shown in Figure 15, that is somewhat faster than the original and less oscillatory, as was desired.

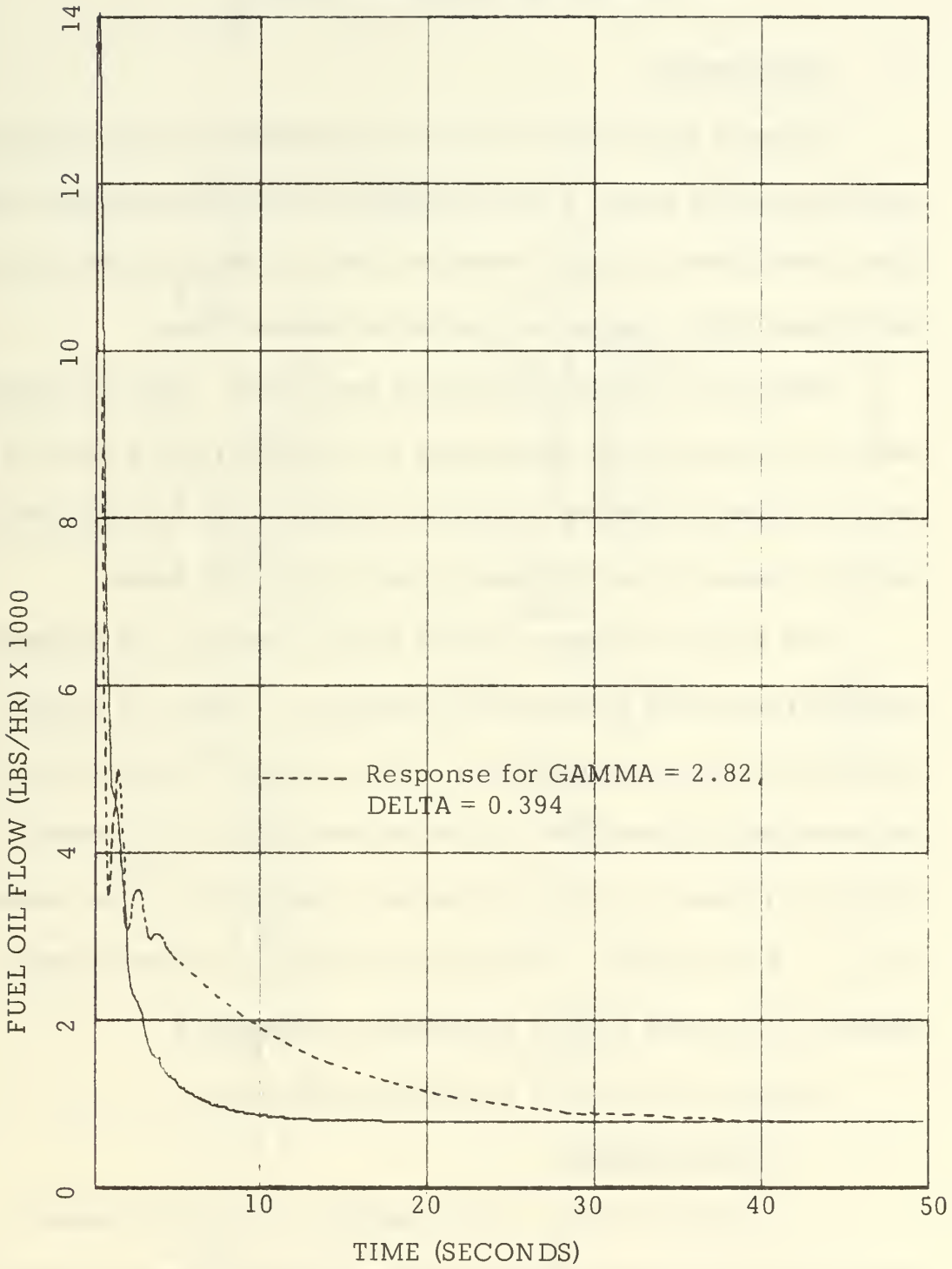

FIGURE 15. UNIT STEP RESPONSE
FUEL OIL LOOP. GAMMA = 2.0, DELTA = 0.80

IV. WATER LEVEL CONTROL SYSTEM

A. DESCRIPTION

The water level control system is a conventional three-element feedwater control system. It is designed so that the proportional plus reset control mode regulates feedwater flow rate while simultaneously maintaining boiler drum water level at the desired value.

Figure 16 is the block diagram of the system. It has as demand index the signal Pgs that corresponds to the steam flow; it also has as input the signal Pl that represents the water level of the boiler drum, and the reference signal Prl which is set to 15 psi as before.

Note that the transfer functions of the controller, the feedwater regulating valve and the water flow transmitter in Figure 16 are different from those given in Figure 1. The changes for the dynamics of the controller and water flow transmitter were made in accordance to Appendix B, where the thesis referenced in paragraph c of the appendix is Ref. 5 of this thesis. The correction for the gain of the feedwater regulating valve was made in accordance to Appendix B.

The system consists of the following elements:

1. The Controller

This controller, also a Standatrol, is a three-element controller which compares the signal Psw' from the steam flow-water flow differential relay, and the drum water level signal, Pl, against the reference signal Prl and develops a pneumatic control signal, Pdw, sent to the feedwater regulating valve.

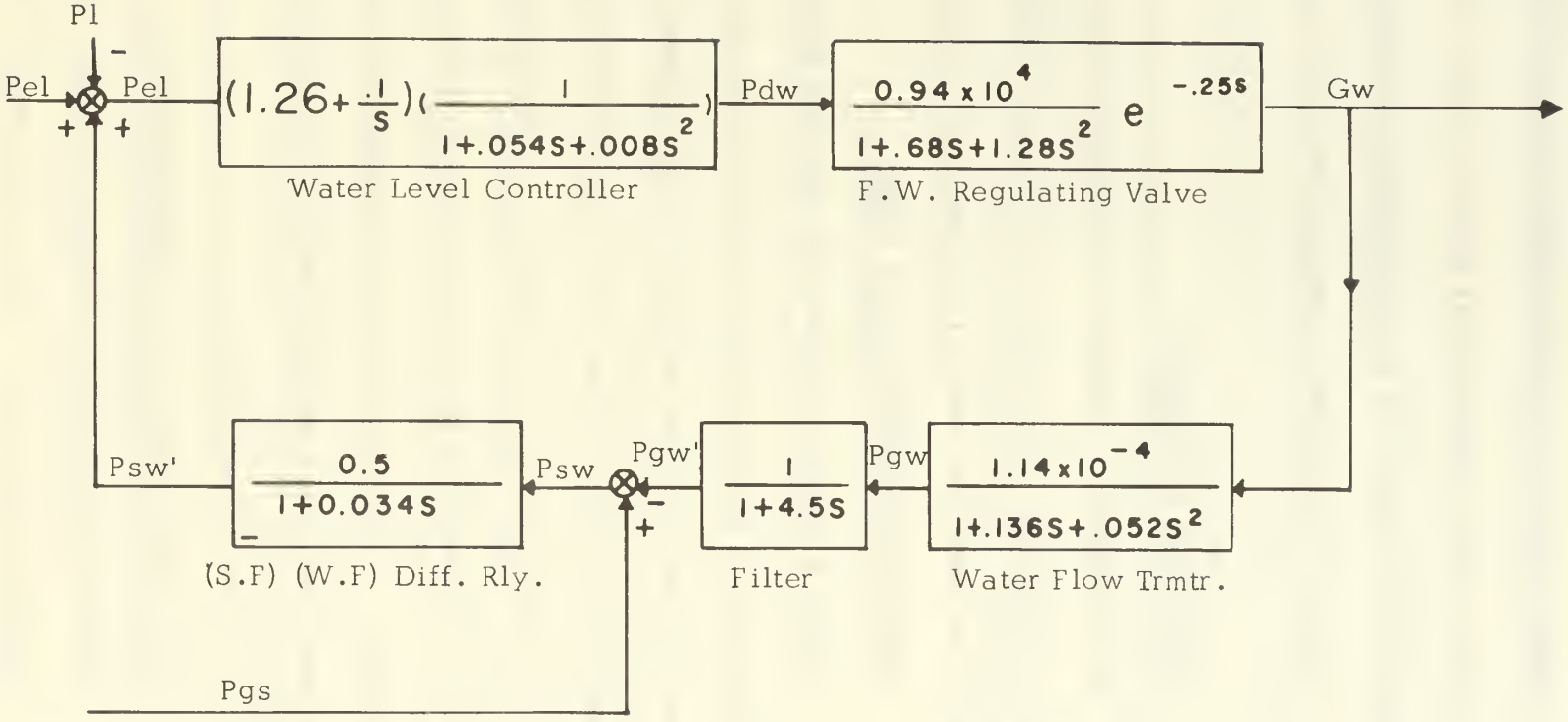

FIGURE 16
BLOCK DIAGRAM. WATER LEVEL CONTROL SYSTEM

2. Feedwater Regulating Valve

This valve is a typical V-ported positioner equipped diaphragm control valve, which has as input the control signal Pdw and according to this signal the valve controls the amount of feedwater flow, Gw. The time delay shown represents the sticking of the valve stem.

3. Water Flow Transmitter

This transmitter measures the differential pressure related to the flow of feedwater, Gw, across an orifice and develops a pneumatic loading pressure Pgw, which is proportional to the feedwater flow.

4. Water Flow Feedback Signal Filter

This is a needle valve-volume tank that serves the function of an R-C filter in the feedwater flow feedback loop, and is designed to attenuate the control system response to high-frequency components in the measured water flow signal, Pgs. The fact that this filter appears in the feedback portion of the loop causes a loop response similar to that obtained with proportional plus derivative response in the forward path. This in turn means that adjustment of the filter natural frequency will produce significant effects on the dynamic characteristics of the closed loop.

5. Steam Flow - Water Flow Differential Relay

This relay subtracts the pneumatic signal, Psw', output of the filter, from the signal Pgs, output of the steam flow transmitter,

and develops a pneumatic signal, Psw', which is linearly proportional to this difference; the output of the relay is sent to the water level controller.

B. ANALYSIS AND SIMULATION

Figure 17 is the step response of the water loop with the parameters and transfer functions as given in the block diagram, Figure 16. As before a parameter plane study was made to attempt the improvement of the loop step response.

Figure 18 is the parameter plane plot for the loop made by defining the gains of the controller as:

$$\text{LAMBDA} + \text{RHO}/S$$

where, as given in Figure 16, Lambda = 1.26, Rho = 0.10, and operating point marked "B" for which zeta $\doteq$ 0.21, Wn $\doteq$ 0.828 and sigma $\doteq$ 0.033. The parameter plane for this loop has certain resemblance with the one for the oil loop, with the major difference that the complex roots are much closer to the origin in the present case making the loop more oscillatory. Then to damp the oscillation, zeta should increase or Lambda decrease which will also increase Wn; by increasing Rho, sigma is increased. The overall result of these adjustments is the transient response shown in Figure 19 made for Lambda = 0.5, Rho = 0.2, and it is seen that the response is faster and less oscillatory.

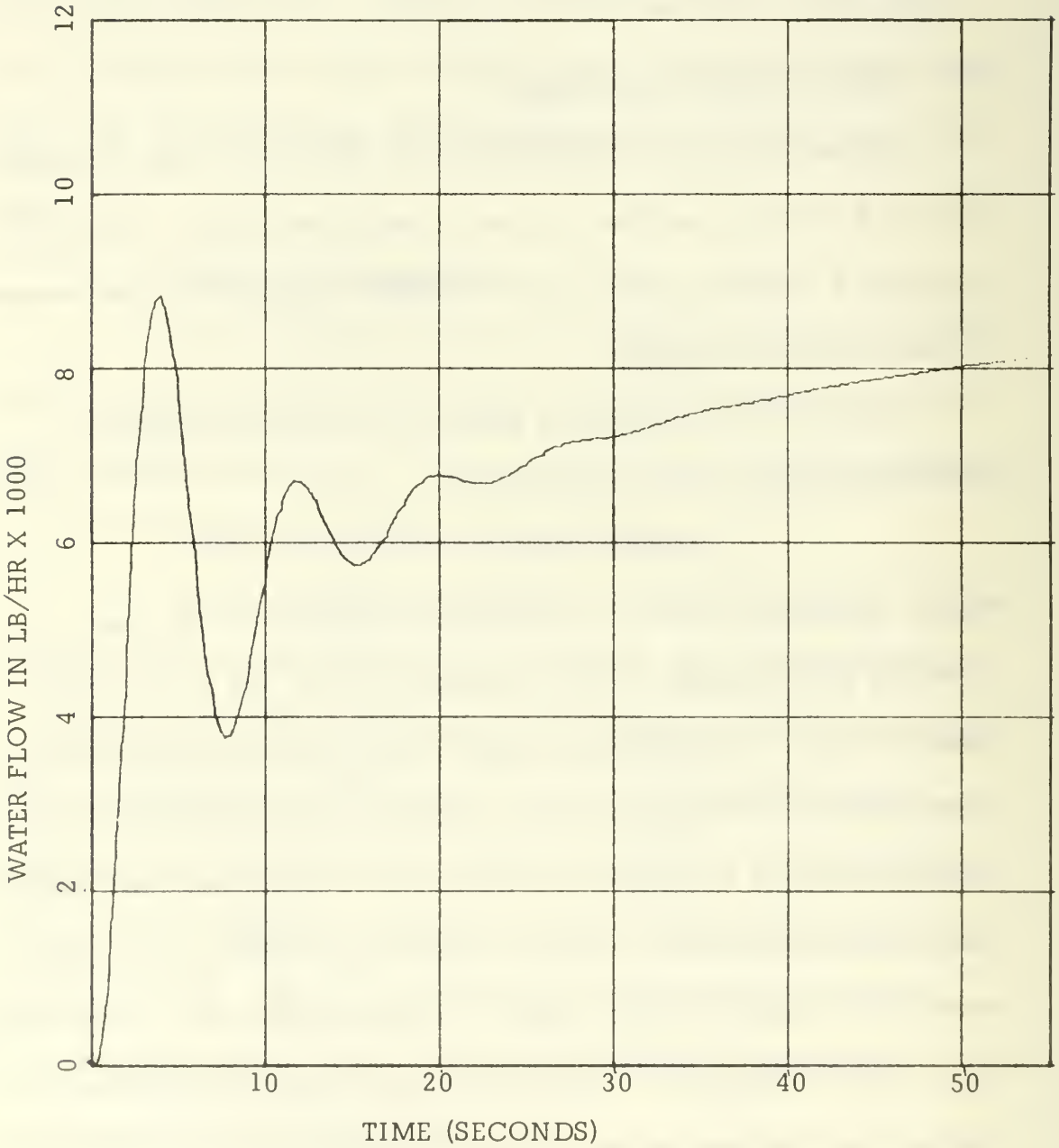

FIGURE 17. UNIT STEP RESPONSE
WATER LEVEL LOOP. LAMBDA = 1.26, RHO = 0.10

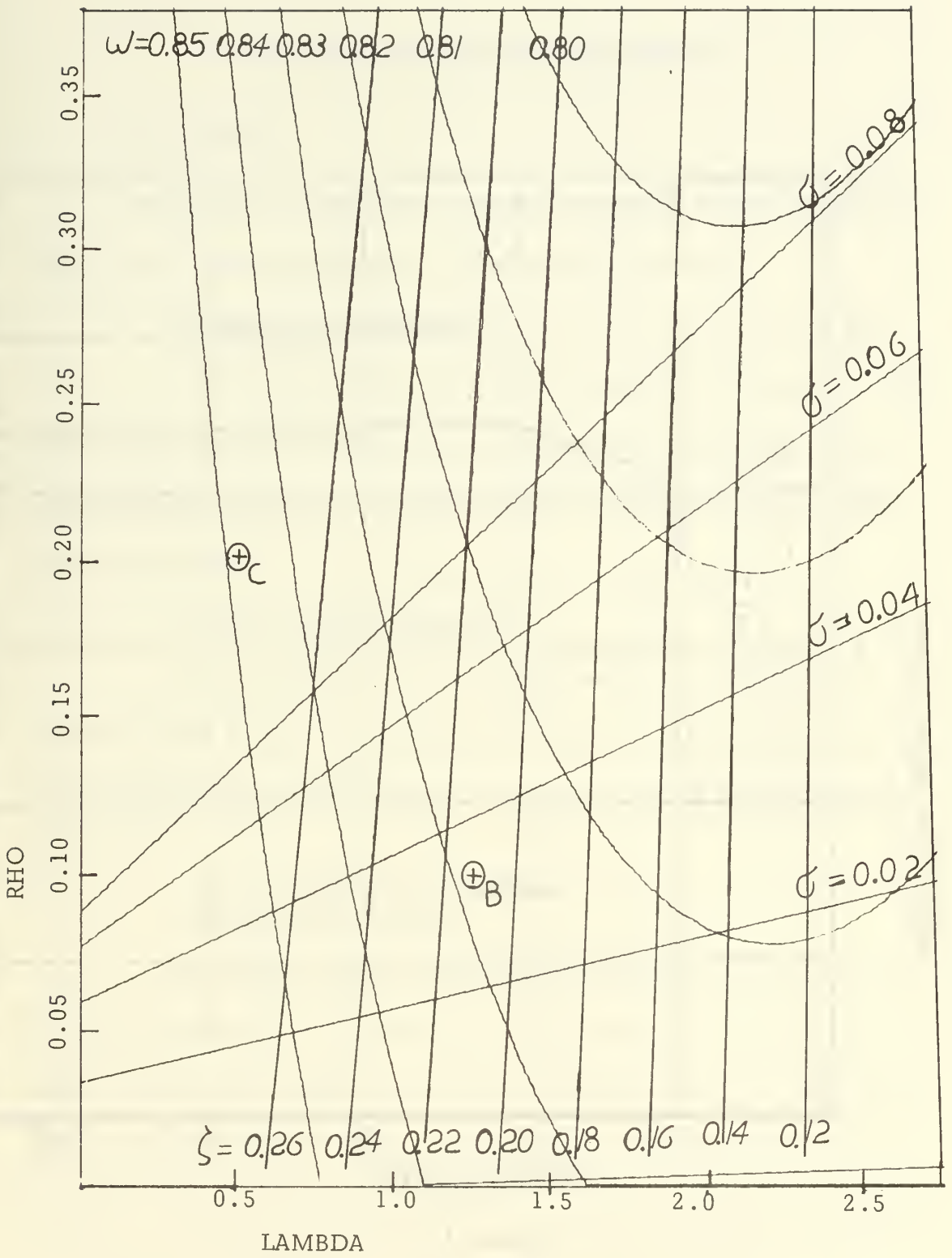

FIGURE 18. PARAMETER PLANE
WATER LEVEL CONTROL LOOP

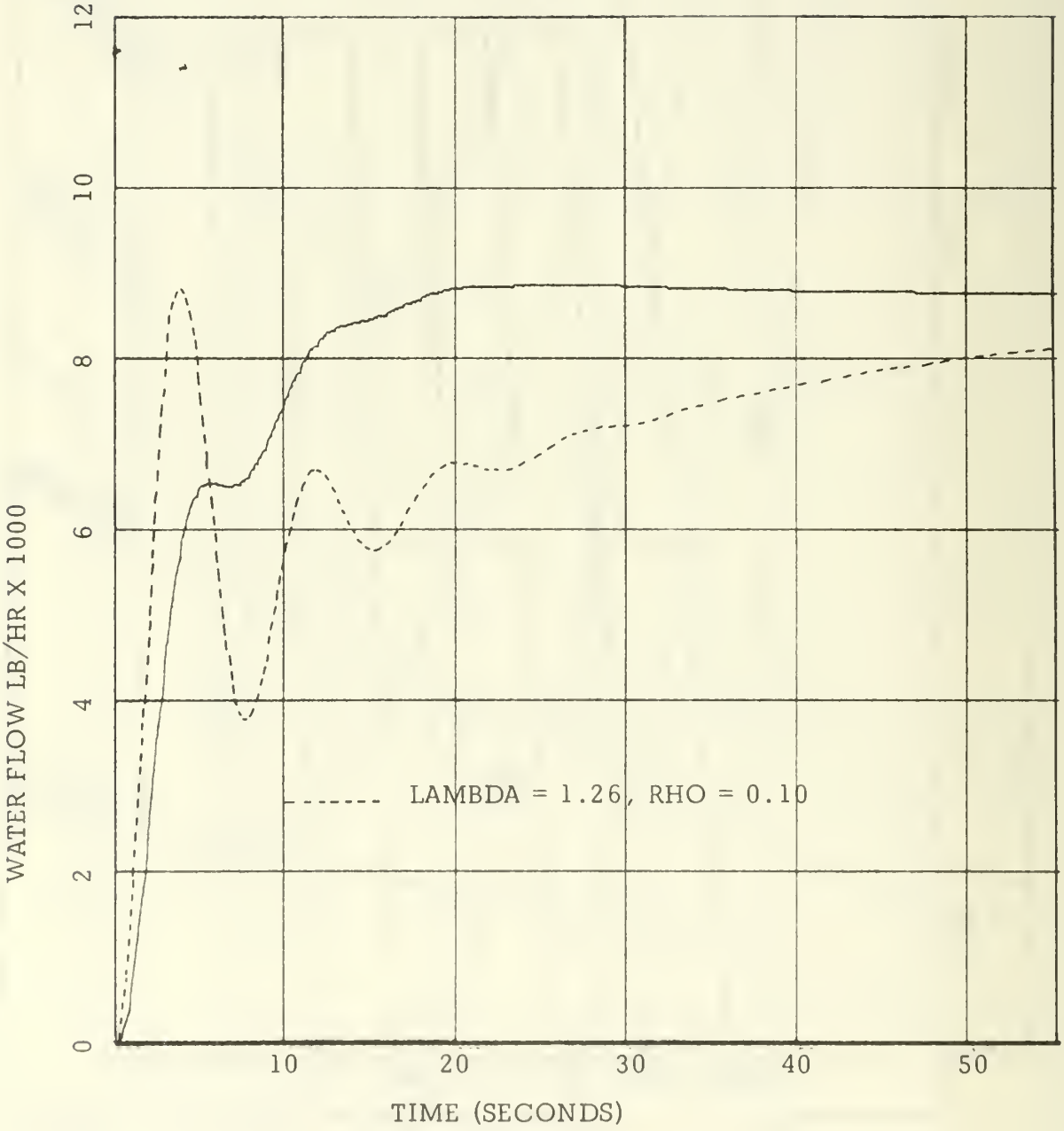

Figure 19

UNIT STEP RESPONSE WATER LEVEL CONTROL LOOP
LAMBDA = 0.50, RHO = 0.20

V. SIMULATION OF COMPLETE SYSTEM

A. DESCRIPTION

The complete boiler control system consists, in addition to the already described components, of the following ones:

1. Steam Flow Transmitter

This transmitter is identical to that of the water flow. The input is the load, Gs, steam flow; its output is proportional to the steam flow and is sent to the water level control loop and the steam pressure controller.

2. Steam Pressure Controller

This instrument is a summing device that performs the operation KPep + Pgs, and the output is the control signal Pm, that is the input to the air loop, which is sent also to the signal selector relay.

3. Signal Selector Relay

This relay selects the smaller of the two signals: Pm, from the steam pressure controller, and Pbg from the air loop, and sends it as demand index, to the fuel oil control loop. The reason for this is that the quantity of fuel oil supplied to the boiler furnace, in this way, can never be excessive for the amount of air flow measured by the air flow transmitter. In this manner, smoking is presented under conditions of rapidly increasing boiler load.

4. Main Propulsion Steam Generator

The steam generator was modeled by the NBTL [1] by simulating triangular pulses for the steam flow, the fuel oil flow and the feedwater flow, and measuring the response of steam drum pressure and water level to these forcing triangular pulses. As a result the steam generator was represented by a total of seven parallel transfer functions, three representing the dynamic behaviour of the steam pressure due to disturbances in steam flow, fuel oil flow and feedwater flow respectively, and four representing the dynamic behaviour of the water level to the same disturbances. As explained in Ref. 1, the response of the water level due to steam flow disturbances was separated in two parallel transfer functions, one attributable to the mass balance integration, since the boiler water level integrates at a rate proportional to the steam flow - water flow difference, the other attributable to the boiler water level "shrink and swell".

5. Water Level Transmitter

This a bellows type inverse acting differential pressure transmitter. It is designed to measure and transmit differential head pressure between water level in the boiler drum and a reference column of condensate connected into the steam space above the water level in the steam drum; the steady state calibration curve changes one psi for each one inch of boiler level change. The output, P1, is sent to the water level controller.

6. Superheater Pressure Transmitter

Measures the superheater outlet pressure and produces an output, Pp, between 3 and 27 psi which is compared against the reference signal Prp, set at 15 psi, and the difference is the input to the steam pressure controller.

7. Superheater

The pressure drop across the superheater was represented as a linear function, based on the derivatives of the pressure drop curves evaluated at the two load conditions. In reality these pressure differentials vary with the square of the steam flow, and this fact is taken into account for the simulation of part VI of this thesis.

B. SIMULATION

The system was modeled by NBTL, as illustrated in Figure 1, at two load conditions, the cruising condition (Gs = 56000 lb/hr) and the 90% of full power (Gs = 152000 lbs/hr). No data was found concerning the behaviour of the actual boiler to small perturbations of the load around the two conditions given, to be compared with the results of this simulation; therefore, a forcing function was chosen similar to the one used in Ref. 5 so that a comparison could be made, at least, of two different simulation methods for the same system.

1. Increasing Steam Load Condition

For the condition of increasing load, a positive ramp was used for Gs. When the steam load on the boiler increases, the initial

effect is a decrease in superheater outlet pressure. As the pressure decreases, the output signal of the steam pressure transmitter decreases, causing a corresponding increase in the output signal from the steam pressure controller.

The increasing signal from the steam pressure controller represents an increased signal of air demand. Since the air demand signal increases, the signal of air flow is less than the signal of air demand, and the air flow controller transmits an increased correcting signal. The increased signal pressure, in turn, increases blower speed and opens the forced draft dampers to increase air flow across the boiler air registers.

On increasing the boiler load, the signal of air flow is less than the signal of boiler load; therefore, the signal of air flow is transmitted by the minimum signal selector relay as the minimum of the two signal pressures.

As air flow across the air registers increases, the increased flow is sensed by the air flow transmitter which sends an increasing signal through the control circuit to increase air loading to the fuel oil pressure control valve. The increased loading on the diaphragm of the fuel oil control valve closes off the valve to increase the oil pressure in the fuel oil return line which increases the flow of oil to the burners to the amount required for optimum combustion.

When the firing rate of the boiler has been increased to the level required to restore superheater outlet pressure to set point,

the combustion control system remains at the steady-state condition until again disturbed by variations in boiler load.

a. Cruising Condition Response

The load perturbation used for this condition and shown in Figure 20A was as follows: the steam flow was set initially at 56000 lb/hr and held for 60 seconds, so that all variables of the system reach steady-state condition; then it was ramped to 59000 lb/hr in five seconds and held at that value for fifty seconds. The responses were recorded as follows:

(1) Water Level Response. Figure 20B, where it is seen that a peak of 0.19 inches is reached in 19 seconds and then the level approaches zero again.

(2) Superheater Outlet Pressure Response. Figure 20C. It has a minimum of -4.32 psi reached in 10 seconds after the perturbation was applied and then it approaches the steady state which is seen to be about one psi above 1200 psi.

(3) Air Flow Response. Figure 20D. It goes from 19.1% to 20.6% following the ramp with an overshoot that has a peak of 21% at 7 seconds, and then approaches the steady state.

(4) Fuel Oil Flow Response. Figure 20E. This response is similar in shape to the air flow response, has an overshoot that peaks at 17 seconds with a value of 4400 lb/hr and then settles to a value of 4230 lb/hr in a much faster rate than the air flow does.

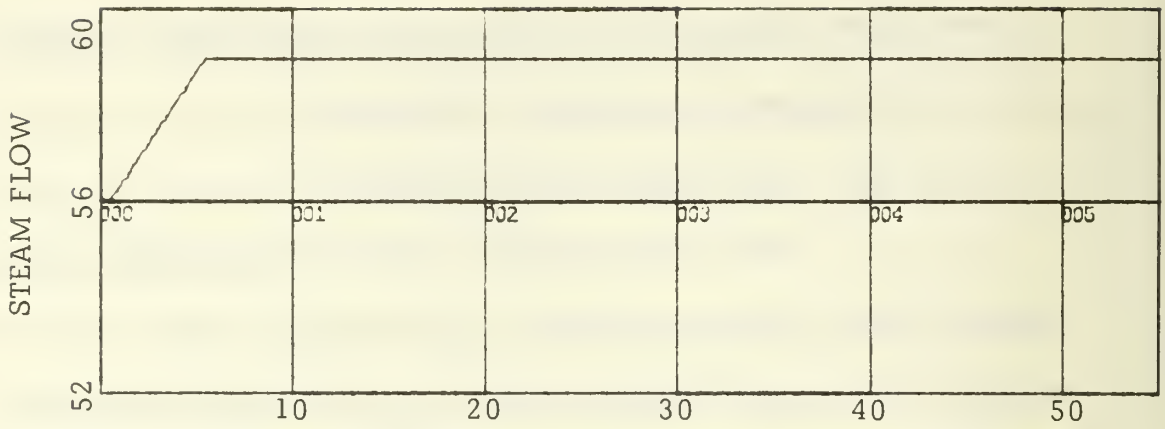

Figure 20A. Increasing Steam Load (Cruising)
Given in lb/hr x 1000.0, vs. time in seconds

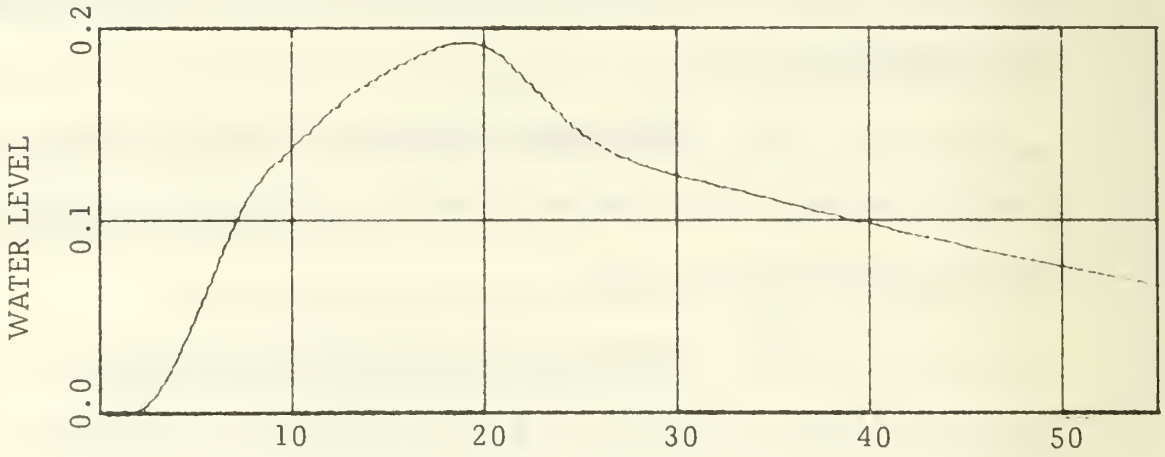

Figure 20B. Water Level Response
Given in inches of variation from set level, vs. time in seconds

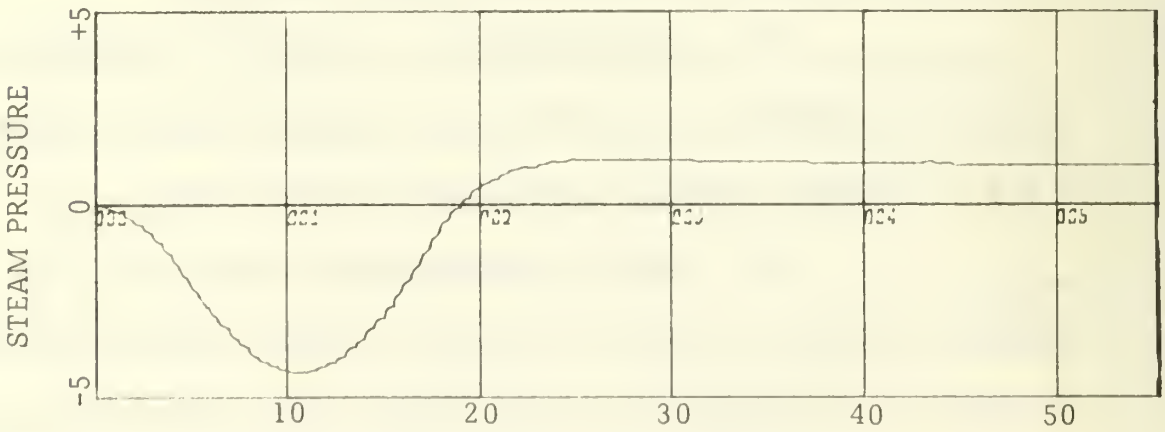

Figure 20C. Steam Pressure Response
Given in psi variation from 1200psi, vs. time in seconds

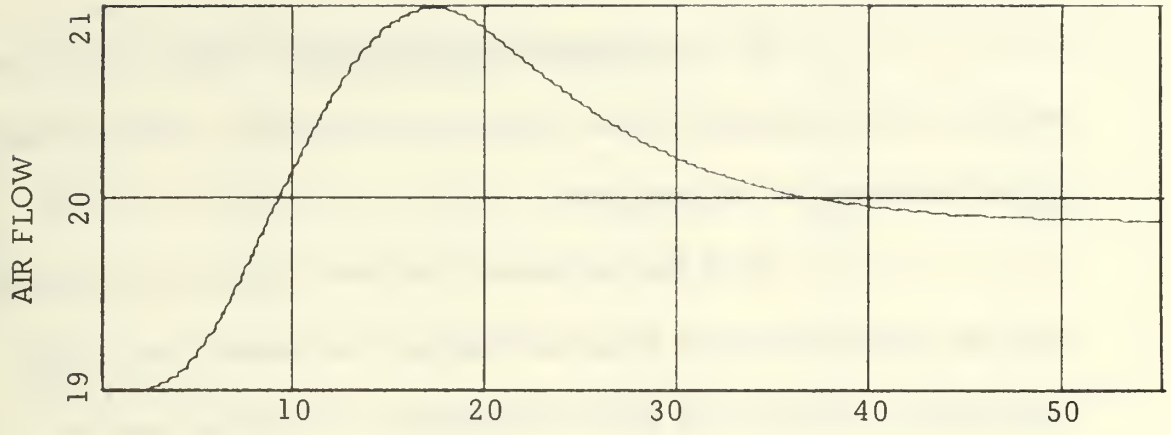

Figure 20D. Air Flow Response
Given in percentage of full power, vs. time in seconds

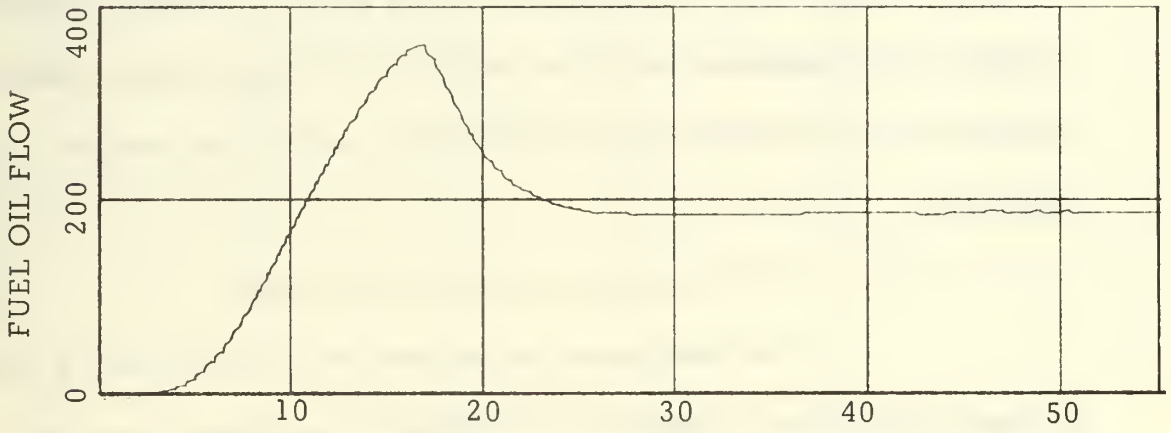

Figure 20E. Fuel Oil Flow Response, vs. time in seconds
Given in lb/hr variation from steady state value (4040.)

Figure 20F. Feedwater Flow Response, vs. time in seconds
Given in lb/hr x 1000.0 variation from 56000.0 lb/hr

(5) Feedwater Flow Response. Figure 20F. The response of the feedwater flow is seen to be very slow, and oscillatory at the beginning of the transient.

All of the responses specified above are in agreement with the type of response expected from the discussion given at the beginning of this part. If these responses are compared with the corresponding ones given in Ref. 5, it is seen that they are very similar; the shapes of the responses are the same. The major difference is noted in the feedwater response, which for the case of this simulation is much less oscillatory, due to the changes made in the transfer functions.

b. 90% Full Power Condition Responses

The load perturbation used for this condition is shown in Figure 21A and was simulated as follows: after steady state was reached for 152000 lbs/hr of steam flow it was ramped to 160000 lbs/hr in five seconds and held for fifty seconds. The corresponding responses were:

(1) Water Level Response. Figure 21B. It shows a peak of 0.38 inches at 16 seconds after the perturbation was applied, and then the steady state is approached.

(2) Superheater Outlet Pressure Response. Figure 21C. It has a minimum of -3.8 psi at 8 seconds, and then goes to the steady state in about 9 seconds more, with a small error of less than one psi above 1200 psi.

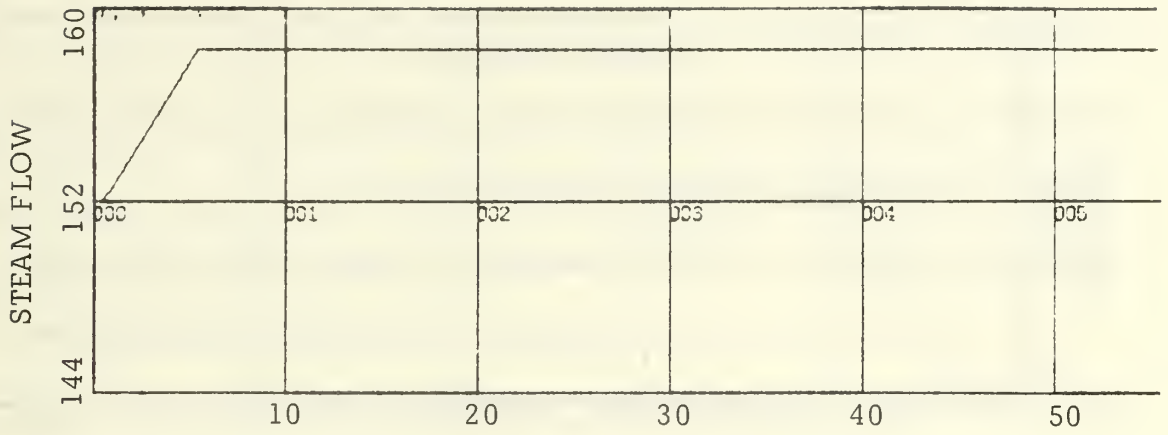

Figure 21A. Increasing steam load (90% FP)
Given in lb/hr x 1000.0, vs. time in seconds

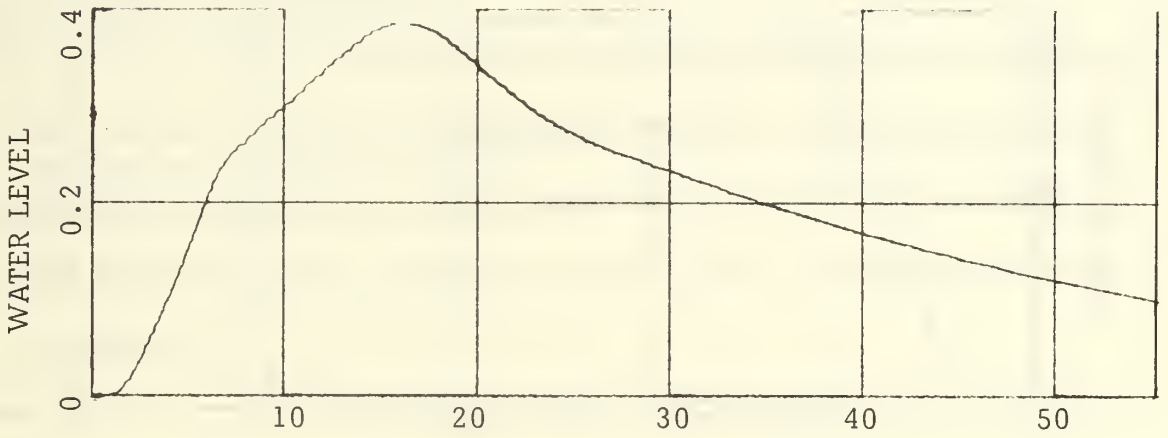

Figure 21B. Water Level Response, vs. time in seconds
Given in inches of variation from set level

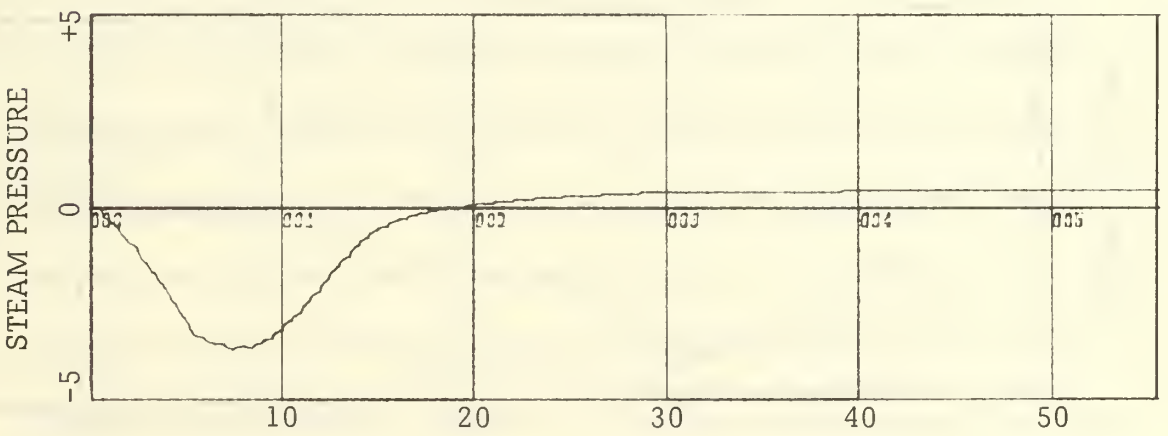

Figure 21C. Steam Pressure Response, vs. time in seconds
Given in psi variation from steady state

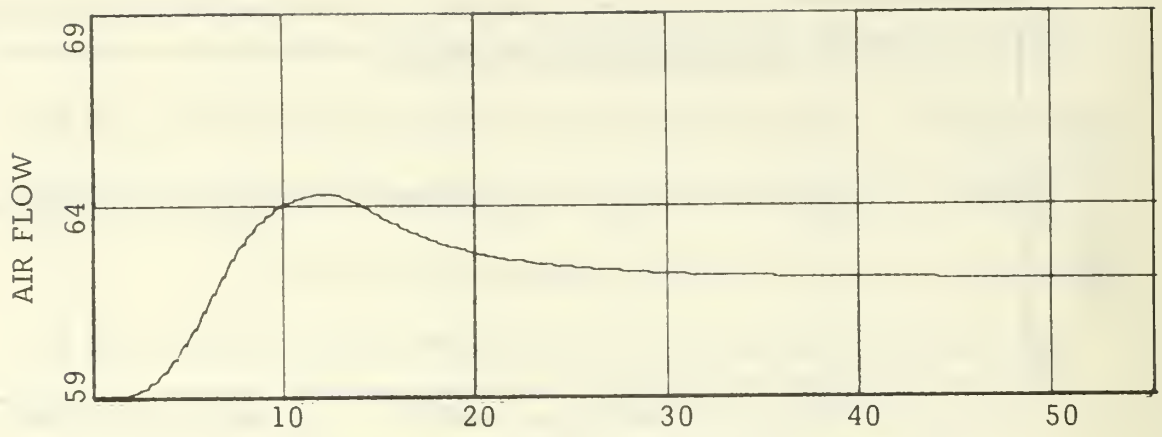

Figure 21D. Air Flow Response, vs. time in seconds
Given in percentage of full power

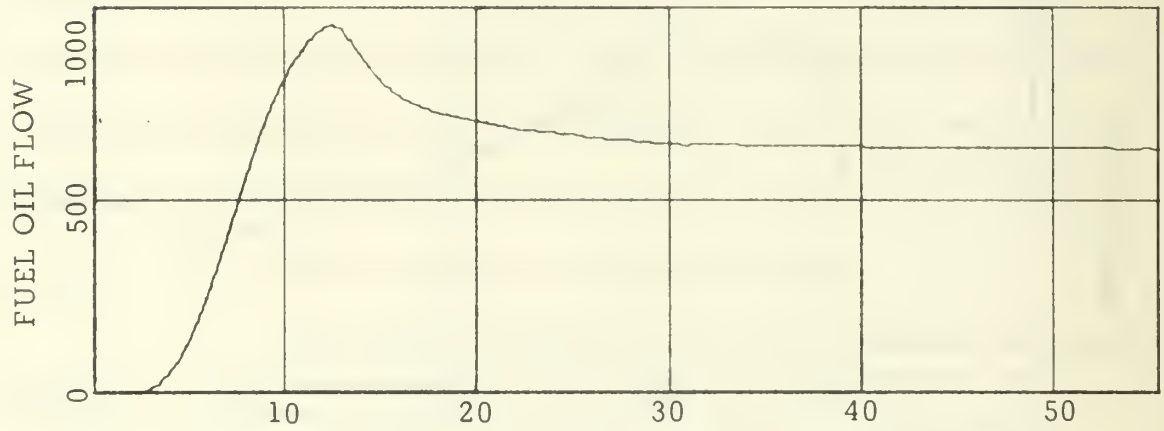

Figure 21E. Fuel Oil Response, vs. time in seconds
Given in lb/hr from steady state (12480 lb/hr)

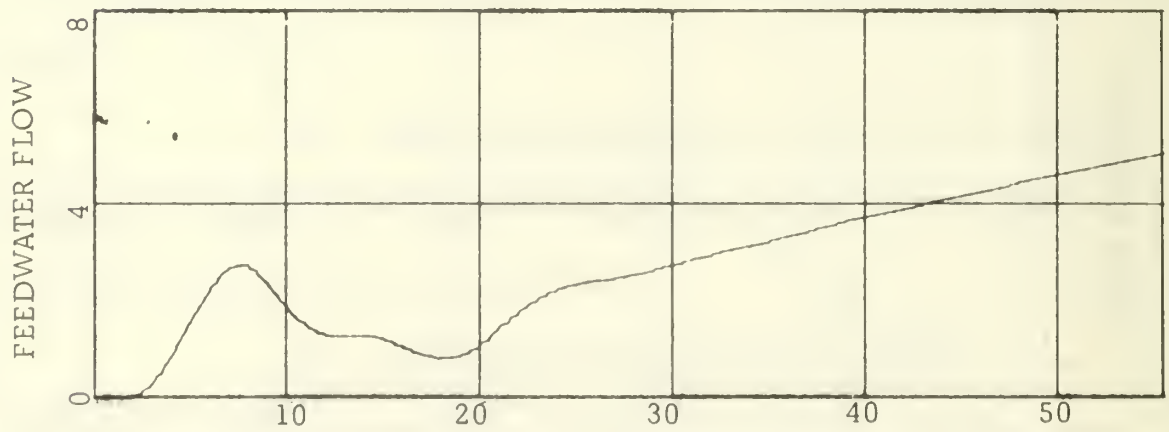

Figure 21F. Feedwater Flow Response, vs. time in seconds
Given in lb/hr x 1000 variation from 152000 lb/hr)

(3) Air Flow Response. Figure 21D. It goes from 59% to 62% in 25 seconds, with an overshoot of 64.2% at 12 seconds.

(4) Fuel Oil Flow Response. Figure 21E. Goes from 12480 lb/hr of fuel oil flow to 13100 lb/hr in about 23 seconds, overshooting to 13440 at 12 seconds.

(5) Feedwater Flow Response. Figure 21F. Very slow to reach steady state and also shows some oscillation at the beginning of the transient.

Comparison of these responses with the corresponding ones of Ref. 5 shows good agreement, with the following noticeable differences: variation in steam pressure is less for this simulation; the feedwater flow is also seen to be much less oscillatory for this simulation.

As was said before these differences are attributable to the corrections made to some of the transfer functions.

2. Decreasing Steam Load Condition

For this condition a negative ramp was used to simulate the load, Gs. When this reduction of steam load occurs an instantaneous increase in superheater outlet pressure takes place. With increasing pressure there is an increasing output signal from the steam pressure transmitter which causes a proportional decreasing signal from the steam pressure controller. This decreasing signal indicates a reduced signal of air demand at the air flow controller. Therefore, the signal of air flow will be greater than the signal of air demand

which causes a correcting decreased signal to be transmitted by the air flow controller. This decreased signal pressure decreases blower speed and closes off the forced draft dampers to reduce combustion air flow to the boilers.

With decreasing boiler load, the boiler load signal to the minimum signal selector relay is instantaneously less than the signal of air flow.

When the boiler load signal is less than the signal of air flow, the minimum signal selector relay immediately transmits the lower boiler load signal to reduce oil flow to the burners.

As the firing rate is adjusted to restore superheater outlet pressure to set point, the automatic combustion control system returns to its steady-state condition until variations in boiler load again cause a change in superheater outlet pressure.

a. Cruising Condition Response

The load perturbation used for this condition is shown in Figure 22A, and was as follows: after steady state was reached by the system at 56000 lb/hr of steam load a negative ramp was applied for five seconds to bring Gs to 53000 lb/hr. The responses were as follows:

(1) Water Level Response. Figure 22B. Has a maximum decrease of 0.185 inches at 11 seconds after the perturbation and then goes to the set level again.

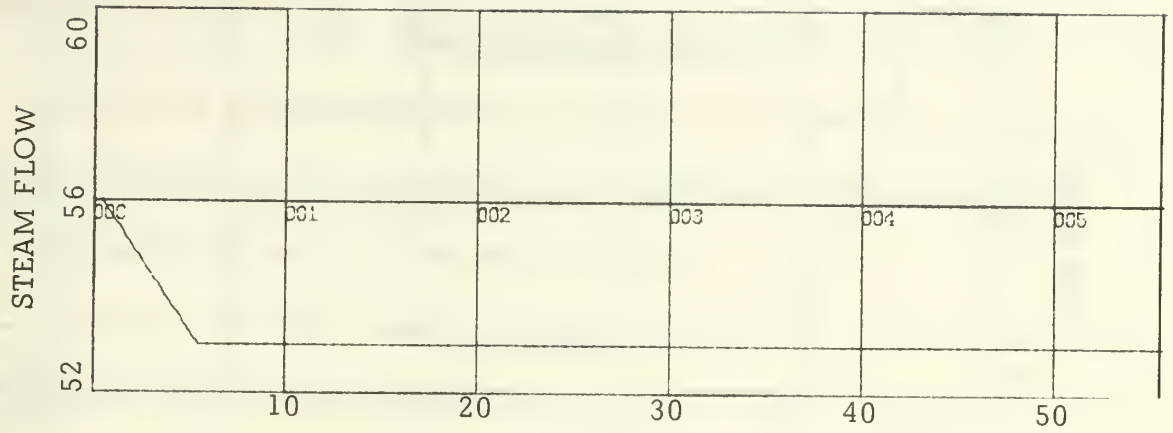

Figure 22A. Decreasing Steam Load (cruising)
Given in lb/hr x 1000, vs. time in seconds

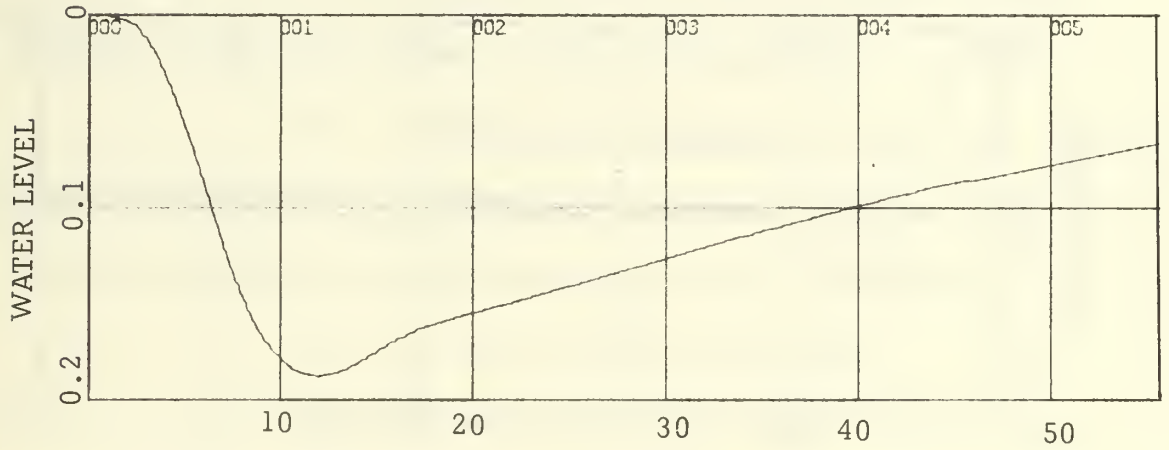

Figure 22B. Water Level Response, vs. time in seconds
Given in inches of variation from set level

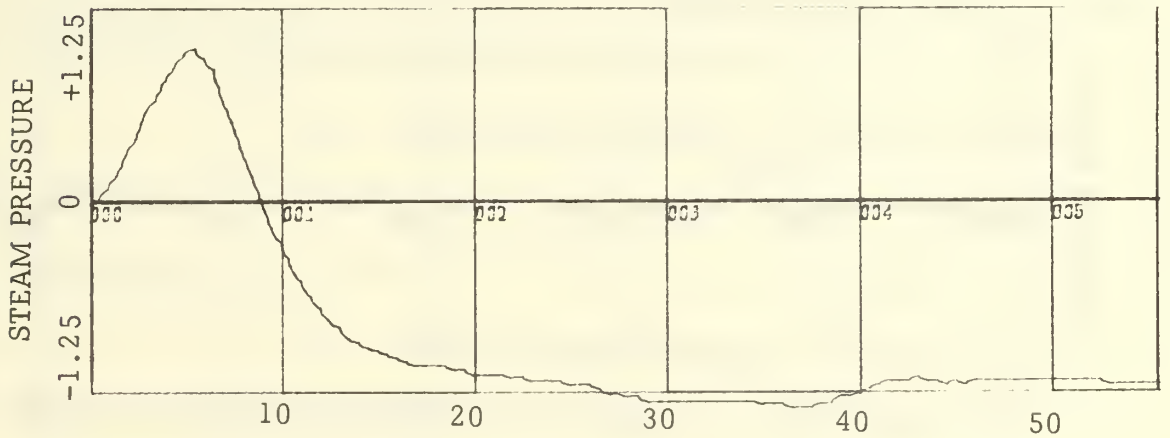

Figure 22C. Steam Pressure Response, vs. time in seconds
Given in psi variation from steady state

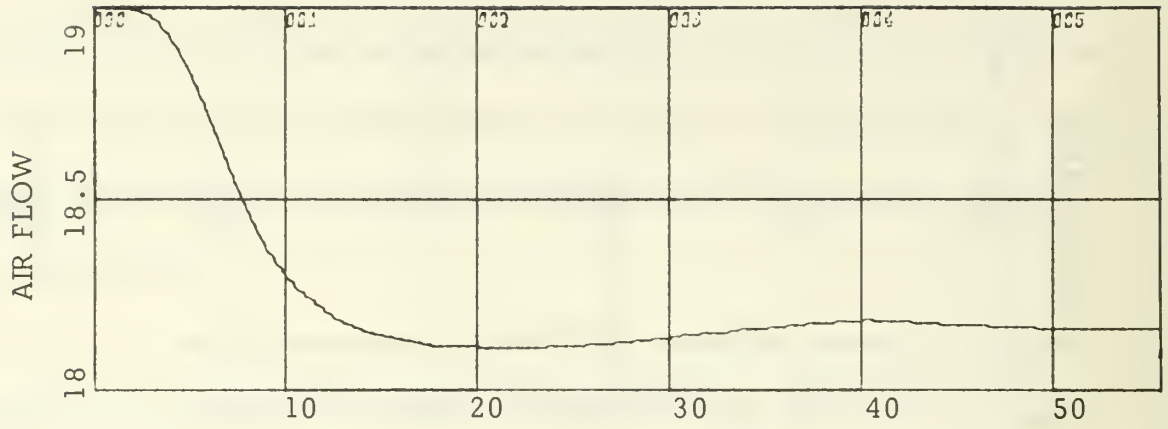

Figure 22D. Air Flow Response, vs. time in seconds
Given in percentage of full power

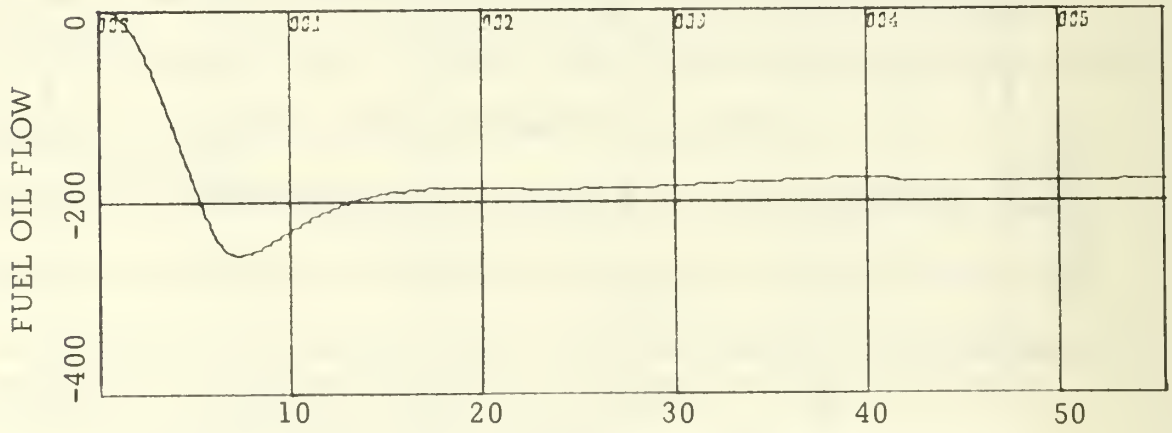

Figure 22E. Fuel Oil Response, vs. time in seconds
Given in lb/hr variation from steady state (4040 lb/hr)

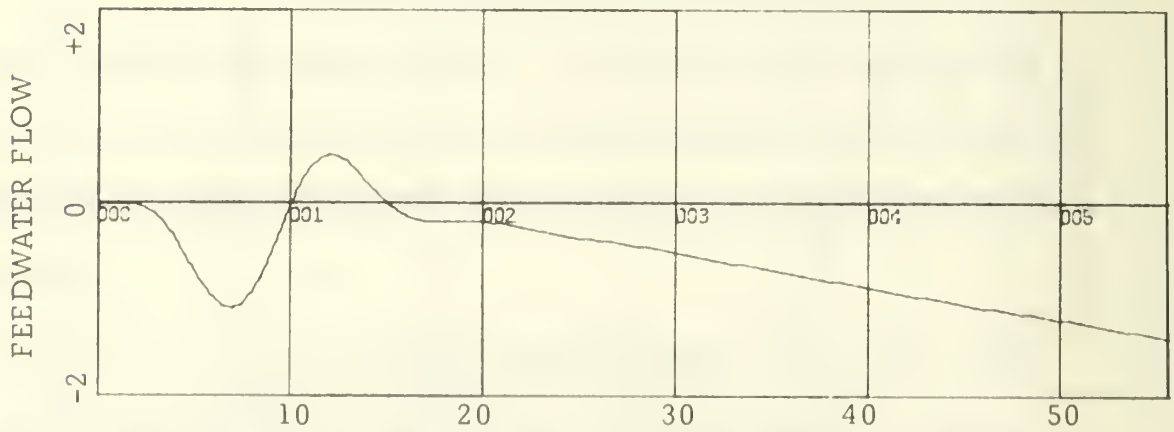

Figure 22F. Feedwater Flow Response, vs. time in seconds
Given in lb/hr x 1000 variation from 56000 lb/hr

(2) Steam Pressure Response. Figure 22C. Initially the pressure increases to about 1 psi above the steady state in five seconds, then decreases to -1.25 psi below the steady state and keeps this value as new steady state.

(3) Air Flow Response. Figure 22D. Varies from 19% to 18.2% in fifteen seconds.

(4) Fuel Oil Flow Response. Figure 22E. Decreases from steady state with a small overshoot at seven seconds after the perturbation and then settles to a value of 3860 lb/hr.

(5) Feedwater Flow Response. Figure 22F. Presents some oscillation during the first fifteen seconds of the response and then decreases steadily to its new steady state value of 53000 lb/hr.

b. 90% Full Power Condition Responses

The load perturbation used, Figure 23A, was, as before, letting the system reach steady state at 152000 lb/hr and then a negative ramp was applied for five seconds to bring the load, Gs, to 144000 lb/hr. The responses were as follows:

(1) Water Level Response. Figure 23B. Shows a minimum of -0.39 inches at 11 seconds and then goes to the set level again.

(2) Steam Pressure Response. Figure 23C. Initially the pressure increases to about 4 psi above steady-state value at 6 seconds, then decreases to its steady-state value in about six seconds more and settles at a value of about one psi below 1200 psi.

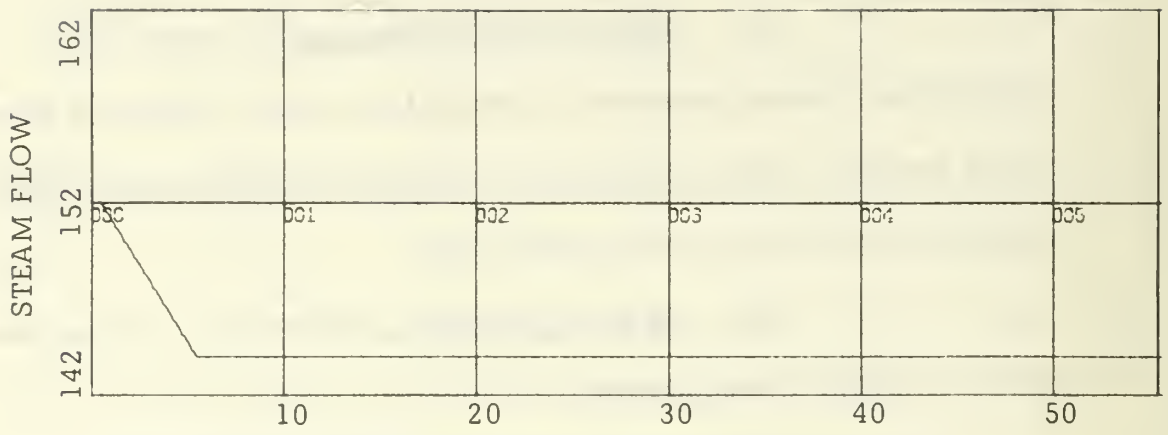

Figure 23A. Decreasing Steam Load (90% FP)
Given in lb/hr x 1000.0, vs. time in seconds

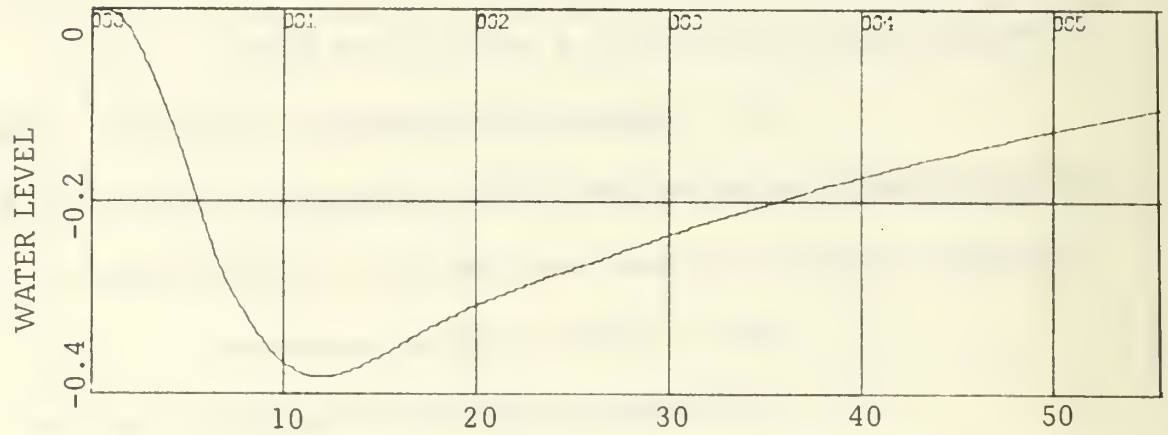

Figure 23B. Water Level Response, vs. time in seconds
Given in inches of variation from set level

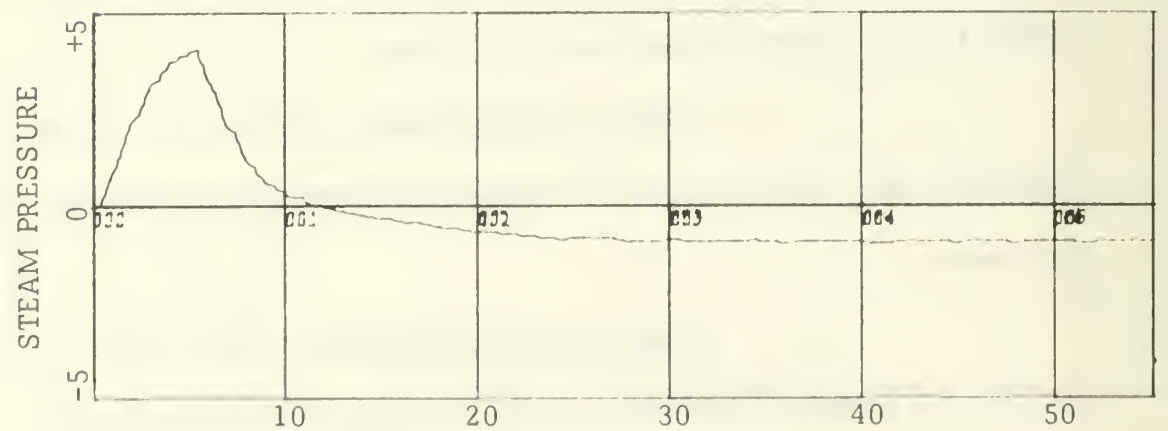

Figure 23C. Steam Pressure Response, vs. time in seconds
Given in psi variation from steady state

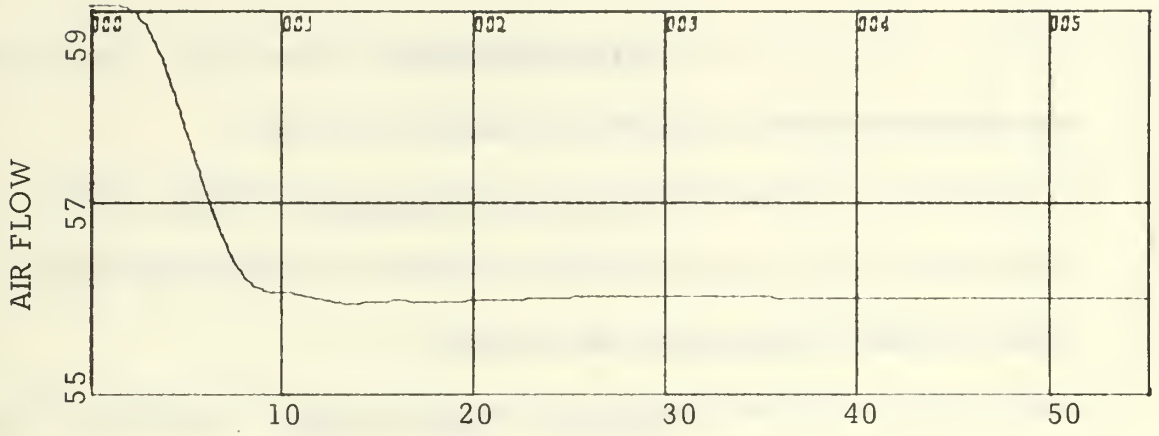

Figure 23D. Air Flow Response, vs. time in seconds
Given in percentage of full power

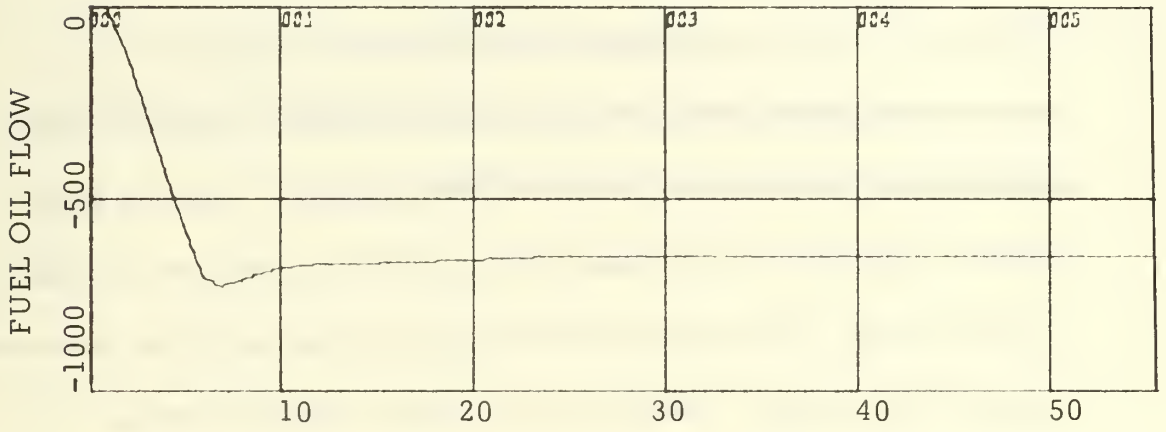

Figure 23E. Fuel Oil Flow Response, vs. time in seconds
Given in lb/hr variation from steady state value (12480 lb/hr)

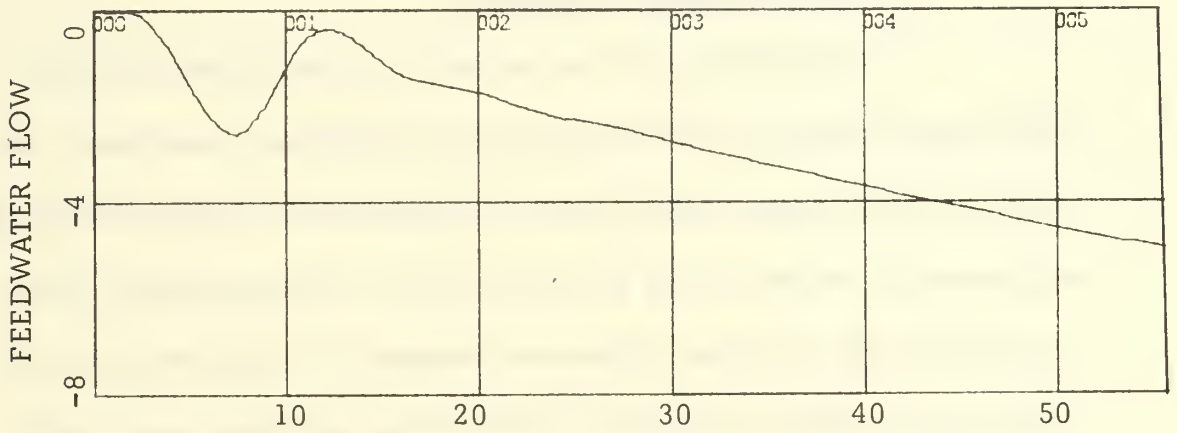

Figure 23F. Feedwater Flow Response, vs. time in seconds
Given in lb/hr x 1000 variation from 152000 lb/hr

(3) Air Flow Response. Figure 23D. Goes in eight seconds from 59.0% to 55.7%, its new steady state.

(4) Fuel Oil Flow Response. Figure 23E. Decreases from steady-state value (12480 lb/hr) to its new steady state (11790 lb/hr) in about 10 seconds.

(5) Feedwater Flow Response. Figure 23F. Again shows oscillation during the beginning of the response and then decreases steadily to its new value of 144000 lbs/hr.

Comparison of the decreasing responses to the corresponding ones of Ref. 5 shows good agreement, with the same exception as before of the feedwater flow response. For the steam pressure response to a decreasing ramp, 90% FP condition, in Figure 7-12(a) of Ref. 5 the steam pressure at the beginning of the response is shown to decrease, which is not consistent with the physical behaviour of steam pressure under decreasing load condition.

3. New Parameters Simulation

The simulation of the system using small perturbations was repeated using as gain settings for the different controllers, the values found in parts II, III, and IV of this thesis. The general shape and values of the responses were very close to those obtained using the original gain settings. The most noticeable change for all of the responses is that the feedwater response was less oscillatory and somewhat faster.

a. Increasing Steam Load

(1) Cruising Condition. Shown in Figures 24A to 24F. Responses are very close to those previously obtained; the feedwater response is less oscillatory.

(2) 90% Full Power Condition. Figures 25A to 25F. Same behaviour as noted for cruising condition; here the feedwater response is noticeable faster than before.

b. Decreasing Steam Load

(1) Cruising Condition. Figures 26A to 26F. Same observations as noted for the increasing load condition.

(2) 90% Full Power Condition. Figures 27A to 27F.

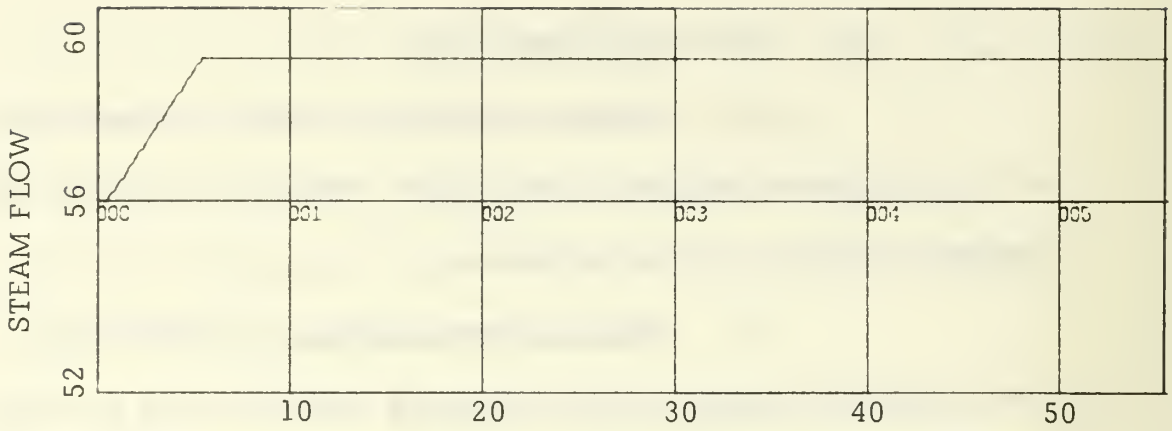

Figure 24A. Increasing Steam Load (cruising)
Given in lb/hr x 1000.0, vs. time in seconds

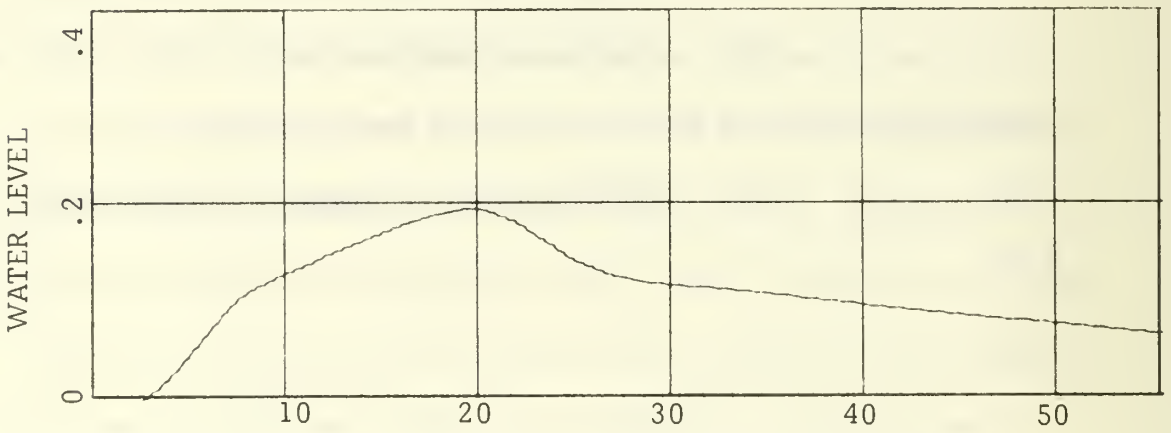

Figure 24B. Water Level Response, vs. time in seconds
Given in inches of variation from set level

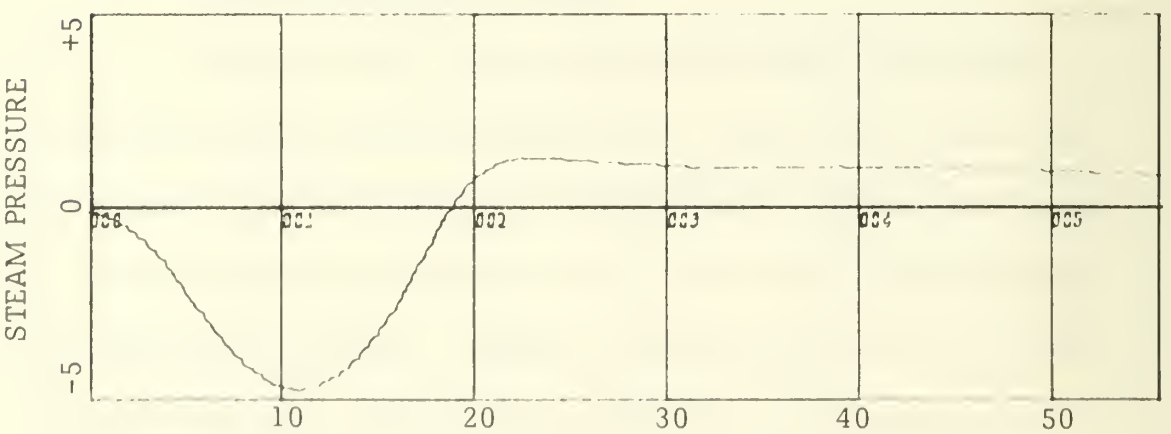

Figure 24C. Steam Pressure Response, vs. time in seconds
Given in psi variation from steady state

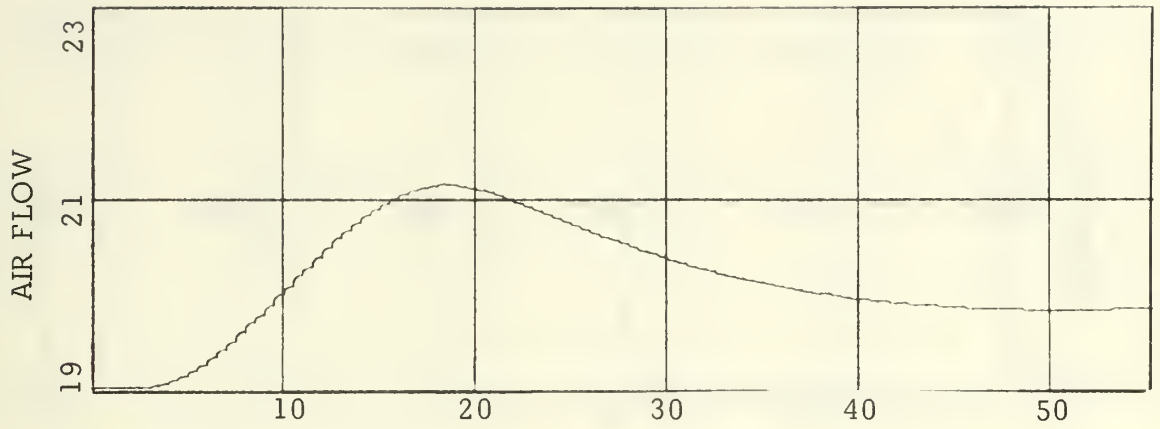

Figure 24D. Air Flow Response, vs. time in seconds
Given in percentage of full power

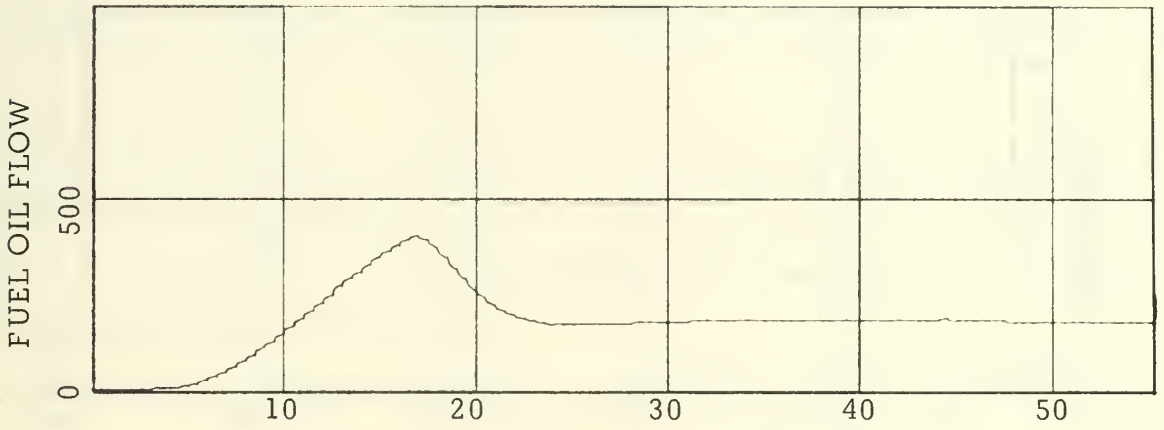

Figure 24E. Fuel Oil Flow Response, vs. time in seconds
Given in lb/hr variation from steady state

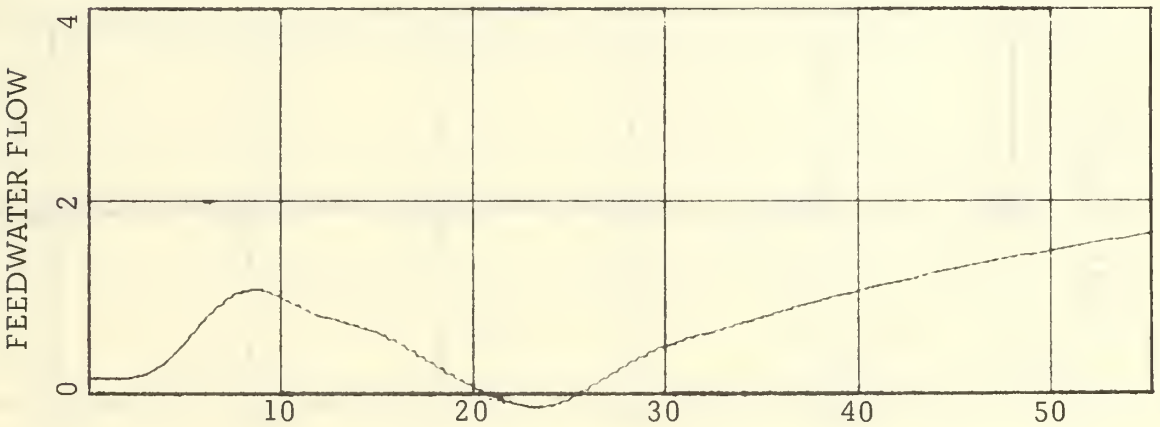

Figure 24F. Feedwater Flow Response, vs. time in seconds
Given in lb/hr x 1000 variation from 56000 lb/hr

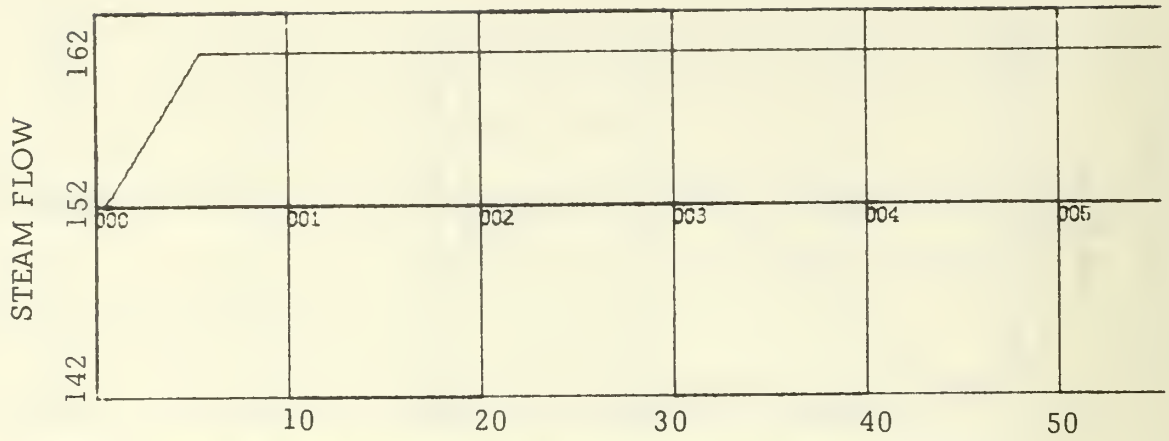

Figure 25A. Increasing Steam Load (90% FP)
Given in lb/hr x 1000.0, vs. time in seconds

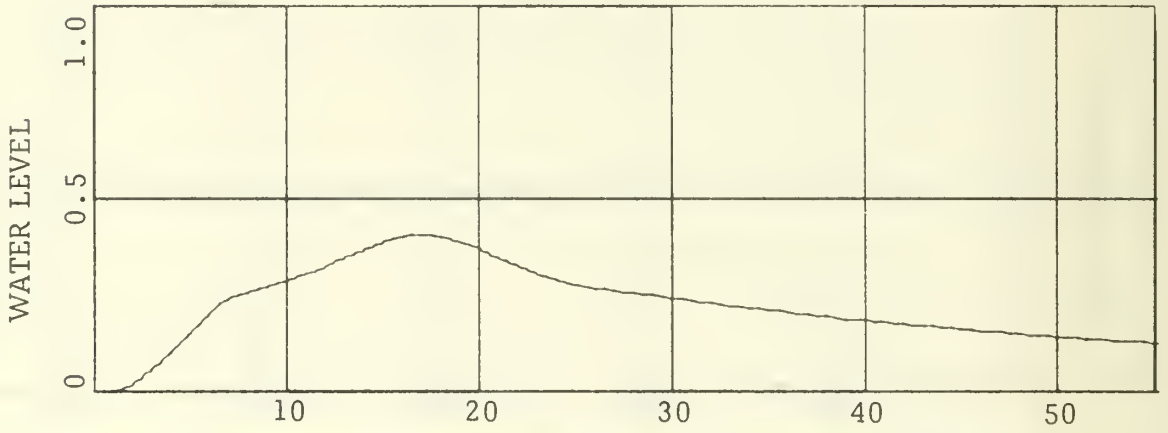

Figure 25B. Water Level Response, vs. time in seconds
Given in inches of variation from set level

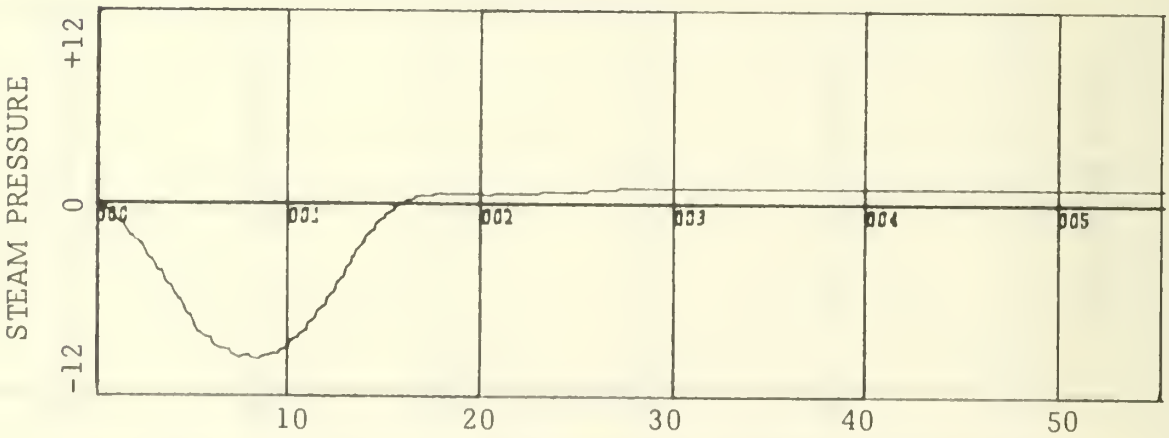

Figure 25C. Steam Pressure Response, vs. time in seconds
Given in psi variation from steady state

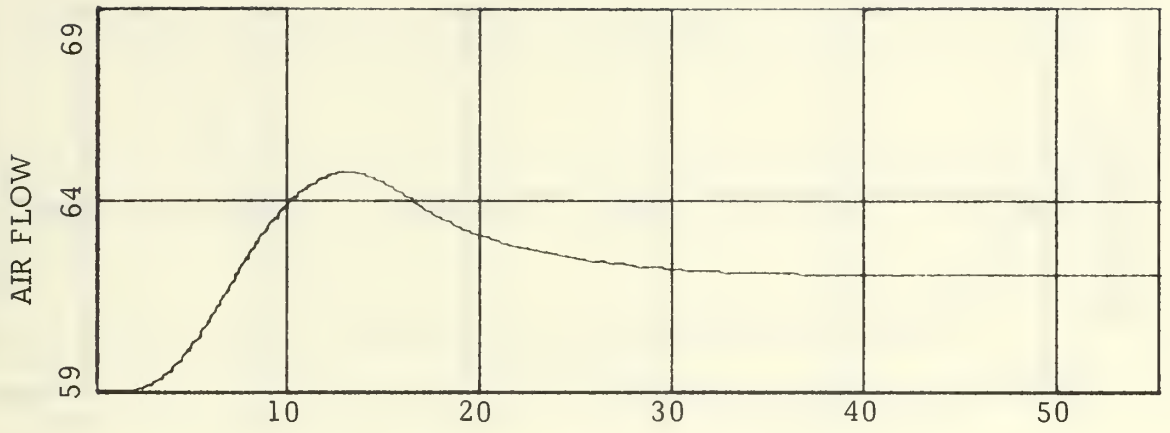

Figure 25D. Air Flow Response, vs. time in seconds
Given in percentage of full power

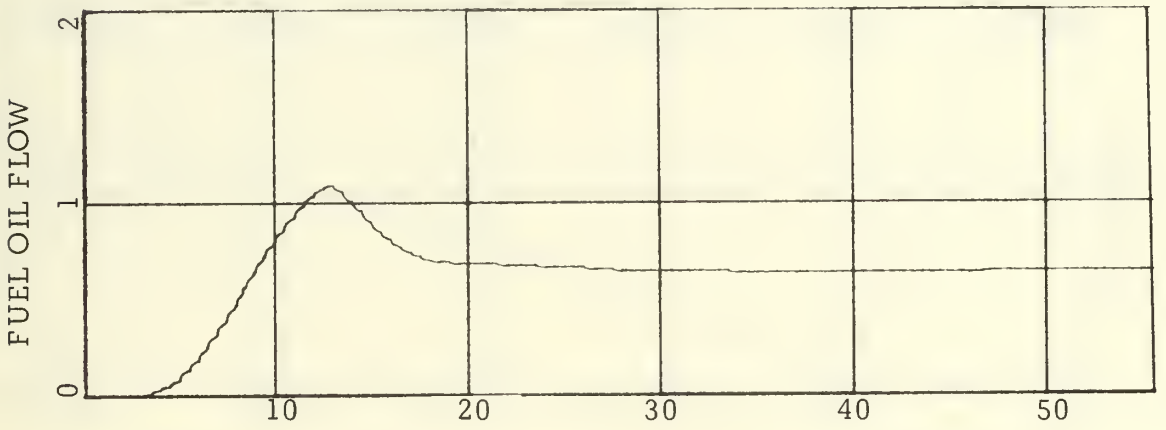

Figure 25E. Fuel Oil Flow Response, vs. time in seconds
Given in lb/hr x 1000 variation from steady state

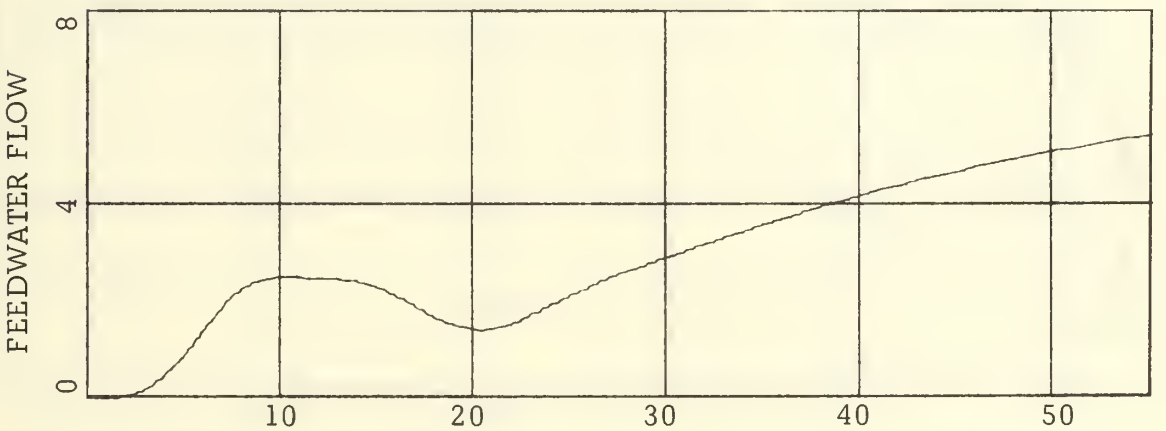

Figure 25F. Feedwater Flow Response, vs. time in seconds
Given in lb/hr x 1000 variation from 152000 lb/hr

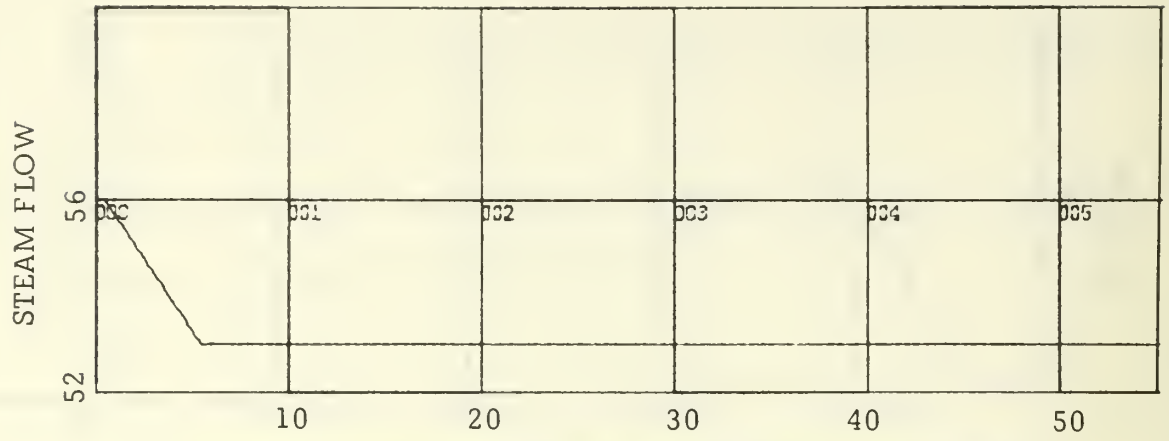

Figure 26A. Decreasing Steam Load (cruising)
Given in lb/hr x 1000.0, vs. time in seconds

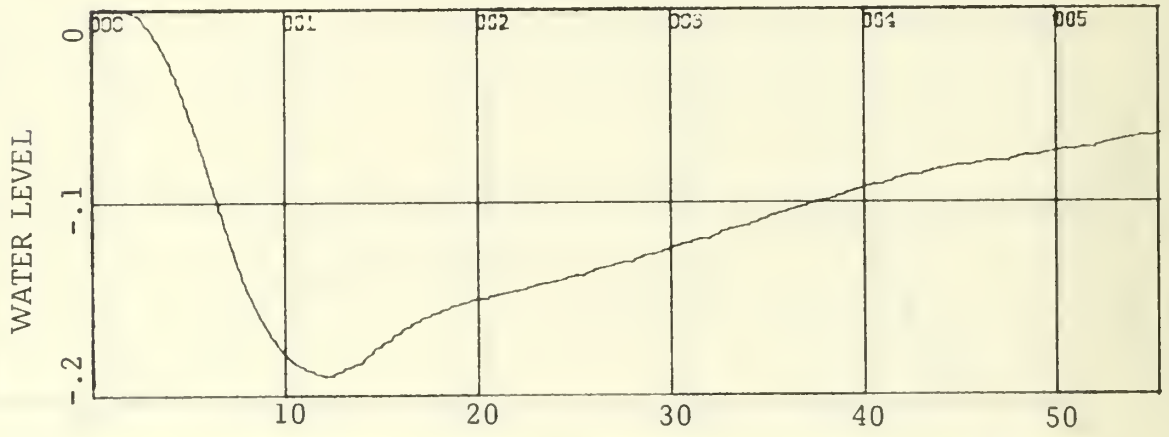

Figure 26B. Water Level Response, vs. time in seconds
Given in inches of variation from set level

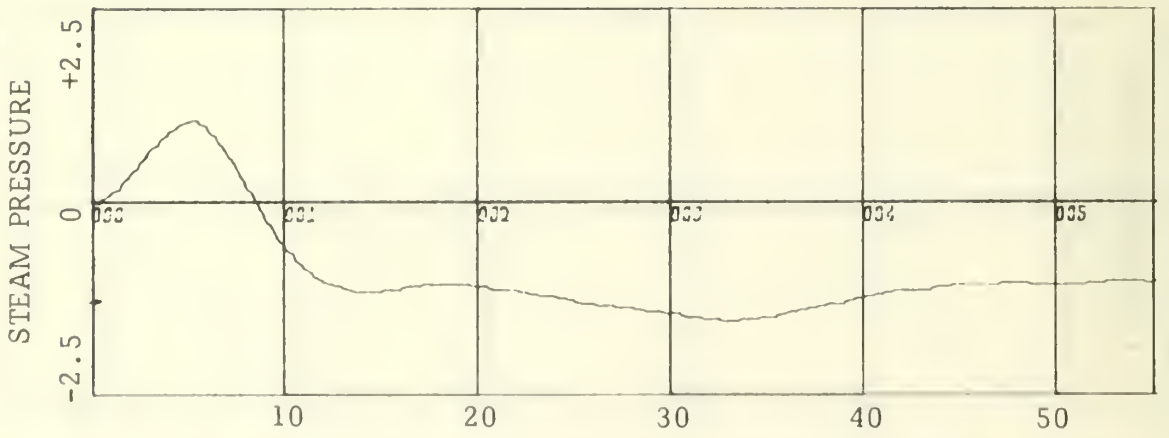

Figure 26C. Steam Pressure Response, vs. time in seconds
Given in psi variation from steady state

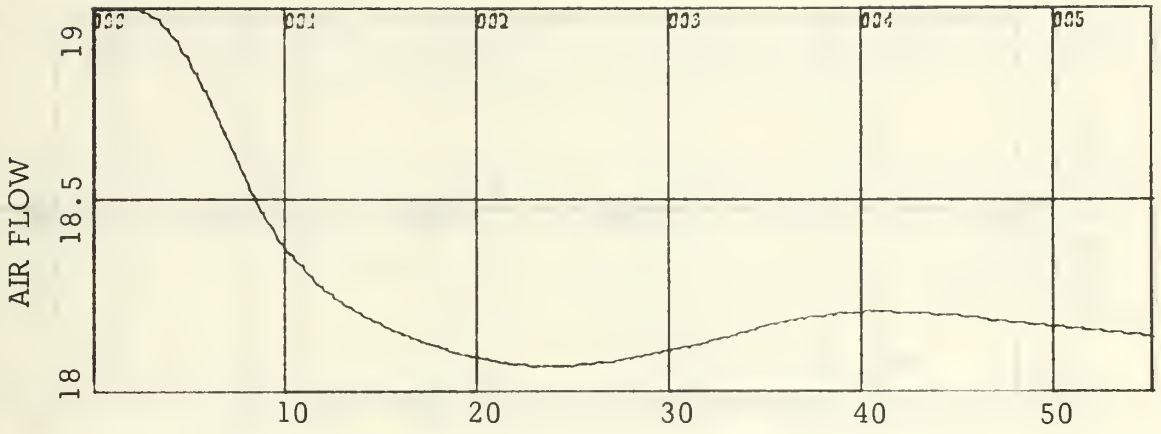

Figure 26D. Air Flow Response, vs. time in seconds
Given in percentage of full power

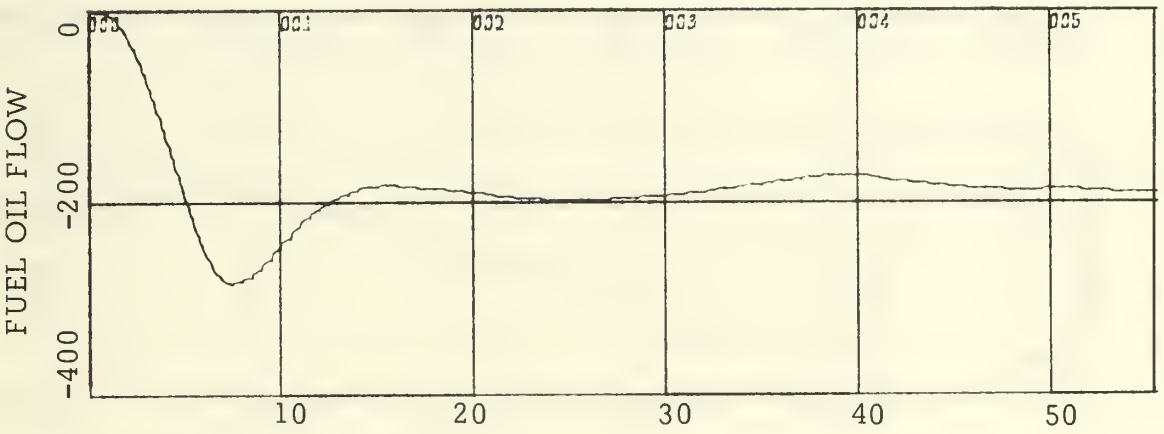

Figure 26E. Fuel Oil Flow Response, vs. time in seconds
Given in lb/hr variation from steady state

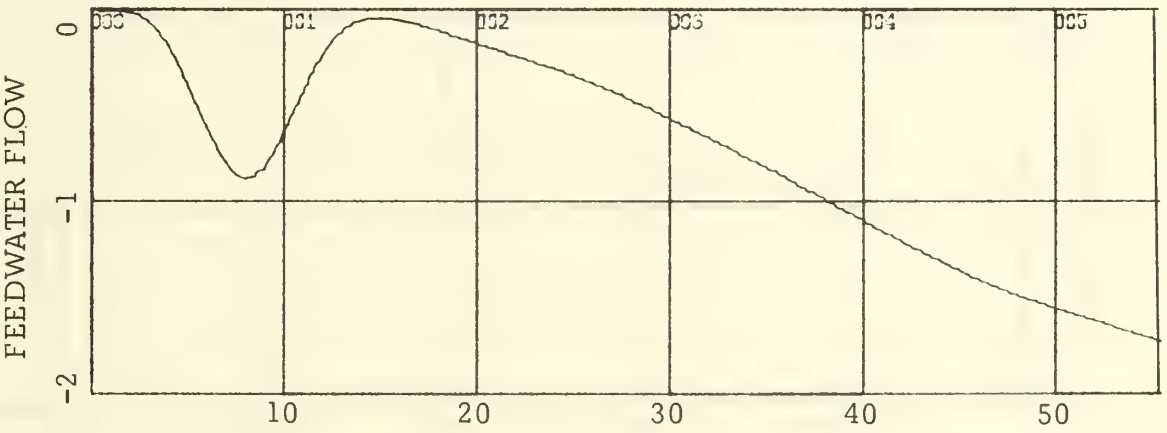

Figure 26F. Feedwater Flow Response, vs. time in seconds
Given in lb/hr x 1000 variation from 56000 lb/hr

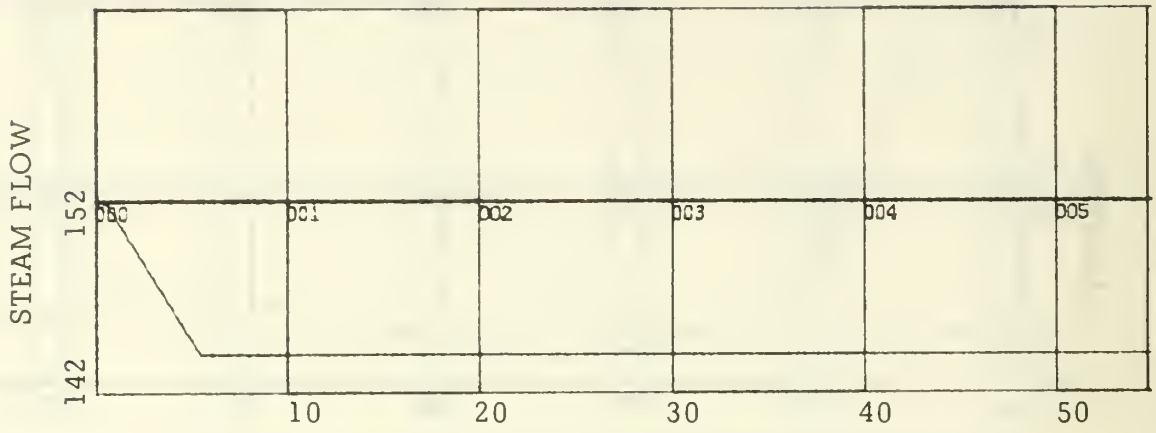

Figure 27A. Decreasing Steam Load (90% FP)
Given in lb/hr x 1000.0, vs. time in seconds

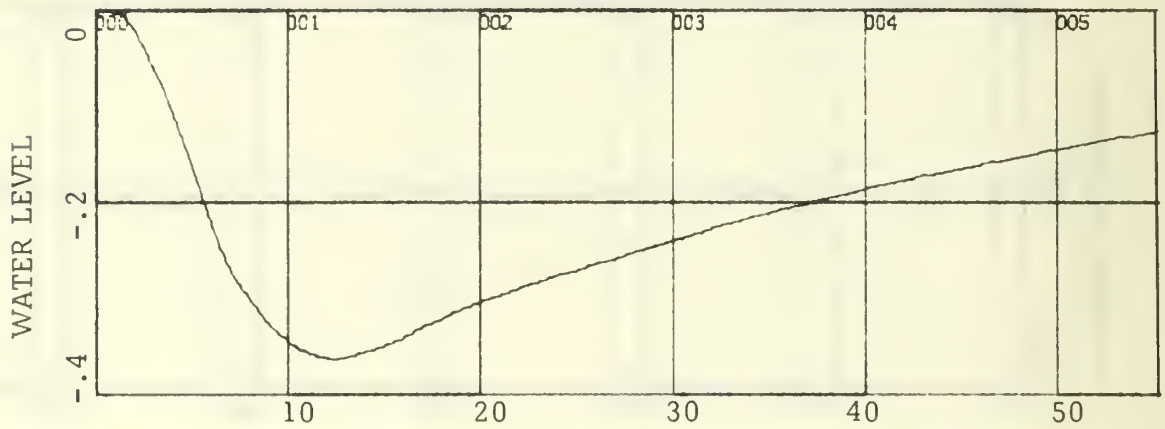

Figure 27B. Water Level Response, vs. time in seconds
Given in inches of variation from set level

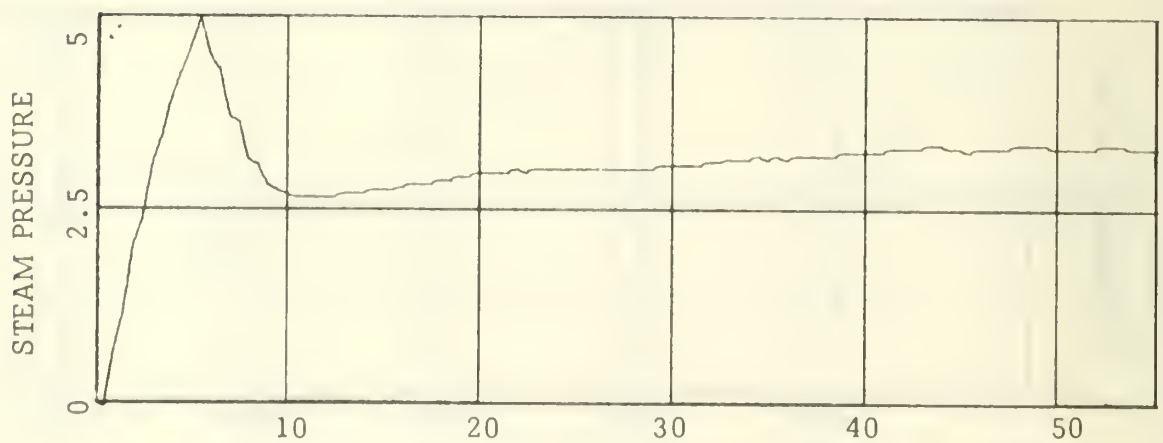

Figure 27C. Steam Pressure Response, vs. time in seconds
Given in spi variation from steady state

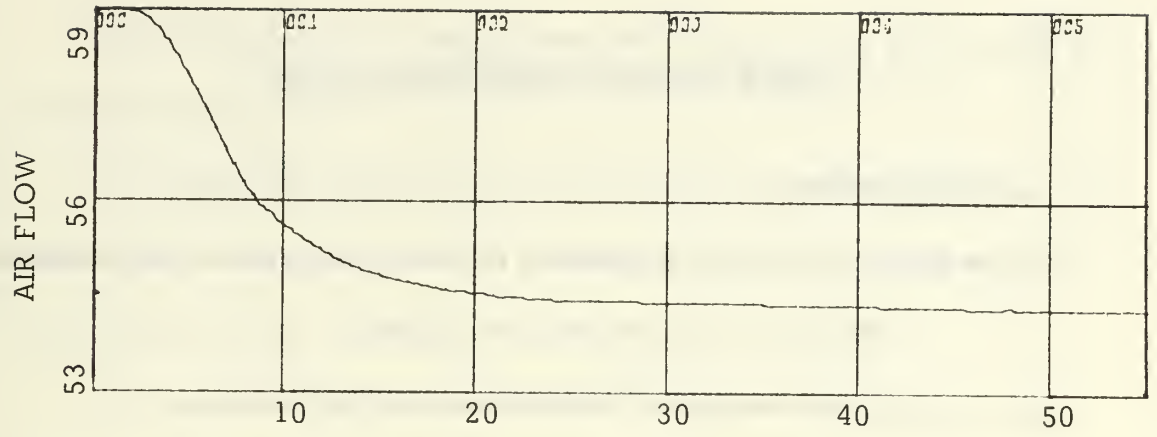

Figure 27D. Air Flow Response, vs. time in seconds
Given in percentage of full power

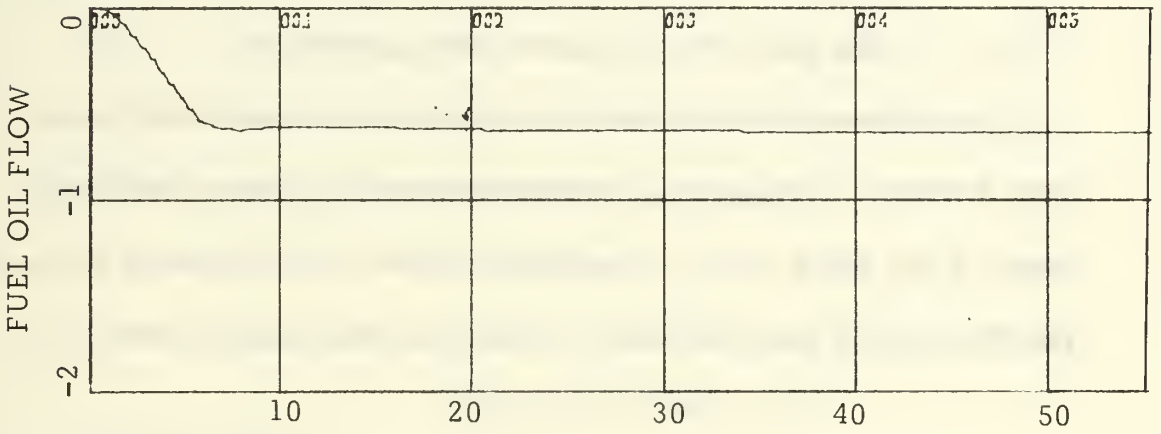

Figure 27E. Fuel Oil Flow Response, vs. time in seconds
Given in lb/hr x 1000 variation from steady state

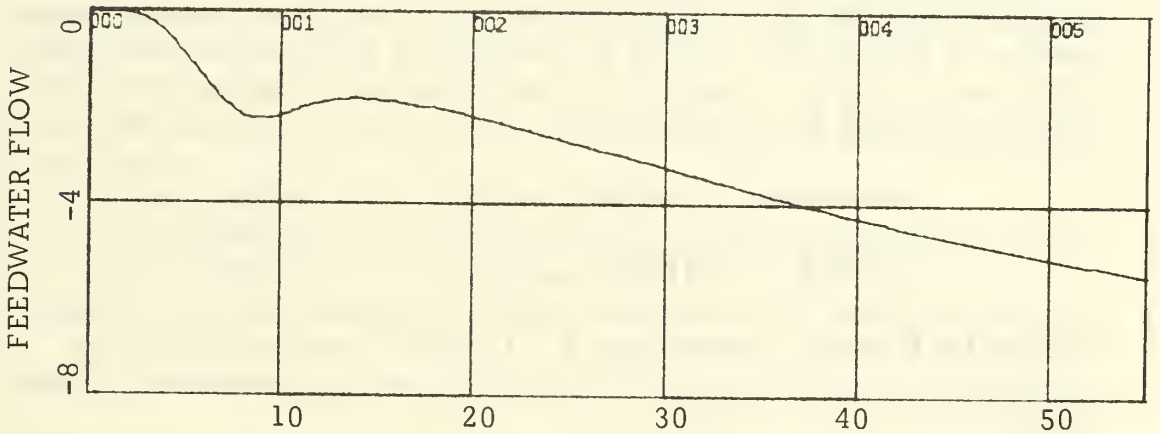

Figure 27F. Feedwater Flow Response, vs. time in seconds
Given in lb/hr x 1000 variation from 152000 lb/hr

VI. LINEAR INTERPOLATION SIMULATION

A. DISCUSSION

As already has been discussed the nonlinearities of the model are:

-The gain of the blower actuators

-The dynamics of the main forced draft blowers

-The seven transfer functions representing the steam generator

-The pressure drop across the superheater

The pressure drop across the superheater is represented as a linear function in the model, but this pressure drop varies with the square of the steam flow, as explained before. The following expression was used in the simulation to represent this pressure drop:

$$Pp = (Gs)^2/(1.86 \times 10^8)$$

where Pp is the superheater outlet pressure in psi, and Gs is the steam flow in lb/hr. The constant of proportionality was chosen as the inverse of 1.86×10^8, so that the two points given in the model for cruising and 90% FP are contained by the square law curve; that is:

for cruising: $(56000.0) \times (3 \times 10^{-4}) = (56000.)^2 \times K$

for 90% FP: $(152000.) \times (8.2 \times 10^{-4}) = (152000.)^2 \times K$

Solving for K gives: for cruising $K = 1.87 \times 10^8$ and for 90% FP $K = 1.85 \times 10^8$.

All the other gains and time constants of the nonlinear functions were simulated as follows:

For loads of 90% FP and above, the values given for the 90% FP condition were used.

For loads between 90% FP and Cruising conditions, a linear interpolation was made between the values given for these two conditions by the NBTL report.

For loads below Cruising (56000. lb/hr) an extrapolation was made continuing the same straight line used for the interpolation, down to a value of Gs equal to 28000. lb/hr.

The extrapolation was not continued for lower values of Gs, or above 90% FP, because some values get very close to the imaginary axis and the results obtained were very oscillatory.

For loads below 28000. lb/hr the values of gains and time constants were held constants at the values calculated for 28000.0 lb/hr.

B. SIMULATION

The simulation was done using a forcing function that represented a linear variation of load from 10% FP to 90% FP and vice versa, which was the same load variation used in Ref. 4 to drive a test DLG-9 Class boiler.

For comparison, the responses to the same driving force, but using the cruising condition transfer functions only, and the 90% FP transfer functions only, are also shown, along with the interpolation and the actual responses.

1. Increasing Load Condition

As before, the system was allowed to reach steady-state condition for all variables by applying a load of 10% FP, that is, 16880. lb/hr of steam flow, for a period of 60 seconds. Then a linear increasing ramp was applied up to 90% FP, in 23 seconds. The responses to this load variation are shown in Figures 28 to 31, where the first graph of each figure is the response of the test boiler to the same load disturbance, as reported in Ref. 4. The second graph is the response using for the model the cruising condition transfer functions only; the third graph is the response of the model using the 90% FP transfer functions only and the fourth graph is the response of the model using the interpolation as explained above.

Water Level response, (Figure 28). The model responses are similar in shape to the actual response; they peak at about 28 seconds, and then tend to the normal level. However, all of the model responses are larger in magnitude than the actual response.

Steam Pressure response, (Figure 29). The actual response peaks at about 23 seconds, with a value of 1115 psi while the model responses peak at about 16 seconds with the following magnitudes: Cruising, 1125 psi; 90% FP, 1144 psi; and interpolation, 1082 psi. The actual response settles to 1200 psi, while the model responses settle to values higher than 1200 psi, as seen in Figure 29.

Air Flow response, (Figure 30). Model responses are similar in shape to the actual, but cruising and 90% FP responses are

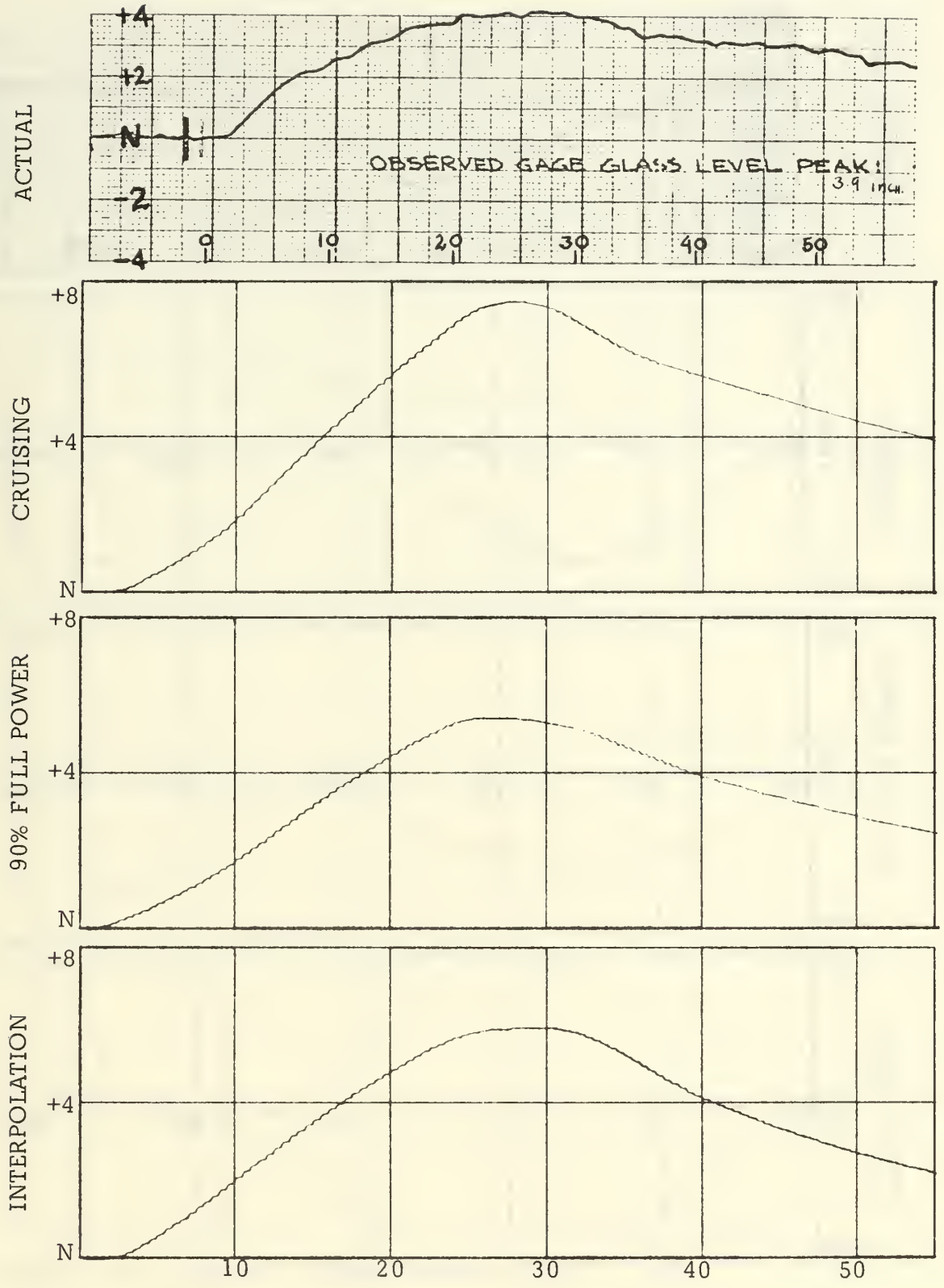

Figure 28. Water Level Response to increasing load
Inches of variation from set level N, vs. time in seconds

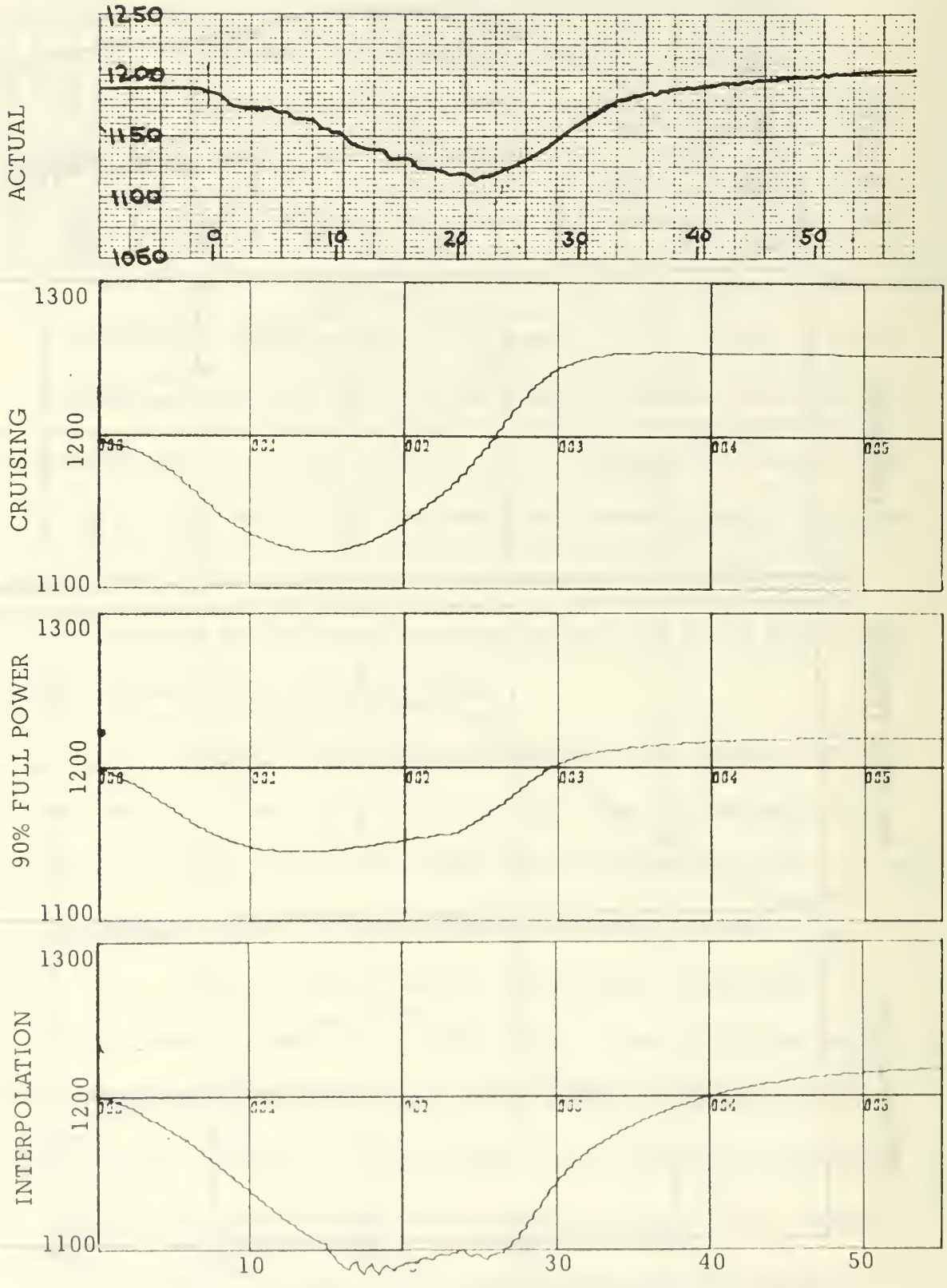

Figure 29. Steam pressure response to increasing load
Given in psi, vs. time in seconds

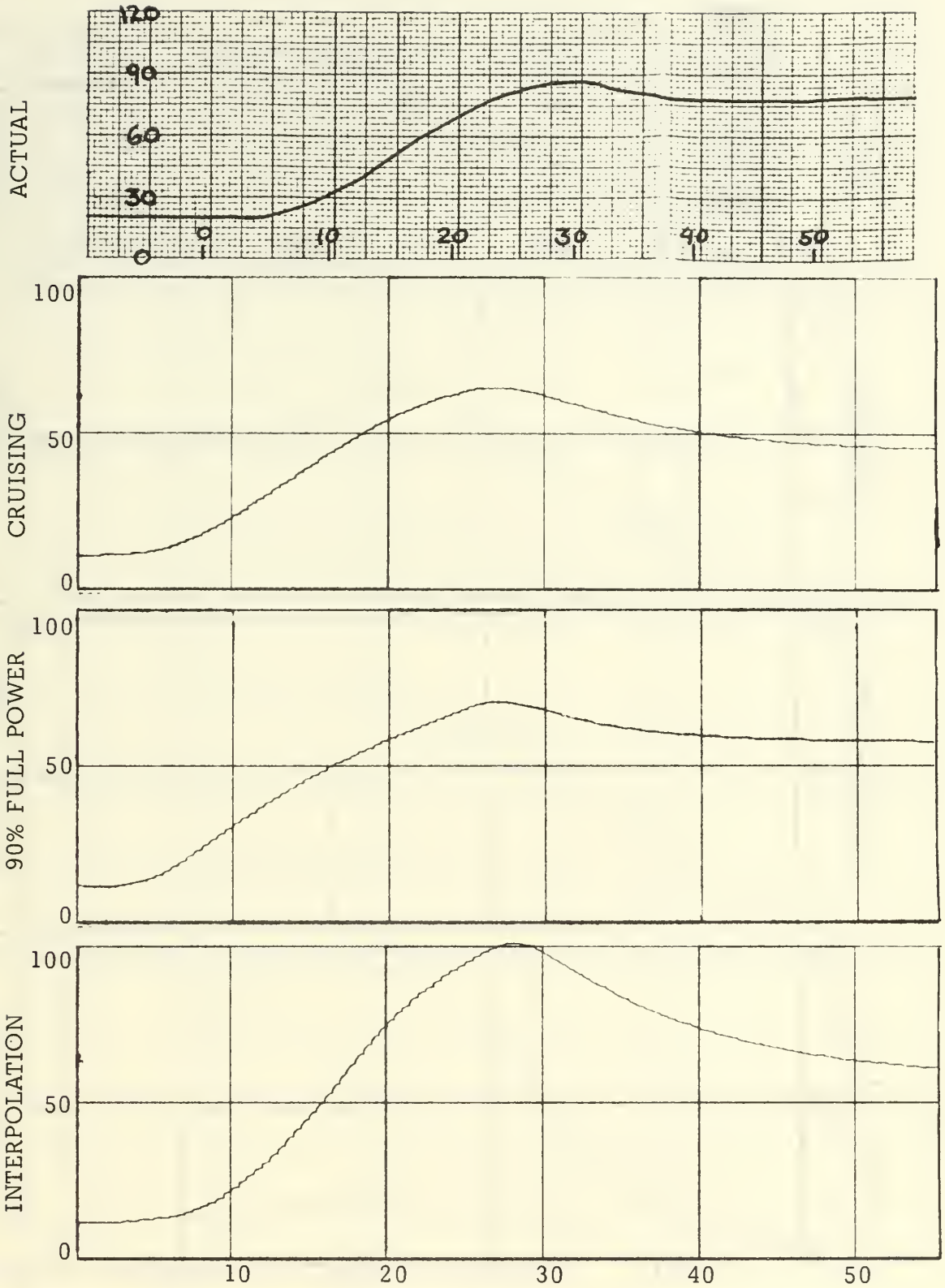

Figure 30. Air Flow response to increasing load
Given in percentage of FP, vs. time in seconds

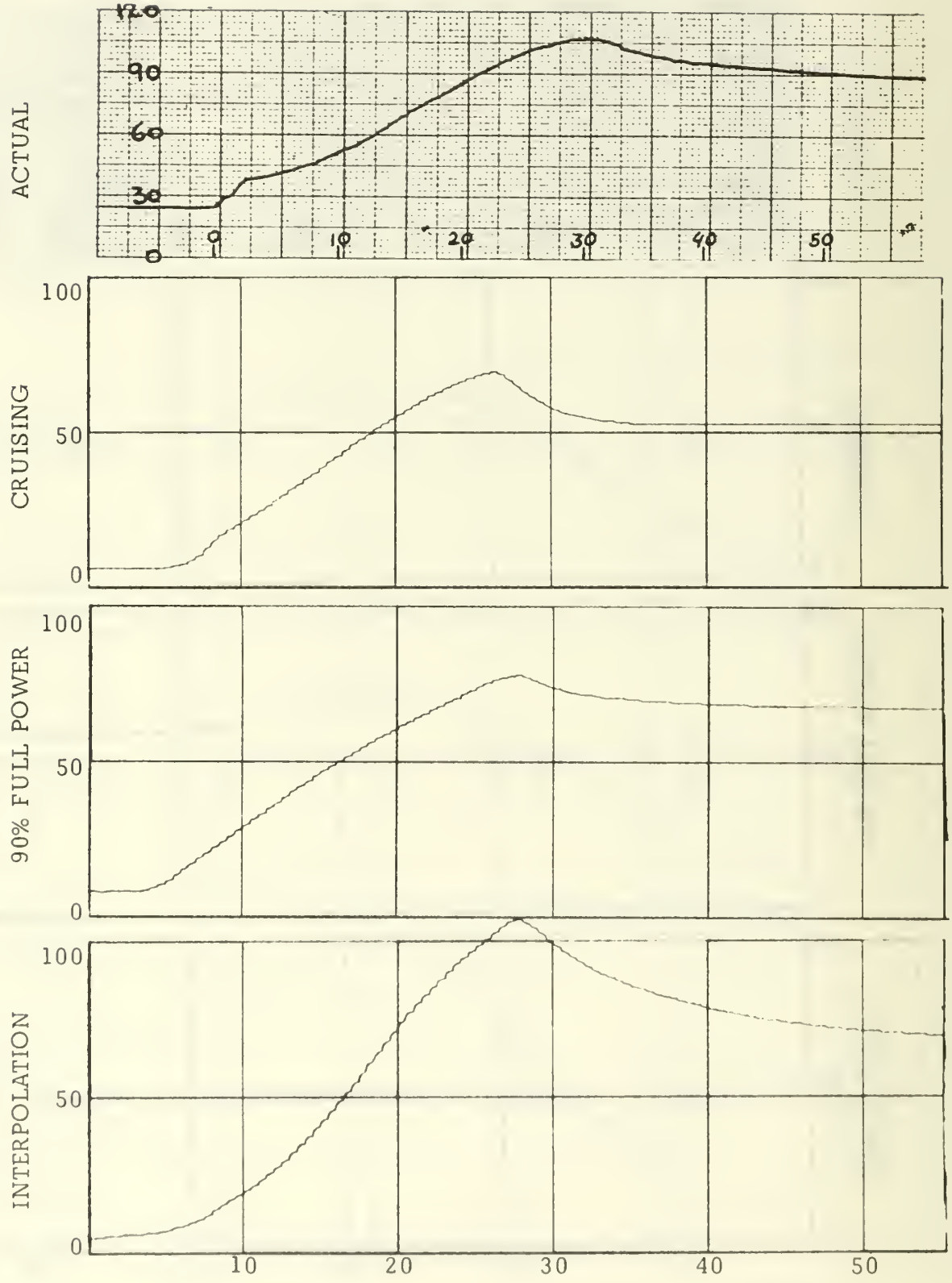

Figure 31. Oil Flow response to increasing load
Given in percentage of FP, vs. time in seconds

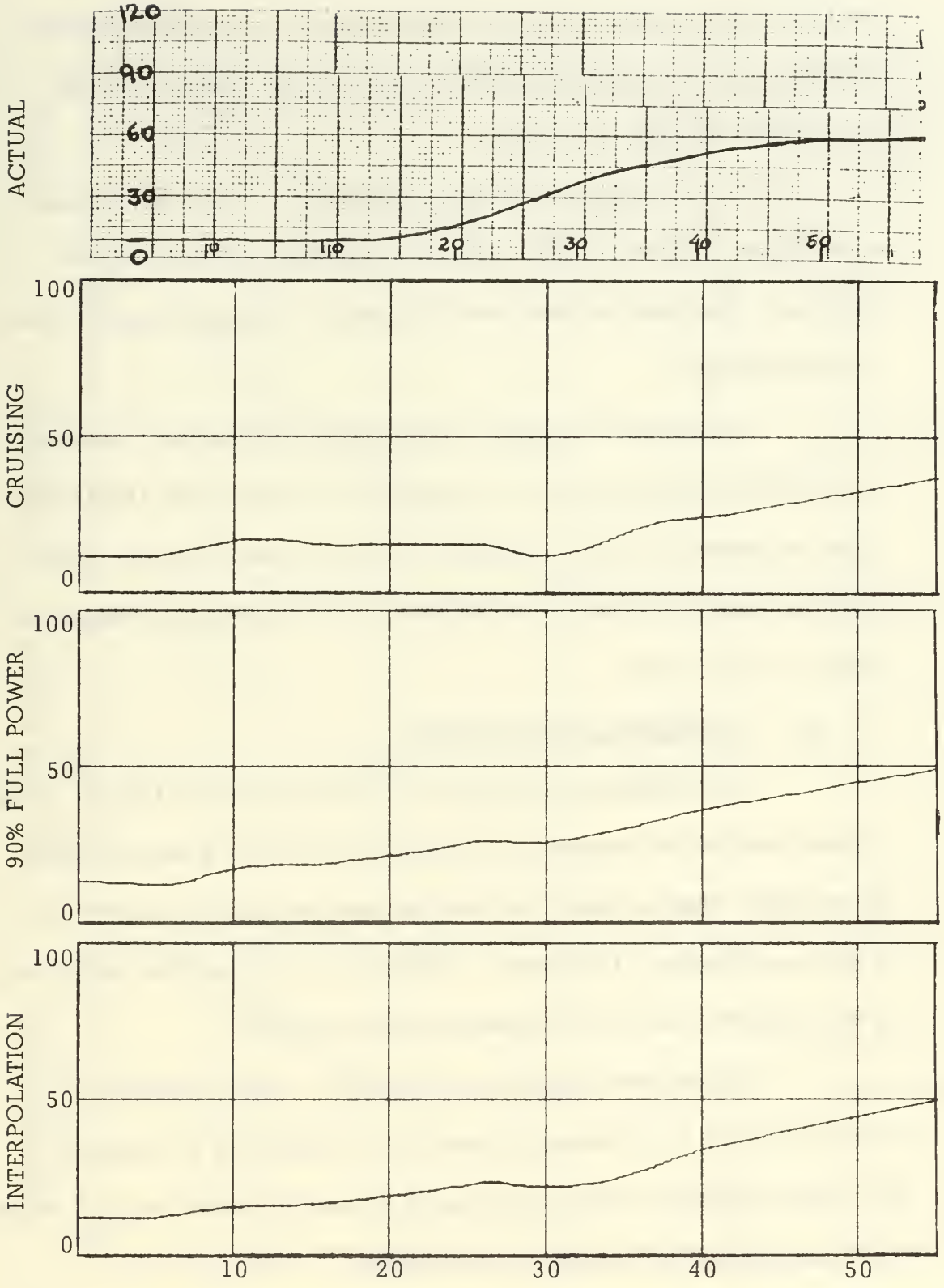

Figure 32. Water Flow response to increasing load
Given in percentage of FP, vs. time in seconds

smaller in magnitude of peak and settling values. The interpolation response values are closer to the actual response values than the cruising and 90% FP values are.

Fuel Oil Flow response, (Figure 31). The observations made for the air flow response are valid also for the fuel oil flow response. Interpolation responses are closer to actual than the other two simulations.

Water Flow response, (Figure 32). The actual response is observed to begin at about 13 seconds while the model simulations begin responses at about 4 seconds; also the actual response settles to 60% at about 50 seconds, while the model responses are slower to reach the steady state.

2. Decreasing Load Condition

The system was driven with a steady load of 152000. lb/hr of steam load for 60 seconds until steady-state values were reached for variables; then a steady decreasing ramp was applied down to 10% of full power during 23 seconds. Figures 33 to 37 show the responses, in the same form as for the increasing load condition.

Water level response, (Figure 33). Actual response of water level was a decreasing of level of 3.9 inches in 25 seconds; the model responses show a decreasing of level of more than 5.5 inches in 27 seconds for all the three simulations.

Steam pressure response, (Figure 34). Actual response shows that superheater pressure goes from steady state (1210 psi) to

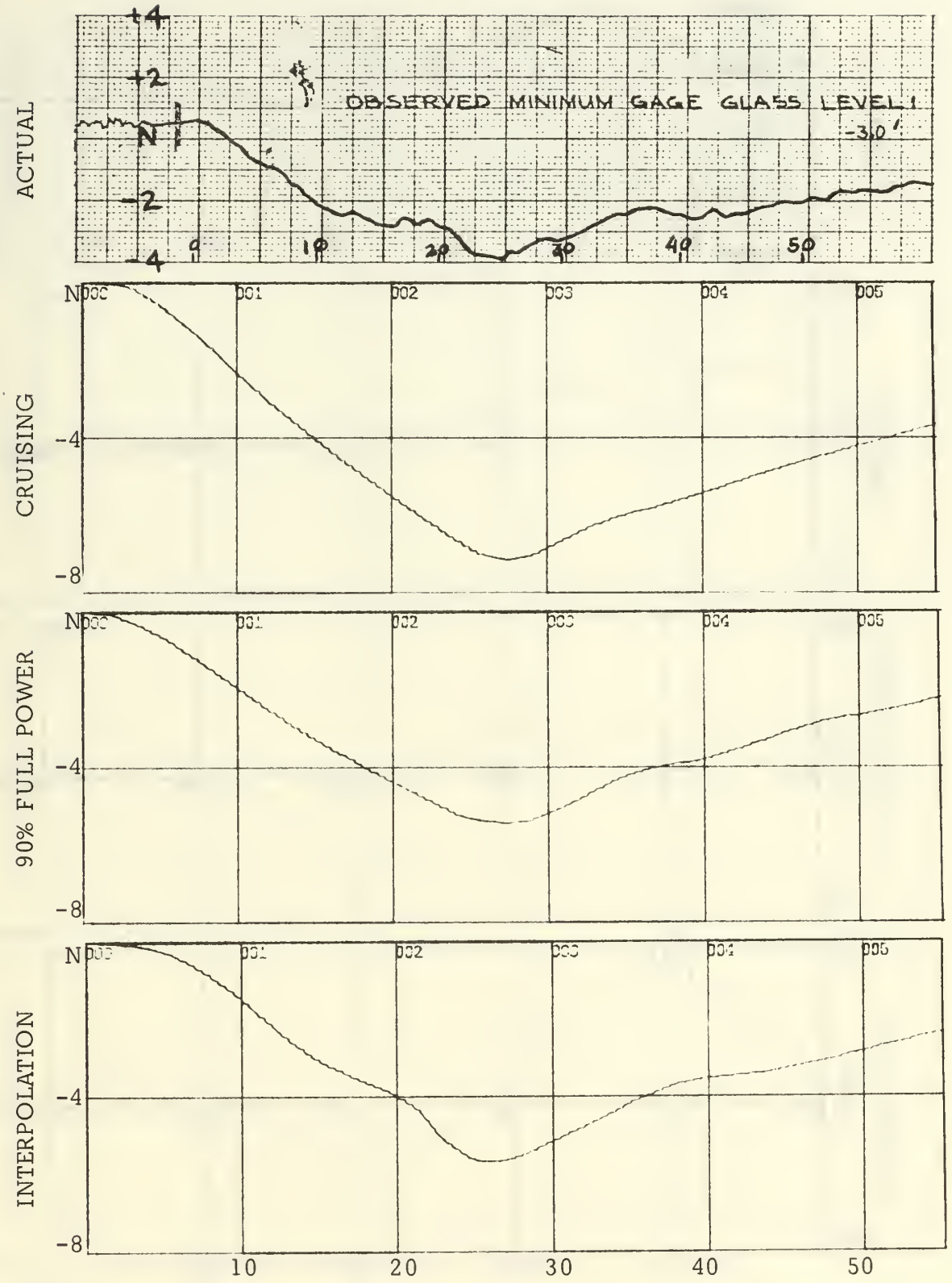

Figure 33. Water level response to decreasing load
Inches of variation from set level N, vs. time in seconds

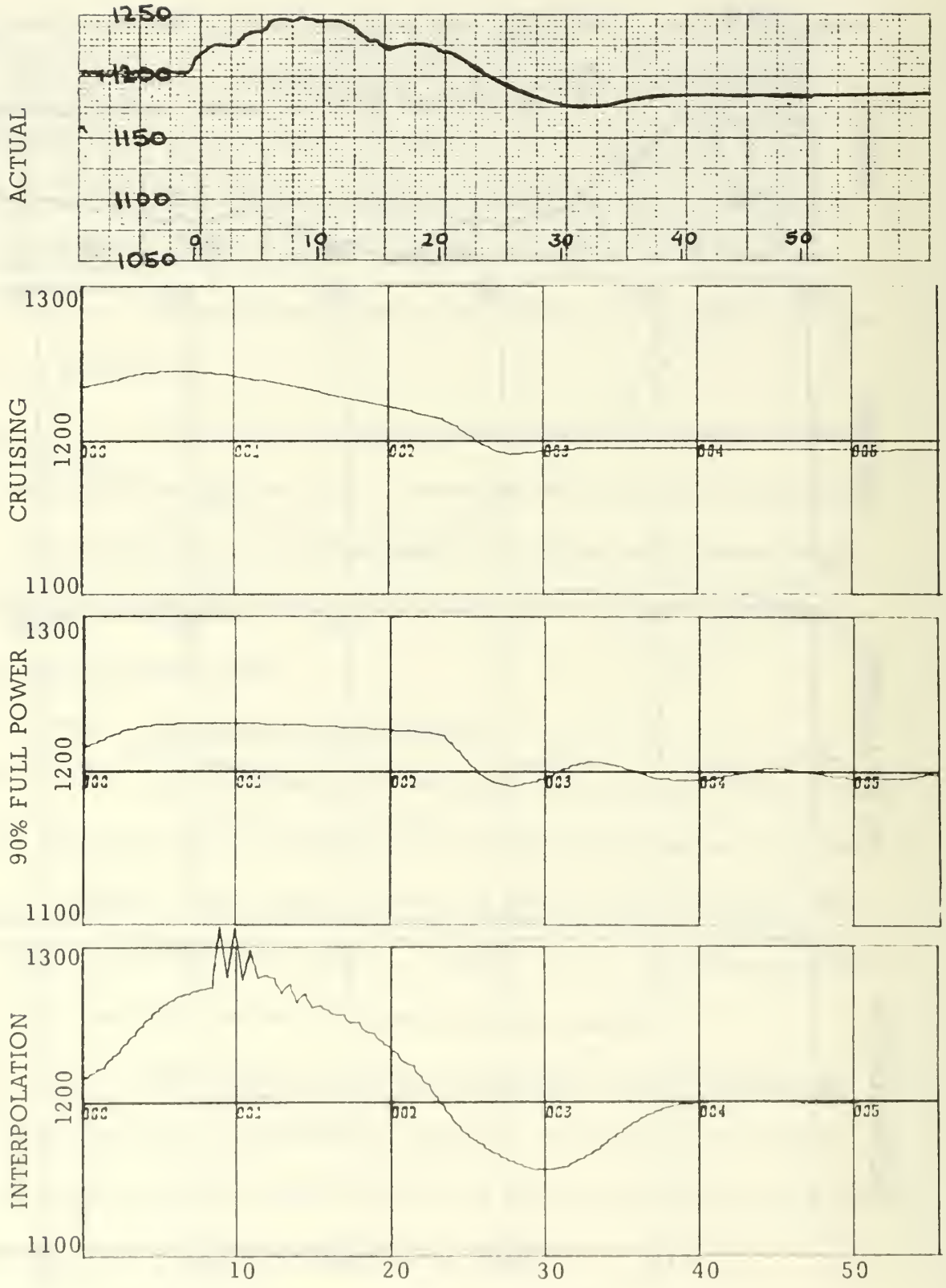

Figure 34. Steam pressure response to decreasing load
Given in psi, vs. time in seconds

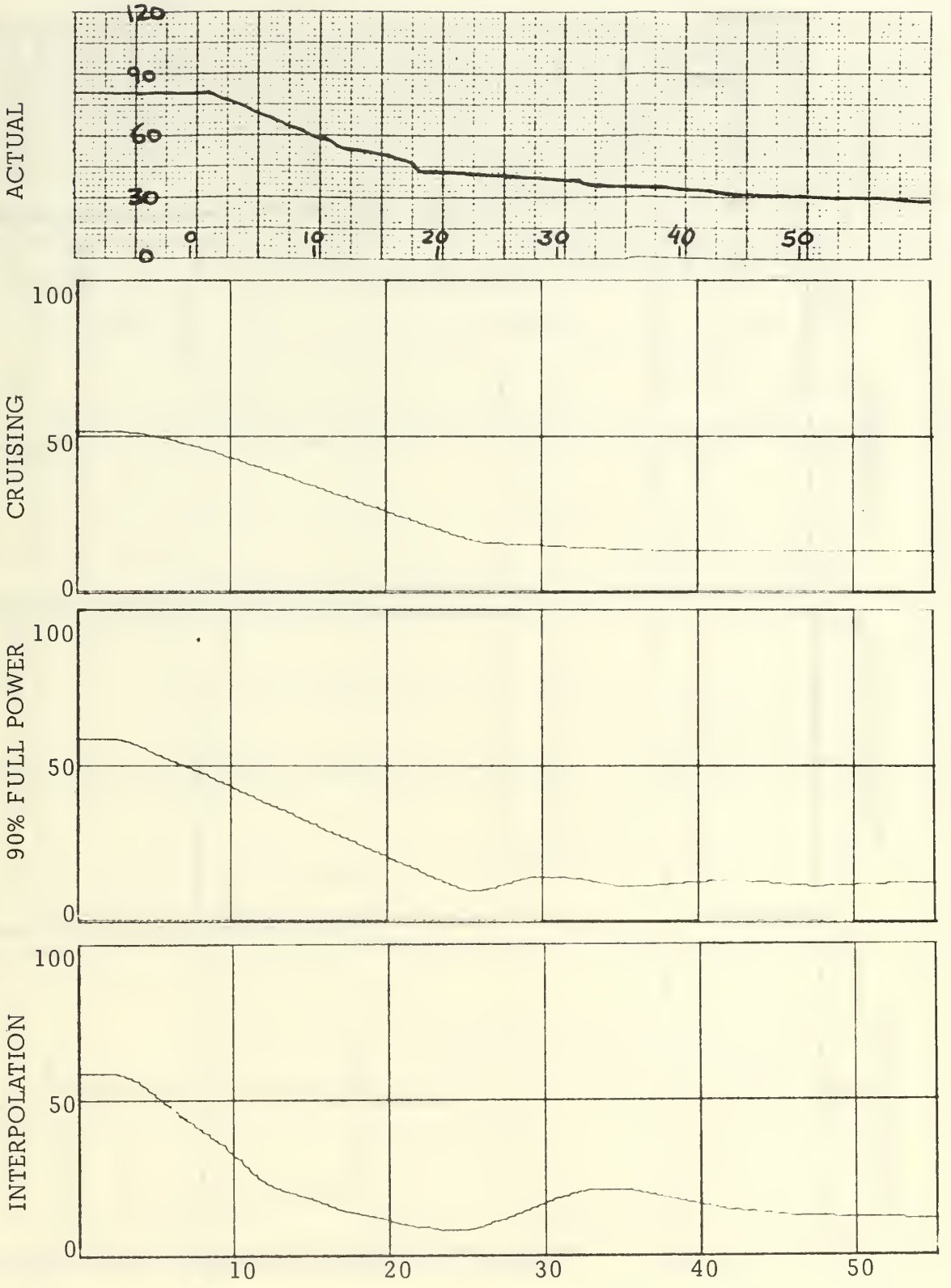

Figure 35. Air Flow response to decreasing load
Given in percentage of FP, vs. time in seconds

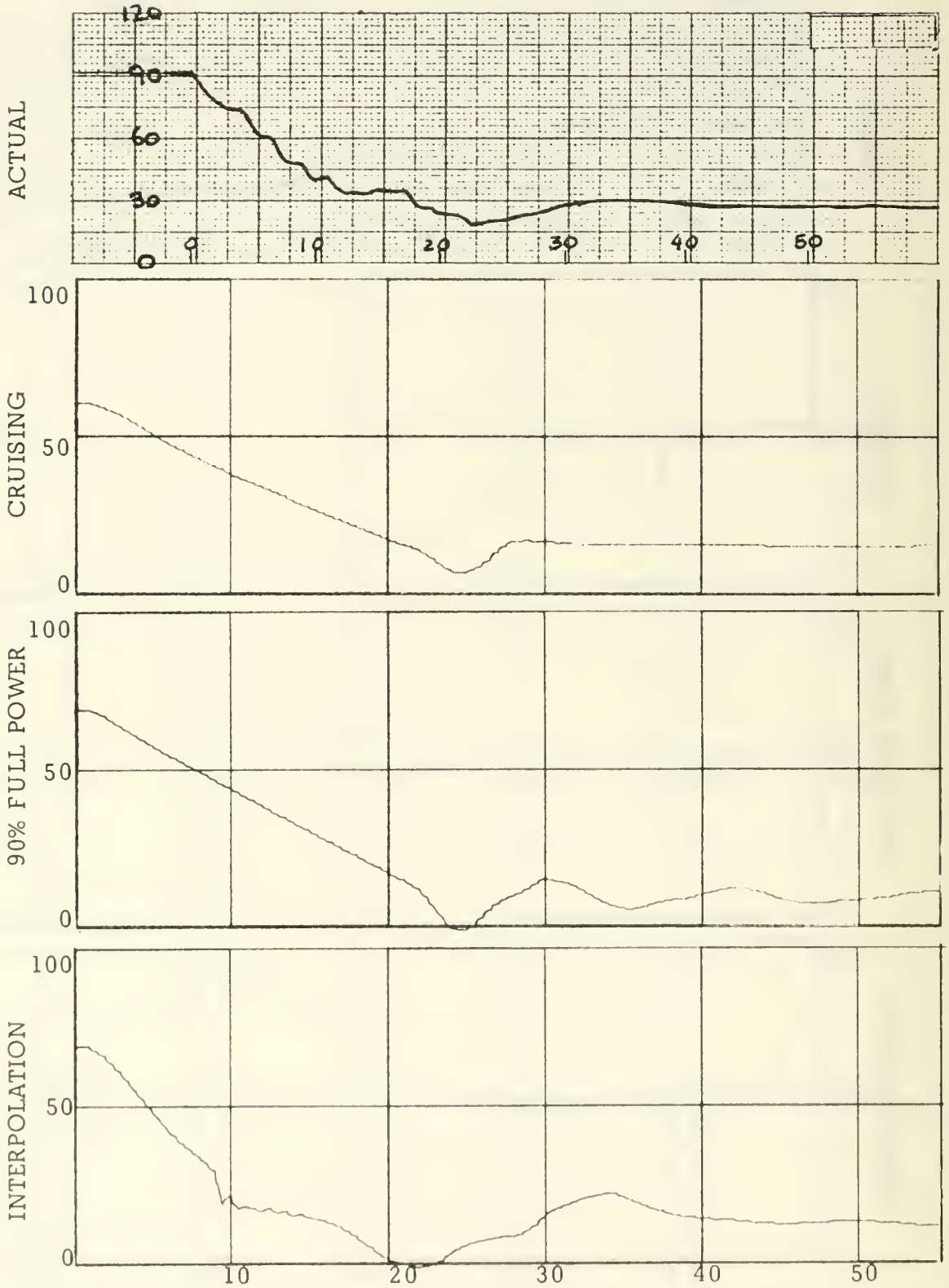

Figure 36. Oil flow response to decreasing load
Given in percentage of FP, vs. time in seconds

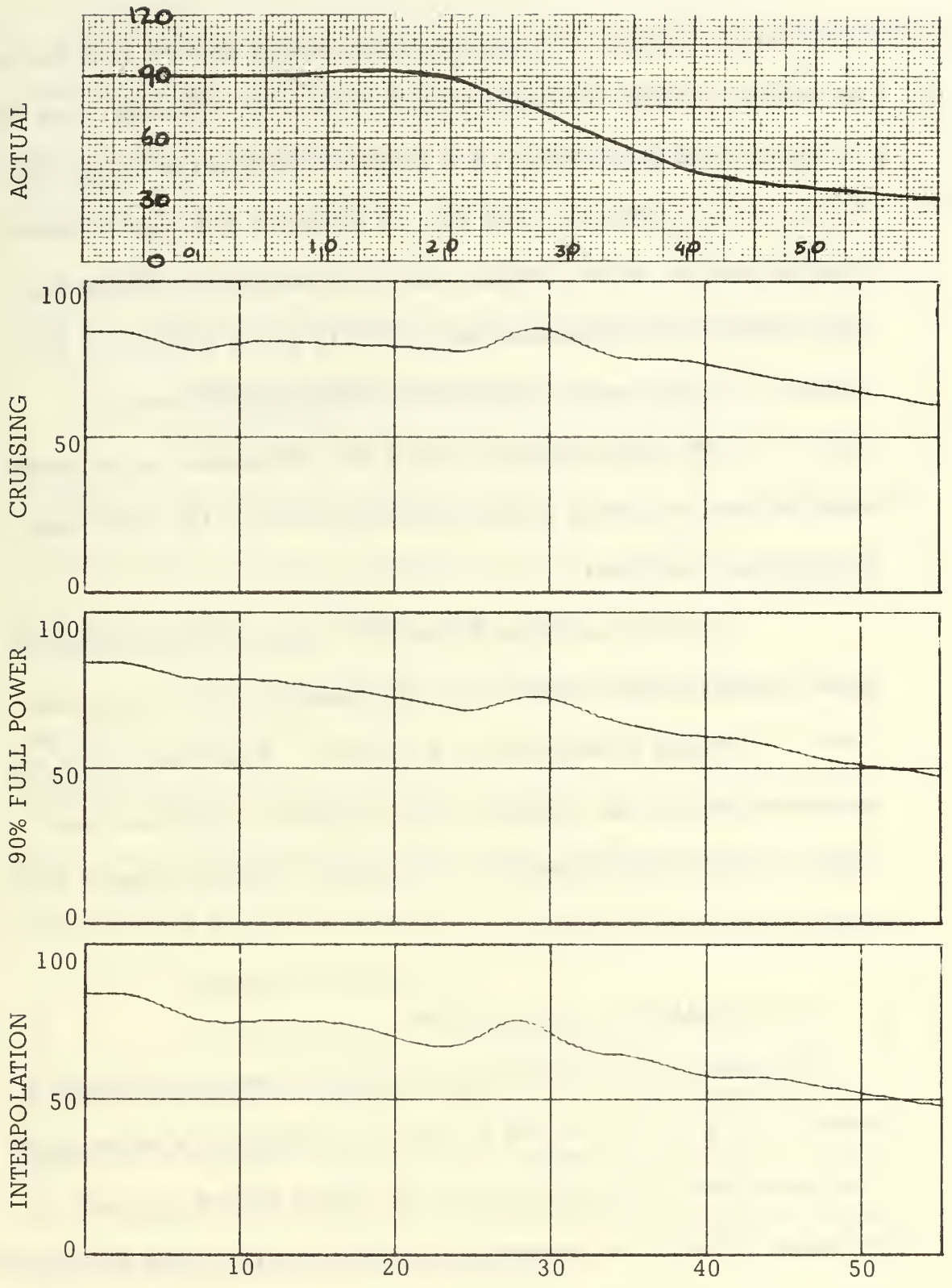

Figure 37. Water flow response to decreasing load
Given in percentage of FP, vs. time in seconds

1248 psi in 8 seconds and reaches a new steady state of 1185 psi at 40 seconds. Model simulations were as follows: Cruising, from 1235 psi to 1248 psi in 7 seconds, and settles to 1195 psi at 28 seconds; 90% FP, from 1220 psi to 1230 psi in 7 seconds, and reaches steady state of 1200 psi at 35 seconds with small oscillations around this value; interpolation response was from 1215 psi to 1310 psi in 10 seconds, reaching new steady state of 1200 psi at 40 seconds.

Air flow response, (Figure 35). Responses of the model were the same as actual in shape but magnitudes of the model were smaller than the actual.

Oil flow response (Figure 36). Again the magnitudes of model responses were smaller than magnitudes of actual responses.

Water flow response, (Figure 37). Same observation as for the increasing load condition. The water flow responses were faster to initiate their response, but slower to reach the steady state than the actual responses.

C. NEW PARAMETERS SIMULATION

Comparison of the responses presented in the preceding part B, shows that the model with 90% FP transfer functions is a better model to represent the steam generator and its control system, for large variations of load, than the cruising condition or the linear interpolation model. Therefore, the 90% FP transfer functions were used to perform a simulation using the new parameters and variations of load from 10% to 90% of full power, and vice versa.

Of course, there are no actual boiler responses for the new parameters to compare with; such is the case of the designer who is presented with a model of the plant and he is to find the controller gains, to make the plant respond according to certain specifications.

In the discussion to follow, comparison will be made with the 90% FP responses of the model using the original parameters.

1. Increasing Load Condition

The forcing function is the same as the one used in part B, that is, the system is allowed to reach steady-state values at 10% of full power, and then it is ramped linearly, and in 23 seconds, to 90% of full power, as shown in Figure 38A.

The responses, shown in Figures 38B to 38F, are not significantly different from those for the original parameters, they are somewhat faster in the sense that the peaks and settling times are about 3 seconds earlier than before. The steam pressure response peaks about 6 seconds earlier than previously.

2. Decreasing Steam Load

The forcing function is shown in Figure 39A and the responses are shown in Figures 39B to 39F; they are similar in shape, magnitude and times of peaking to the responses using the old parameters, however, the settling time is increased since some oscillation is noted at the latter part of the response.

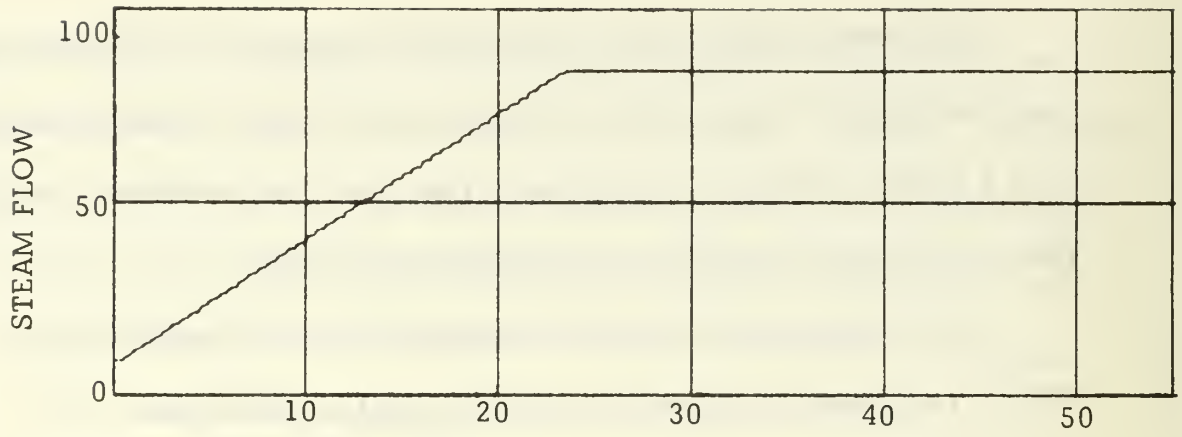

Figure 38A. Increasing Steam Load
Given in percentage of FP, vs. time in seconds

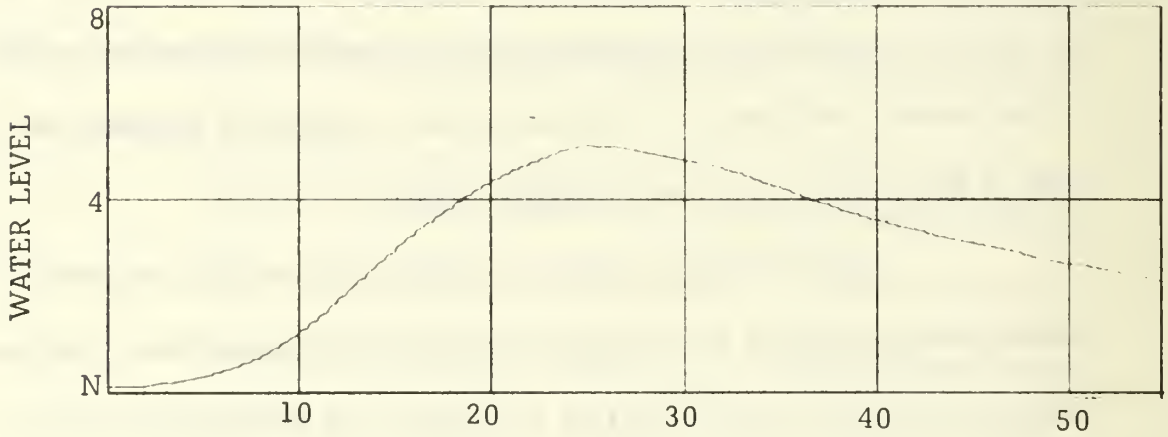

Figure 38B. Water Level Response
Inches of variation from set level N, vs. time in seconds

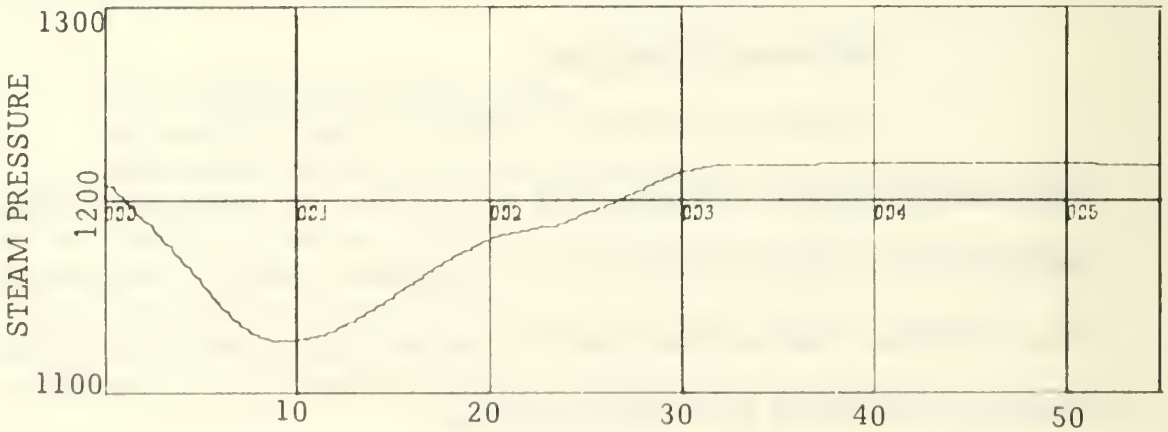

Figure 38C. Steam Pressure Response
Given in psi, vs. time in seconds

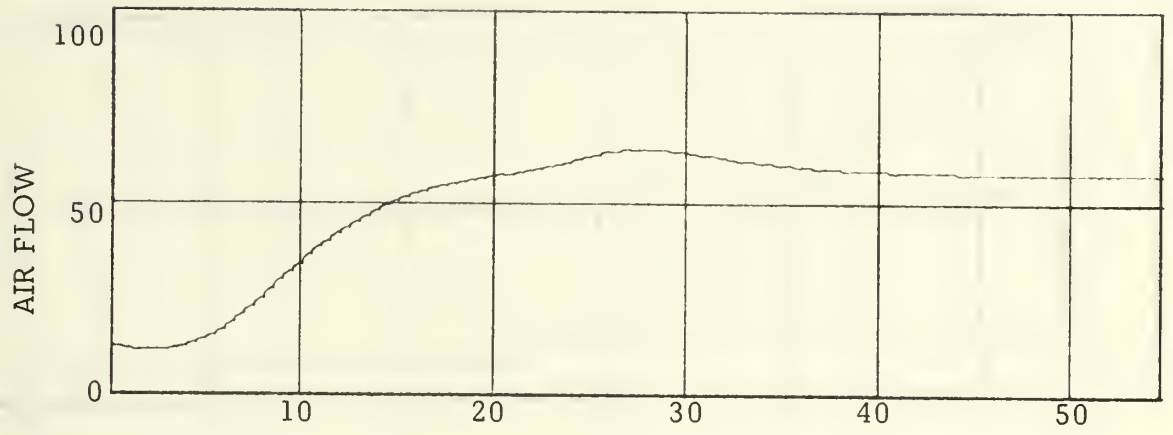

Figure 38D. Air Flow Response
Given in percentage of FP, vs. time in seconds

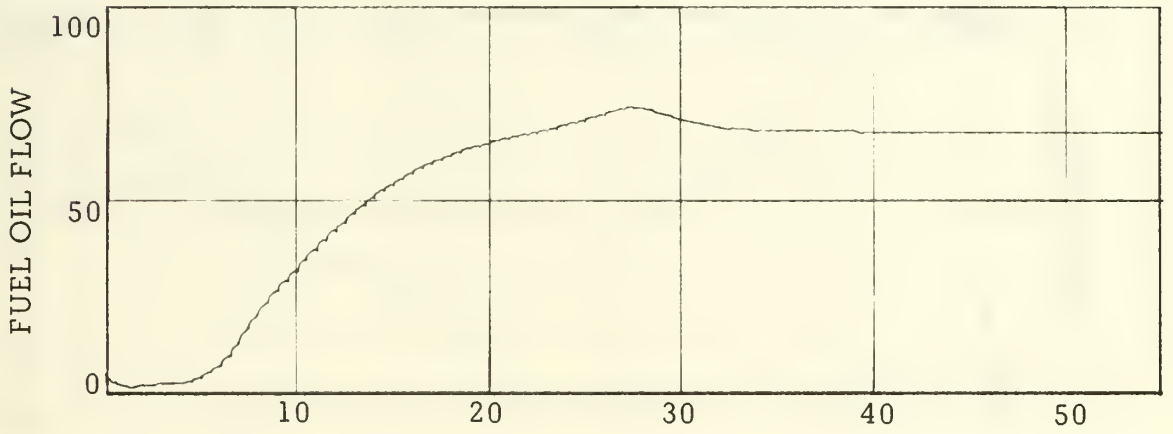

Figure 38E. Fuel Oil Flow Response
Given in percentage of FP, vs. time in seconds

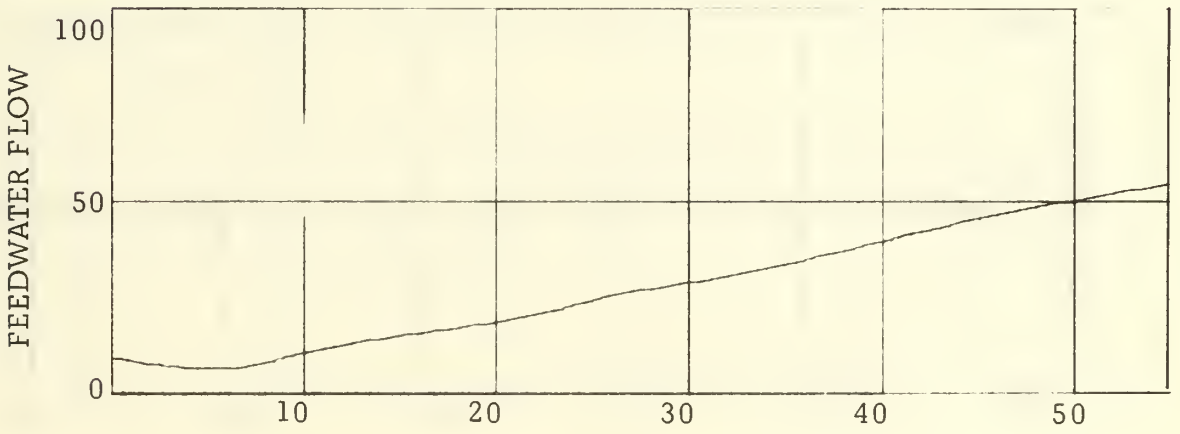

Figure 38F. Water Flow Response
Given in percentage of FP, vs. time in seconds

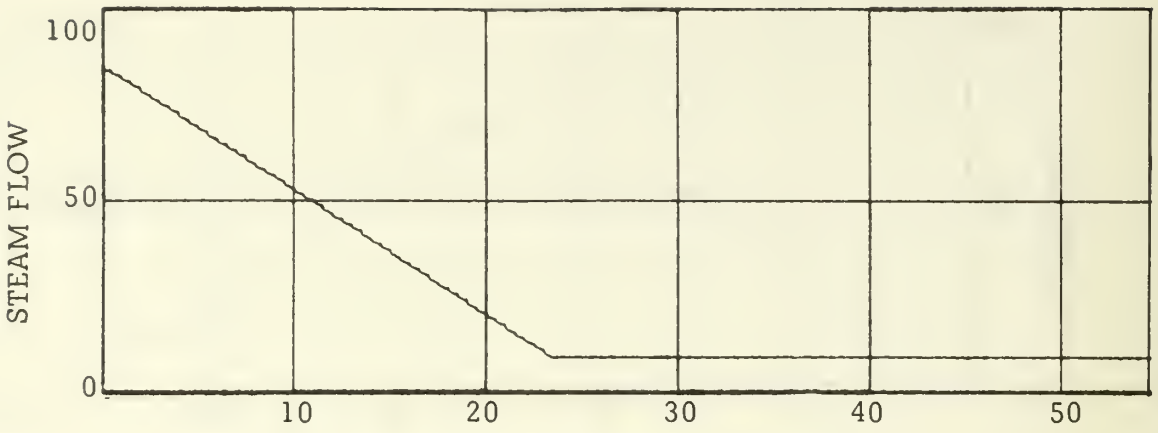

Figure 39A. Decreasing Steam Load
Given in percentage of FP, vs. time in seconds

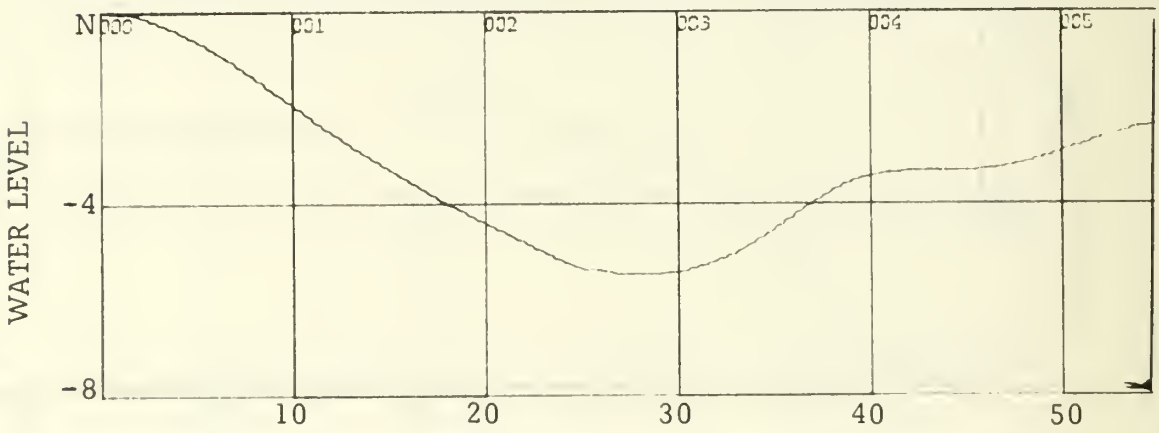

Figure 39B. Water Level Response
Inches of variation from set level N, vs. time in seconds

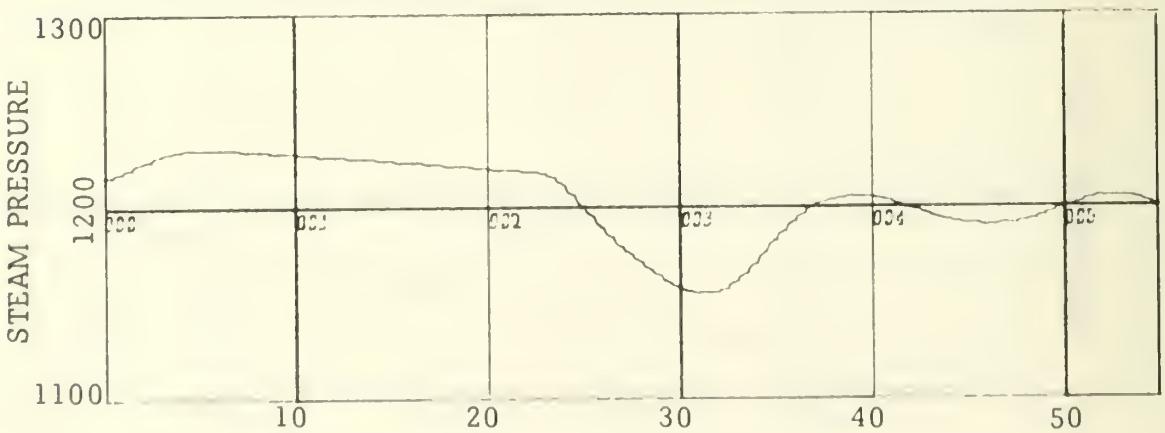

Figure 39C. Steam Pressure Response
Given in psi, vs. time in seconds

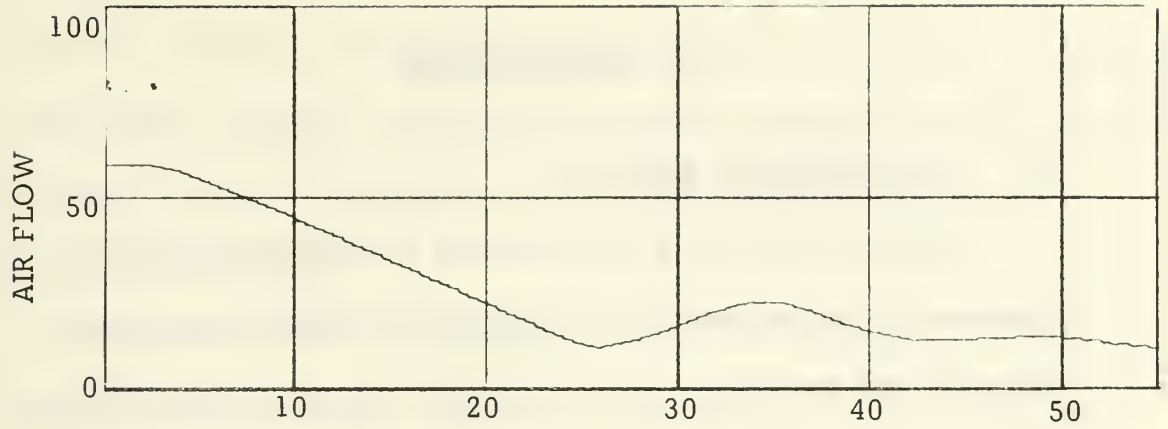

Figure 39D. Air Flow Response
Given in percentage of FP, vs. time in seconds

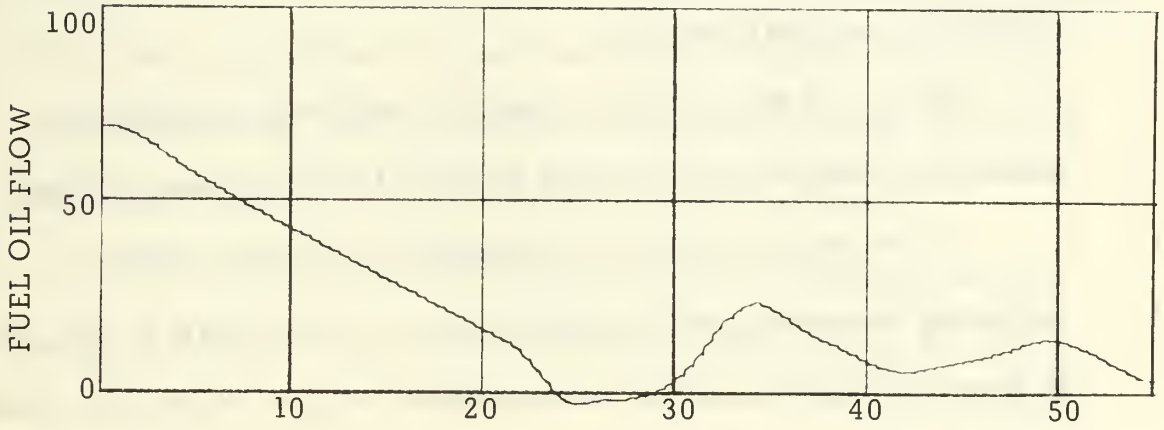

Figure 39E. Fuel Oil Flow Response
Given in percentage of FP, vs. time in seconds

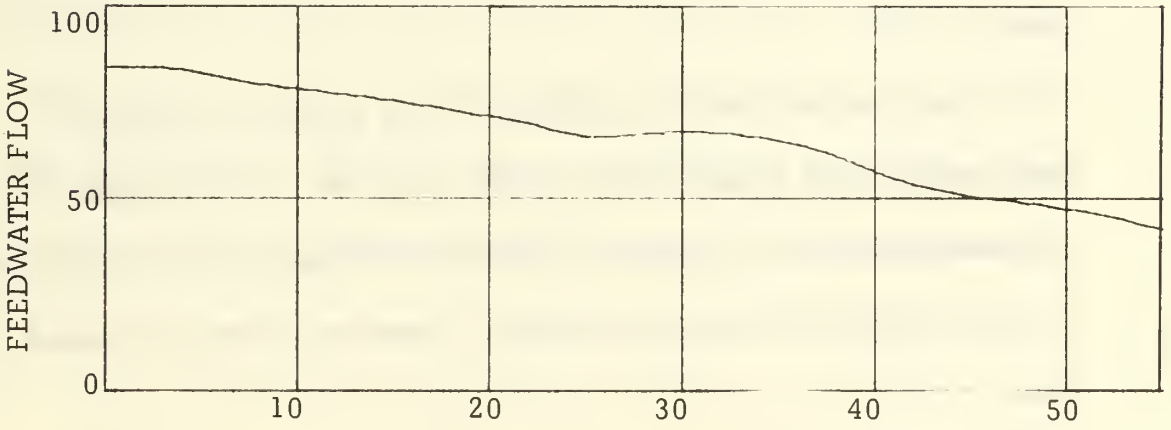

Figure 39F. Water Flow Response
Given in percentage of FP, vs. time in seconds

VII. CONCLUSIONS

A. DISCUSSION OF RESULTS

Parts II, III, and IV of this thesis demonstrate the use of parameter plane techniques, as applied to complex control loops, where all the parameters of the loop had been selected and there remains only the problem of selecting the parameter settings (gain values) of the controllers to provide acceptable, (according to certain criterion), loop performance.

The use of the parameter plane will reduce by a significant amount the time expended in field trials to find these gain settings.

It is to be noted that the optimization of several subloops according to certain specifications, as was done in parts II, III, and IV does not imply that when these subloops are put together the entire system will perform as expected from the specifications used in the optimization of the subloops, because of the many interactions between them.

Part V shows that the behaviour of the system to small disturbances was as expected from theory; however, the magnitude of the variations of the responses could not be compared with responses of actual boiler to small perturbations, because of lack of relevant data.

Part VI assesses the validity of the model, since the responses of this mathematical model are close to the responses of the actual

boiler. However, some discrepancies in magnitude were noted, because the transfer functions were found at two fixed operating conditions, and hence the model is valid only for small perturbations about these operating conditions.

The responses of the model shown on part VI indicate that the 90% Full Power condition transfer functions provide a better model for large excursions of load, than the cruising condition transfer functions. It also shows that the linear interpolation did not bring the magnitudes of the responses closer to actual values than those for the 90% FP transfer functions, and in the case of steam pressure the variations were larger than when using cruising transfer functions.

The use of the DSL/360 digital simulation language was very useful, and easy to use, to obtain the time responses of the model.

B. RECOMMENDATION

In order to have a model that closely represents the behaviour of the actual boiler for large changes in steam flow, further work is recommended in the interpolation and extrapolation of the nonlinear transfer functions, since the linear approximation done in part VI of this thesis did not improve the 90% FP transfer functions responses.

APPENDIX A

PERSONAL LETTER

DEPARTMENT OF THE NAVY
NAVAL SHIP ENGINEERING CENTER, PHILADELPHIA DIVISION
PHILADELPHIA, PA. 19112

IN REPLY REFER TO
6770:JWB:jm
Ser 30
3 Feb 1970

LCDR Humberto Medina, Venezuelan Navy
U. S. Naval Postgraduate School
SMC No. 1486
Monterey, Calif. 93940

Dear LCDR Medina:

Thank you for your interesting letter concerning your simulation studies of the DLG-9 Class steam generator. It appears that you have indeed identified one of the trouble spots in our "model" of this system. This same difficulty was not recognized by us until 1966 when we operated a control system on the boiler; the system had been designed with the aid of simulation based upon the "model" reported in our Project No. B-502-III.

Let us first clear up your confusion concerning our block diagram, Figure 3 of the report. It is true that the constant term of the characteristic of the closed loop fuel system is negative; this is compensated by the fact that the fuel control valve, G_V, is reverse acting, thus placing a negative sign in front of the dynamic terms of both numerator and denominator of the closed loop transfer function. The negative signs of course cancel out, leaving us with a potentially stable system. You have correctly concluded that the system is not stable for the controller settings indicated. This results from the fact that the elements of the control loop were individually identified by open-loop testing; as a result, the effects of impedance mismatching on the system dynamics were not revealed. It turns out that the loading effect of the fuel control valve diaphragm operator on the fuel controller effectively adds a two-second first order time constant to the system. Thus the control valve transfer function should be properly specified as $G_V = -795/(1 + 2.0S)$. This problem is discussed in some detail in our Report No. B-584-II, which may be obtained from the Defense Document Center using AD No. 805-700L. I believe that you will find that the addition of this first order lag to the system will stabilize your simulation. You should not have to alter the dynamics of either the controller or the transmitter to achieve stability.

6770:JWB:jm
Ser 30

In addition to the correction to the high frequency components of the water level controller, the only other correction to the system is that of the gain of the feedwater control valve. It should be changed from 3.12×10^4 to 0.94×10^4. The new figure represents the average gain of the valve over the full load range, whereas the original figure represents a perturbation result at one load level.

The control devices in the system were manufactured by the Bailey Meter Company; all operate on a signal range of 3 to 27 psig. The controller settings were obtained by trial-and-error adjustment in the field based on transient response specifications of +5 in. of water level and -120 psi superheater outlet pressure as load varies from 8 to 75%, and -5 in., +20 psi as load varies from 75 to 8%, both in 25 seconds and linearly. Remember that pressure drop through the superheater varies with the square of steam flow and amounts to 75 psi at 83.3% of rating.

I hope that the foregoing information will be of value to you in your work; please feel free to correspond if additional assistance is required.

Very truly yours,

James W. Banham Jr.

JAMES W. BANHAM, JR.
Head, Machinery Automation
Systems Department

APPENDIX B

PERSONAL LETTER

PHILADELPHIA NAVAL SHIPYARD

~~NAVAL BASE~~

PHILADELPHIA, PA. 19112

IN REPLY REFER TO
Code 2725

30 August 1965

Professor Milton L. Wilcox
U. S. Naval Postgraduate School
Monterey, Calif. 93940

Dear Professor Wilcox:

Thank you for your letter of 10 August 1965 expressing your interest in a continuation of the simulation program undertaken by Lieutenants Creager, Fenick, and O'Brien. I apologize for not having replied sooner, but I was on my vacation when your letter arrived.

I would be very pleased to provide whatever assistance and information required that is available here at the Laboratory. In reply to your specific questions, the following information is offered:

a. There is no additional test information available on the feedwater system.

b. The entire boiler and control system has been satisfactorily simulated on the analog computer here at NBTL.

c. There are errors in the transfer functions shown in blocks 29 and 84 of Figure 6-3 of the simulation thesis. These errors resulted from erroneous information originally provided by us, but I had been under the impression that it was subsequently corrected. The correct transfer functions should be $125/(S^2 + 6.75S + 125)$ for block 84, and $19.2/(S^2 + 2.62S + 19.2)$ for block 29. These errors undoubtedly account for the instability of the simulated digital system. It should be noted that the analog simulation was stable, and, in general, duplicated the transient response of the actual boiler.

We are presently preparing a detailed description of the procedure whereby the analog program was developed. A copy of the computer program of the feedwater control system, together with this description, will be forwarded to you as soon as completed.

Code 2725

I have been in touch with Mr. Lackowski concerning our mutual problems and interests; subject to authorization by the Bureau of Ships, some sort of joint effort between our two Laboratories may result from this contact.

As your work progresses, should you find need for additional information, please advise LCDR Ediin and LT Lamb to feel free to contact us directly. I suggest that any correspondence be addressed officially to the Commander, Philadelphia Naval Shipyard (Naval Boiler and Turbine Laboratory), and marked to my attention. In this manner we can maintain such correspondence as a matter of record.

Very truly yours,

JAMES W. BANHAM, JR.
Head, Controls Branch

BIBLIOGRAPHY

1. Naval Boiler and Turbine Laboratory Report NBTL RT&E Project B502 - III, Experimental Determination of Open Loop Frequency Response Characteristics of DLG-9 Class Steam Generator System, by J. W. Banham, Jr., 31 August 1964.

2. Syn, Turner, Wyman, DSL/360 - Digital Simulation Language Manual, IBM Technical Publication, November 1963.

3. Siljak, D.D., "Analysis and Synthesis of Feedback Control Systems in the Parameter Plane, Part I: Linear Continuous Systems," IEEE Transactions on Applications and Industry, Vol. 83, November 1964.

4. Naval Boiler and Turbine Laboratory Report NBTL RDT&E Project B-452-I, Analysis of Automatic Control Systems Design for Main Propulsion Machinery, by J. W. Banham, Jr., 24 June 1964.

5. Creager, Fenick and O'Brien, Computer Investigation of a Destroyer Steam Generator, MSEE Thesis, Naval Postgraduate School, Monterey, California, June 1965.

INITIAL DISTRIBUTION LIST

		No. Copies
1.	Defense Documentation Center Cameron Station Alexandria, Virginia 22314	2
2.	Library, Code 0212 Naval Postgraduate School Monterey, California 93940	2
3.	Professor G. J. Thaler Department of Electrical Engineering Naval Postgraduate School Monterey, California 93940	5
4.	LCDR Humberto Medina A. Commandancia General de la Marina San Bernardino, Caracas, Venezuela	5
5.	Biblioteca, Escuela de Postgrado Escuela Naval de Venezuela Meseta de Mamo, La Guaira. Venezuela	1
6.	Biblioteca, Esc. de Ingeneieria Electrica Universidad Central de Venezuela Ciudad Universitaria, Caracas, Venezuela	1
7.	Professor Milton L. Wilcox Department of Electrical Engineering Naval Postgraduate School Monterey, California 93940	1
8.	Mr. J. W. Banham, Jr. Naval Ship Engineering Center Philadelphia Division Philadelphia, Pa. 19112	1
9.	LT Charles A. Vinroot c/o Supervisor of Shipbuilding 97 East Howard St. Quincy, Mass. 02221	1

Security Classification

DOCUMENT CONTROL DATA - R & D

(Security classification of title, body of abstract and indexing annotation must be entered when the overall report is classified)

ORIGINATING ACTIVITY (Corporate author)	2a. REPORT SECURITY CLASSIFICATION
Naval Postgraduate School Monterey, California 93940	Unclassified
	2b. GROUP

REPORT TITLE

Digital Computer Model Study of a Destroyer Steam Generator System Control

DESCRIPTIVE NOTES (Type of report and inclusive dates)

Master's Thesis; June 1970

AUTHOR(S) (First name, middle initial, last name)

Humberto Medina Arellano

REPORT DATE	7a. TOTAL NO. OF PAGES	7b. NO. OF REFS
June 1970	111	5

8. CONTRACT OR GRANT NO.	9a. ORIGINATOR'S REPORT NUMBER(S)
b. PROJECT NO	
c.	9b. OTHER REPORT NO(S) (Any other numbers that may be assigned this report)
d.	

10. DISTRIBUTION STATEMENT

This document has been approved for public release and sale; its distribution is unlimited.

11. SUPPLEMENTARY NOTES	12. SPONSORING MILITARY ACTIVITY
	Naval Postgraduate School Monterey, California 93940

13. ABSTRACT

The steam generator of a DLG-9 Class Destroyer is studied and simulated by means of the Digital Simulation Language DSL/360. Parameter plane studies are made for each one of the principal subloops of the control system and determination of optimal controller settings is attempted. The entire steam generator and control system are simulated and the responses to small disturbances are analyzed. Finally a linear interpolation is attempted for the nonlinear transfer functions, and the responses compared with data from an actual DLG-9 Test Boiler.

DD FORM 1 NOV 65 1473 (PAGE 1)

S/N 0101-807-6811

Security Classification

A-31408

14 KEY WORDS	LINK A		LINK B		LINK C	
	ROLE	WT	ROLE	WT	ROLE	WT
Boiler Control Simulation						
Parameter Plane						

17 MAY 72 20118
16 NOV 72 21441
17 APR 73 21441
16 NOV 76 24937

Thesis 120525
A648 Arellano
c.1 Digital computer model study of a destroyer steam generator system control.
17 MAY 72 20118
16 NOV 72 21441
17 APR 73 21441
16 NOV 76 24937

Thesis 120525
A648 Arellano
c.1 Digital computer model study of a destroyer steam generator system control.

thesA648
Digital computer model study of a destro
3 2768 001 00627 3
DUDLEY KNOX LIBRARY